Shallow landslide cluster propagation in tropical mountainous terrains. Case study Colombian Andes

Johnnatan Arley Palacio Cordoba

Universidad Nacional de Colombia
Facultad de Minas, Departamento de Ingeniería Civil
Medellín, Colombia
2023

Shallow landslide cluster propagation in tropical mountainous terrains. Case study Colombian Andes

Johnnatan Arley Palacio Cordoba

A thesis submitted in partial fulfillment of the requirements for the degree of:
Msc. Geotechnical Engineering

Advisor:
Ph.D. Edier Vicente Aristizábal Giraldo
Co-advisors:
M.Sc. Óscar Echeverri Rámirez
Ph.D. Martin Mergilli

Research Field:
Landslide and risk management
Research Group:
Semillero Geohazards
Grupo de Investigación en Geología Ambiental - GEA

Universidad Nacional de Colombia
Facultad de Minas, Departamento de Ingeniería Civil (Civil Engineering Department)
Medellín, Colombia
2023

To my mom, who gave me all that she could, and to whom I would give all that I have

To my friends for their support and care along the way

To myself for continuing on the way

"There are no beautiful surfaces without a terrible depth"
— Friedrich Nietzsche

Acknowledgment

The path that has brought me to this point has been a long and transformative one, marked by numerous steps, experiences, and decisions that have shaped my character, especially during challenging times. I owe a debt of gratitude to the many individuals who recognized my potential and consistently encouraged me to persevere. I would like to extend my special thanks to Professor Edier Aristizábal, whose confidence in my abilities provided me with the impetus to embark on this successful academic journey and reach this significant milestone. To Professor Martin Mergili, I am deeply grateful for his continuous support, even from afar, starting from my undergraduate studies. I would also like to express my appreciation to Professor Oscar Echeverri for entrusting me and offering his support, which allowed me to gain valuable teaching experience.

I extend my heartfelt thanks to my dear friends, Dany Rios and Juan Alzate, who have encouraged me over the years. I'm also grateful to the many people who have been part of my life during this time, offering their support, lending a listening ear, and providing invaluable advice. Your trust and encouragement were instrumental in helping me take those crucial first steps.

I want to express my appreciation to my fellow master's program colleagues, with whom I've shared incredible experiences and forged lasting friendships. Special thanks go to Federico Gómez for his continuous contributions and to Mariana Vasquez for her unwavering support. Your presence and belief in me have been a driving force behind my achievements.

Abstract

Approximately one-fifth of the Earth's surface is considered vulnerable to at least one natural hazards such as cyclones, droughts, floods, earthquakes, volcanoes, and landslides. Landslides are one of the most destructive; there are several triggering factors. In the Colombian Andes, rainfall is the primary triggering factor. Historical records of landslide occurrences in the country between 1900 and 2018 found that rainfall was responsible for 87 percent of them. These landslides are typically shallow and can evolve into more rapid movements such as flows or avalanches. According to recent records, debris flows have caused some of the most severe damage and some of them happened as a result of the occurrence of Clustered Shallow Landslides (CSL). In terms of spatial analysis, most study in the country focuses on estimating the areas most susceptible to the occurrence of Shallow Landslides (SL). But what happens when an SL propagates? This research focuses on parameters for modelling the propagation of SL triggered by rainfall occurred on March 31, 2017, in Mocoa that supply mass to bigger chain processes that affect the city and surrounding villages with approximately 306 dead people. The modeling is carried out through two useful tools. The empirical tool Flow-R, it requires little input information, the propagation is performed using different algorithms and friction laws, fundamental factors are the travel distance angle, velocity, and dispersion. And r.avaflow that incorporates various physics-based models. It was established for each tool the best-fit parameters for modeling with minimal requirements. Results indicated a maximum velocity of 10 $m\ s^{-1}$, minimum travel distance angle of 15°, and x value of 2 and 4 for modeling in Flow-R. In addition, the cut-off for the probability of impact was set to 25% as the minimal threshold for zoning. The results concerning to the parameters to modeling SL in r.avaflow suggest; to consider the basal friction equal to the internal friction of the material as the starting value. And to use the minimum heights in the range of 0.51 m to 0.61 m to perform hazard zoning of the possible affected areas.

Keywords: Modeling, landslide, propagation, cluster, runout, r.avaflow, Flow-R..

Resumen

Propagación de deslizamientos superficiales en terrenos montañosos tropicales. Caso de estudio: Andes colombianos

Aproximadamente una quinta parte de la superficie terrestre se considera vulnerable a al menos una amenaza de origen natural, como: ciclones, sequías, inundaciones, terremotos, volcanes y movimientos en masa. Siendo este último uno de los más destructivos; existen varios factores detonantes. En los Andes colombianos, las lluvias son el principal factor detonante, según registros históricos entre 1900 y 2018 el 87% de los movimientos en masa fueron detonados por lluvias, los cuales suelen ser poco profundos y pueden evolucionar a movimientos más rápidos y destructivos como flujos y avalanchas. Según registros recientes, la ocurrencia de decenas a cientos de movimientos en masa detonados por lluvias, resultó en la ocurrencia de avenidas torrenciales causando afectaciones sobre la población y la infraestructura. En términos de análisis espacial, la mayoría de los estudios realizados se centran en estimar las zonas más susceptibles a la ocurrencia de movimientos en masa superficiales. Pero ¿Qué ocurre cuando un movimiento en masa se propaga? Esta investigación se centra en los parámetros para la modelación de la propagación de movimientos en masa superficiales detonados por las lluvias ocurridas el 31 de marzo de 2017, en Mocoa que fueron suplemento para un evento concatenado de mayor poder destructivo, que afecto la infraestructura y causó la muerte de aproximadamente 306 personas. La modelación se realiza mediante la herramienta empírica Flow-R, la cual requiere poca información de entrada, la propagación se realiza utilizando diferentes algoritmos y reglas. Y r.avaflow incorpora varios modelos basados en la física, teniendo como insumo básico la distribución de la fricción interna del material y fricción basal material – superficie. Se estableció para cada herramienta los parámetros de mejor ajuste para el modelado con requisitos mínimos. Los resultados indicaron para Flow-R una velocidad máxima de 10 $m\ s^{-1}$, un ángulo de distancia de viaje de 15°, y un valor de x de 2 y 4. Además, el umbral mínimo de la probabilidad de impacto se fijó en 25% para la zonificación. Respecto a r.avaflow, los resultados sugieren considerar la fricción basal igual a la fricción interna del material como valor de partida. Y utilizar las alturas mínimas en el rango de $0,51\ m$ a $0,61\ m$ para realizar la zonificación de la amenaza de las posibles áreas afectadas. .

Palabras clave: Deslizamiento superficial, modelación, movimiento en masa, propa-

gación, enjambre, r.avaflow, Flow-R.

Contents

1 Introduction

Almost one-fifth of the Earth's surface is considered vulnerable to at least one natural hazard such as cyclones, droughts, floods, earthquakes, volcanoes, and landslides (Dilley et al., 2005). Landslides are one of the natural hazards that cause the highest number of deaths and damages every year (Kjekstad and Highland, 2009; Schuster and Highland, 2001, 2003; Petley, 2012). The area exposed to landslides is about 3.7 million km^2, where 5% of the world's population lives (Dilley et al., 2005). Colombia is one of the countries with the highest landslide risk, classified as medium to high, with an annual occurrence of $0.0125\% - 0.050\%$ per km^2 (Nadim and Kjekstad, 2009). The occurrence of landslides is frequent due to the country's location and rainfall patterns. It is located in the northern zone of South America, with a humid tropical climate and complex weather conditions. The pattern of rainfalls is mainly influenced by the Chocó jet, which transports a stream of moisture from the Pacific Ocean toward the interior of the country (Poveda, 2004). And by the Intertropical Convergence Zone (ITCZ), where cloudiness and concentrated rainfall oscillate from south to north, causing rainfall in the quarters of March-May and September-November (Mesa et al., 2000; Guzmán et al., 2014). On the other hand, the rugged landscape, where the mountain range formation is associated with large reverse and strike-slip faults in an area where the Nazca, South American and Caribbean plates converge. In the country, the Andes are divided into three mountain ranges, creating two large valleys, occupying a third of the territory, presenting steep and mountainous terrains, where 65% of the population and the main economic centers are concentrated (Hermelin and Hoyos, 2010a). In historical records reported, Colombia (2019) shows 92.5% of landslides triggered by rainfall are concentrated in the Andean region, 75% of the deaths are caused by landslides. This shows the high destructive power of these phenomena, with 34198 deaths and losses of more than USD 654 million between 1900 and 2018. In addition, this trend has been on the increase since 1970, which is related to the growth of urbanization in the country (Aristizábal and Sánchez, 2019). The landslides triggered by rainfall generally presented planar failure surfaces and shallow depths, less than 3 m (Anderson and Sitar, 1995). These shallow landslides can mobilize as flows or avalanches, partially or completely depending on the material, topography, and saturation (Caine, 1980; Cruden and Varnes, 1996; Iverson et al., 1998; Hungr et al., 2005). Therefore, can be classified as a complex landslide and are difficult to predict due to uncertainties of rheological characteristics, initiation, and dynamics of mobilization, because it depends on landslide location, volume, and composition (von Ruette et al., 2016). Many of these landslides occur in clusters within minutes to days (Witt et al., 2010). Crozier (2005)

refers to these events as "Multiple-occurrence regional landslide events" (MORLEs), events that can occur with hundreds to thousands of landslides in areas that cover tens to thousands of square kilometers. Clusters occur during heavy and/or prolonged rainfall. In Colombia, this type of event occurs in the central area (the Andina region) during the seasonal rainy season.

1.1 Motivation

In Colombia, empirical-statistical and physics-based methodologies for landslide occurrence and propagation have been established in methodological guidelines for landslide hazard zoning at a scale of 1:25000 (2017) and the most recent guide for torrential flows hazard zoning at a scale of 1:2000 (detailed scale) and 1:25000 (basic scale) (2021) by Colombian Geological Survey (SGC, by its Spanish acronym). However, methodologies to focus on the propagation of hillslope landslides have been the subject of little attention. The occurrence of shallow landslides increases with the intensity of the rainy season, which is greater during the cold phase of the El Niño-Southern Oscillation—ENSO (Sepúlveda and Petley, 2015; Aristizábal and Sánchez, 2019; Carmona Arango et al., 2021), and this landslide-type can mobilize as debris flows, spreading over large areas and potentially causing damage to populations and infrastructure. Hungr et al. (2005) mention that landslide propagation plays an important role in hazard assessment. In Colombia, it is mandatory to include a landslide hazard map in the land use planning process. The inclusion of shallow landslide propagation is an important aspect in land use planning programs in mountainous areas, especially for cluster landslide events and subsequent debris flows, where the greatest damage has often been presented.

1.2 Objectives

General objective

Evaluate the performance of propagation models to identify best-fit parameters for shallow landslides clustered modeling in tropical mountainous terrains.

Specifics objectives

- Identify the variables and dynamics of landslide propagation of shallow landslides in tropical environments and mountainous terrains

- Determine the propagation of shallow landslides with an empirical and physically based model

- Evaluate the performance of different propagation models concerning available inventory to identify best-fit parameters

1.3 Scopes and limitations

The main scope of this research consists in the establishment of best-fit parameters for the modeling of shallow landslides using empirical and physical model. This study use data from shallow landslides clustered occurred in Mocoa (2017). The occurrence of numerous landslides is the most essential feature of the cluster-type event for this investigation. Although each landslide occurs under different geoenvironmental characteristics, they occur apparently in similar conditions in a delimited area. As a result, there is less uncertainty about several factors, such as time and the triggering factor. Understanding the characteristics of individual landslides contributes to setting modeling parameters.
The scope is limited to the exploration and estimation of the best-fit parameters based on the evaluation of the predictive capability of the models. However, it does not evaluate the models' quality. The overall modeling of numerous landslides as a whole is complex, due to the adjustment of the variables that govern the mobilization and their interaction. Each landslide is unique, and the adjustment of the impacted areas to the inventoried area is an arduous task. In cases where the modeling includes events with few or one processes, the tool's predictive capability can be evaluated. In this scenario, the tools support estimating the parameters that best fit the propagation, and then these parameters will work to help in modeling propagation in future susceptibility and hazard studies.

1.4 Document structure

This document is basically presented in the form of a series of articles. There are two major parts to the methodology used to address the issues raised. (i) Theoretical foundations and state-of-art, (ii) models implementation.
First, in the section 2 the theoretical and dynamic basics of shallow landslide and the relevance of propagation in risk management is presented. It explores the methodologies employed in the analysis of landslide propagation. Besides, it briefly discusses the cluster-type events recorded in the country, researches carried out on landslide propagation, and review Colombian risk management regulation.
In the study area - Mocoa - many landslides were triggered by rainfall in a short time, and hundreds of deaths and injuries were caused. For the implementation of models, it's collected the basic inputs of the study area, such as the debugged inventory of the source landslides and the affected areas, geotechnical parameters, and the digital terrain model. The information collected is mostly from studies performed by the SGC after the event (SGC, 2017b, 2018a, 2017,a, 2018b; UNGRD and Universidad Pontificia Javeriana, 2017). This informa-

tion allows the identification of the propagation characteristics for each landslide.
In section 3, the empirical tool Flow-R is implemented, it is a spatially distributed model for regional scale studies, which allows the assessment of propagation from a predefined source areas (inventory), based on several algorithms and simple friction laws (Horton et al., 2013). The section starts exploring the landslide velocity, propagation characteristics, and travel distance angle through geometrical approaches, this data is required in the propagation modeling with Flow-R.
On the other hand, in section 4 the physical modeling is implemented with r.avaflow proposed initially by Mergili et al. (2017), which uses a solid-fluid interaction model to calculate the propagation of mass flows from specified release areas over a defined topography. The tool requires minimum geotechnical data (internal friction angle) to set up the basal friction values. In this case, the basal friction angle is evaluated from 80% to 100% of the internal friction angle.
Finally, is carried out the modeling and set up the best-fit parameters based on the validation criteria of the results in both tools. It established travel distance angle, velocity, propagation coefficient, and cut-off probability affectation with Flow-R. And basal friction angle and, the cut-off height of affectation with r.avaflow.

2 Overview

This chapter was written with support of Edier Aristizábal, Martin Mergili and, Oscar Echeverrí.

Brief review of state of propagation models for flow-like landslides and current state in Colombia

Abstract

In Colombia, seasonal rainfall patterns influence the occurrence of landslides, particularly in mountainous areas such as the central Andean region, generating damage to the population and infrastructure every year. Landslides triggered by rainfall are generally shallow and sometimes occur in clusters in a domino or cascade effect. Clusters have been addressed in the country in terms of landslide susceptibility, but few were addressed in terms of their dynamic propagation. However, the susceptibility to the occurrence of Shallow Landslides (SL) only represents one step in the hazard analysis; propagation and deposition of the failed mass must be included in all types of hazards and risk analysis. This review focuses on models used to estimate hillslope landslide paths and propagation, their implementation, and the current state of risk management in the country.

2.1 Introduction

Landslides, many of which are triggered by rainfall, cause thousands of fatalities and economic losses each year worldwide (Kirschbaum et al., 2015; Kjekstad and Highland, 2009; Petley, 2008, 2012). Colombia has a humid tropical climate and exhibits a rugged topography. Moreover, it features hydro-climatological conditions with bimodal rainfall distribution in the central zone, influenced by the meridional migration of the inner tropical convergence zone and Chocó low-level jet (Mesa et al., 2000; Poveda, 2004). Aristizábal and Sánchez (2019) show how seasonal rainfall patterns influence the occurrence of landslides in Colombia, particularly in mountainous areas such as the central Andean region. Furthermore, they indicate that in 30730 reports, 87% of landslides are triggered by rainfall. The records

show 34198 fatalities, 138290 people affected, and economic losses of more than 650 million dollars.

Landslides triggered by heavy or prolonged rainfall events are often shallow (Crosta, 1998). Many of these Shallow Landslides (SL) occur in clusters and are the sources of domino or cascading events (process chains), which can occur from minutes to days (Witt et al., 2010). And represent components of multi-hazard situations. Crozier (2005, 2017) calls these events as "Multiple-occurrence regional landslide events", events that range from hundreds to thousands of landslides in areas covering tens to thousands of square kilometers.

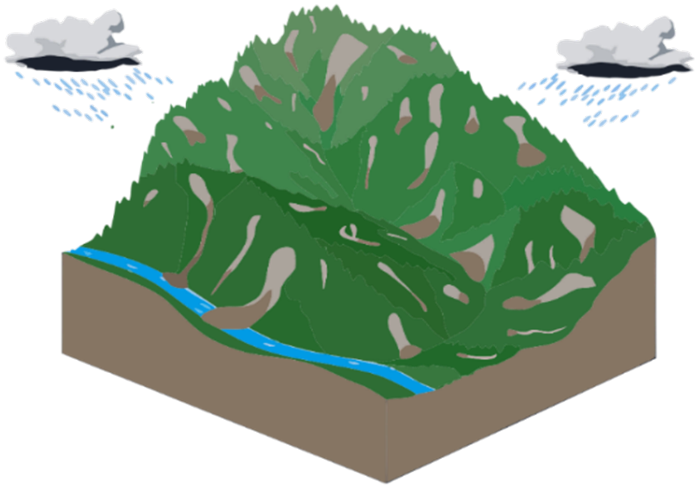

Figure 2.1: Schematic illustration of a cluster event. Modified from Dai et al. (2021).

Cascini et al. (2010) and Cuomo (2020) classify the analysis of SL evolving into extremely rapid flows or avalanches in elementally in three stages, (i) failure stage, where the driving forces overcome resisting forces and failure occurs due to rainfall because pore pressure increases generating changes in the geomechanical properties of the soil; (ii) post-failure stage when the mass accelerates and the transitions from landslide to flow occur; and (iii) the propagation stage, that includes the downslope movement from the source to the deposition area.

Major debris flow occurrences triggered by SL are a very common phenomena in the Colombian Andes, such as those that occurred in Tarazá (2007), Salgar (2015), Mocoa (2017), and Dabeiba (2020), where dozens or hundreds of SL were triggered, and a subsequent debris flow caused many deaths and severe damages. In landslide reports and inventories, a distinction is rarely made between the damage caused in the exact area of occurrence and the damage caused by the propagation of the moving mass. It is often the movement stage that is highly destructive. However, the prediction of the occurrence of SL only represents one step in the hazard analysis; propagation and deposit areas of the failed mass must be included in all types of hazards and risk analysis.

SL are defined by Cruden and Varnes (1996), as a translational slide composes by soil, debris, or rock mass that moves along a planar or slightly undulating failure surface. The failure usually occurs over discontinuities, joints, or material changes (rock, residual soil, or transported sediment). Such processes tend to move continuously if the slope is steep enough and can evolve from slide to avalanche or flow, depending on water content and, slope angle, topography and other factors. SL occur mainly on medium to steep slopes, within topsoil (regolith), or in contact with underlying bedrock (or a less permeable layer) (Borga et al., 1998). Aristizábal et al. (2017) mention that in tropical environments such as Colombia, this type of landslide is controlled by the weathering profile and water storage capacity. Anderson and Sitar (1995) mention that SL are characterized by thicknesses of less than 3 m with a failure surface subparallel to the surface, while other authors consider thicknesses of less than 2 m (Crosta and Frattini, 2001; Moser and Hohensinn, 1983). Skempton and Hutchinson (1969) indicate that this type of landslide generally represents values of ratio Dr/Lr less than 0.1 (maximum depth perpendicular to the slope/length of the landslide).
Data from Shallow Landslides Clustered (SLC) provide the opportunity of to study the occurrence and propagation of numerous individual landslides that occur apparently in similar conditions in a delimited area. In a comprehensive analysis of the possible hazards during SLC, mass flows evolving from SL may cause damage to the population and/or infrastructure and contribute a significant amount of sediment to the channels (see Figure. 2.1). The destructive potential of such debris flows, mud flows, or hyperconcentrated flows (known as *avenidas torrenciales* in Colombia) may increase in a series of concatenated processes. Aristizábal et al. (2020) carry out extensive research on the terminology and definition used in the country for debris flows. They propose to use the term torrential flows to describe flows formed by a mixture of sediment and water in varying proportions, moving at high velocities along channels in mountain catchments, where one or more triggering factors have an influence, such as heavy and intense rainfall, landslide clusters, earthquakes, and dam failures. They also mention three types, (i) channelized debris flows, (ii) debris floods and (iii) sudden rise in water level. Different factors influence the dynamics of landslide propagation and are strongly correlated with each other. For example, the initial mass accelerates as a function of gravity. The velocity change according to topography, material, saturation, and friction between the mass and the basal surface. In addition, there is a constant variation of the composition and internal deformation due to erosion and entrainment. Hungr et al. (2014) illustrates how complex landslides can develop. In our case, e.g., a storm event can trigger a sub-parallel failure in a shallow soil layer, located above an impermeable layer. Failure occurs due to the increase of pore pressure at the contact. The solid/water mixture moves adding material by entrainment, accelerating its movement on a steep slope by the effects of gravity, and deposits in a river channel, contributing material to possible debris flow.

2.2 Cluster events in Colombia

In recent years, the frequency of occurrence of SLC – or at least the number of recorded events – in Colombia has increased (Figure 2.2). In the 1990s, when risk management was incorporated into national regulations, little information about the occurrence of SLC exist. An event such as occurred in the municipality of San Carlos (1990) is known mainly for the damage caused to the infrastructure of the Calderas hydroelectric plant, and investigations focused on risk management two decades later carried out by Aristizábal (2013). On January 31, 1994, in the upper Fraile River basin, about 125 landslides with depths of up to 3 meters were triggered, resulting in the death of 19 people, 86 injured and 22 missing (González et al., 2005). For the following decades, the records have been gradually increasing. On May 29-30 (2000) a debris flow occurred after 7 hours of rain in La Estrella municipality, it was triggered 264 landslides, causing one death and one missing person. In addition, damages close to one million dollars (Hermelin and Hoyos, 2010b).
Generally, the events are reported through the news, and their promulgation is a function of the damages, deaths caused, and seasonal rainfall. For example, information through digital media of events such as those that occurred in Yalí, Anorí (2020) is almost nonexistent, and much information remains unnoticed in regional media or reports of public risk management entities, from municipal to national. Therefore, many events are not known by the community and cannot be used to increase the databases on the occurrence of such events.

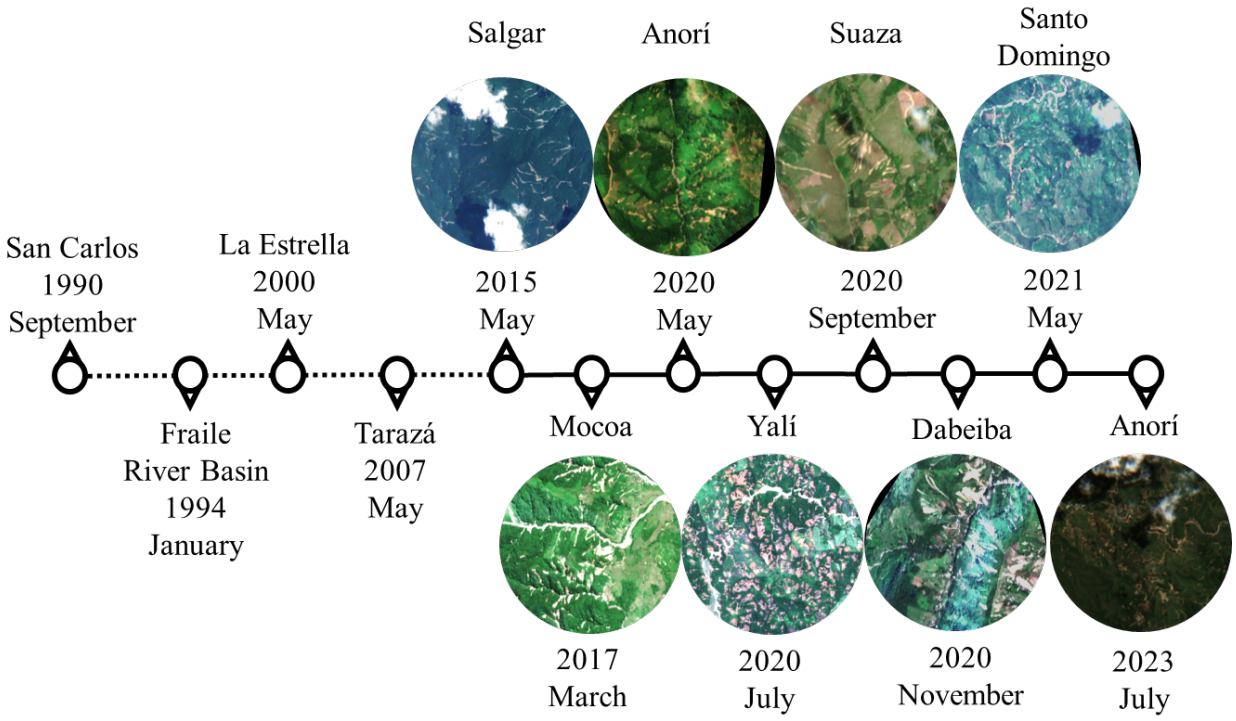

Figure 2.2: Cluster landslides records. Images from `www.sentinel-hub.com/`

In events such as those that occurred in Salgar and Mocoa, it was the propagation (mainly as debris flow) that caused the highest amount of damage to the population. In Mocoa, according to reports from the National Institute of Legal Medicine and Forensic Sciences 2017, on April 6, about 306 victims were identified; according to the press there were 322 deaths, more than 100 missing, and about 330 injured (RCN Radio, 2017) In Salgar 2015 the cluster event and subsequent flash flood caused the death of at least 97 people according to records. To a lesser degree, in Tarazá an event caused the death of at least 7 people and affected more than 600 families (Caracol Radio, 2007; El Tiempo, 2007). The event in Dabeiba caused the death of 5 people and more than 400 were affected (Caracol Radio, 2020a; Noticias RCN, 2020). The event of Yalí resulted in some economic losses and one person dead (Caracol Radio, 2020b).

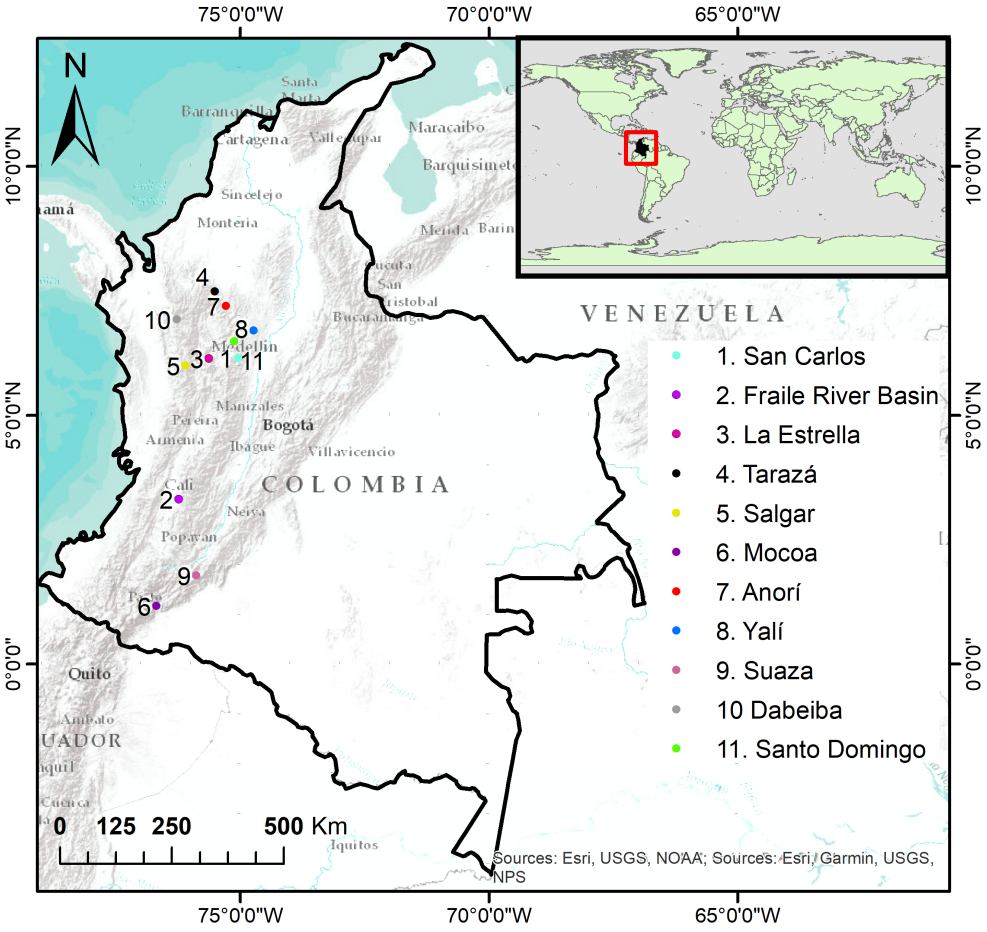

Figure 2.3: Location cluster events

Considering some of those SLC in more detail. In the municipality of Tarazá a rainfall event triggered hundreds of landslides in Cañon de Iglesias creek and San Sereno micro-basin, causing accumulation of material and subsequent debris flow in the Tarazá River, most of the material was deposited 2 km from the urban area. In Salgar is located La Liboriana

creek, which runs through the urban area. Strong rainfalls of 160 mm in two hours in the upper area of the basin, triggering landslides mainly on the Cerro Plateado mountain located about 29 km from the municipal head (UNGRD and Fundación Instituto Geofísico Universidad Javeriana, 2016). The concatenated event resulted in the death of about 100 people and extensive damage to infrastructure and agricultural areas (Hernández, 2015).
The municipality of Mocoa is in the southwest of Colombia in the department of Putumayo, between the Andes Mountain range and the Amazonian lowland. In 2017 between the night of March 31 and dawn on April 1, approximately 129 mm of rainfall triggered hundreds of landslides and concatenated events over the urban area and nearby villages. The event corresponds to a return period of 25 years (SGC, 2017b). In the rainy season of 2020 (more exactly, in the night of November 13), rainfall triggered about 170 landslides in the municipality of Dabeiba. In September of the same year, an event occurred in Suaza (Eastern Mountain range). Also, in the northeast of Antioquia, the municipalities of Anorí and Yalí experienced SLC on 2020 on May 19 and July 5, respectively. Recent recorded event occurred on May 31 (2021), in the first rainy season of the central Andean region, in the municipality of Santo Domingo, where a little more than 120 landslides were triggered. The most recent recorded SLC occurred on July 17 (2023), in the municipality of Anorí, about 3 hours of rainfall triggered dozens of landslides near the urban area.

2.3 Methods

Broadly, authors consider several groups of methods of propagation analysis, the main methods of propagation analysis are analytical methods based on lumped mass, empirical–statistical methods based on geometric correlations, landslide characteristics, and the path derived from observed data to determine the runout path. And Numerical methods considering continuum and discontinuum models (Hungr et al., 2005; Scheidl et al., 2013; Rickenmann, 2005; Crosta et al., 2003). McDougall (2017) indicates that continuum models have developed more in the last decades, and some models can be classified as semi-empirical models with a dynamic basis that requires calibration.

2.3.1 Analytical methods

In analytical methods, formulations generally are based on lumped mass approaches, where the mass sliding is reduced (condensed) in a single point. Therefore, internal deformation is not allowed (Dai et al., 2002; Quan Luna, 2012). The Figure 2.4 show how the analysis focus in the center of mass and friction loss during motion; the mass accelerates according to Newton's second law and stops when the angle of inclination is lower than the critical angle (Pirulli, 2005). According to Dai et al. (2002) the method is suitable to estimate paths in small rock slides; without regard to disintegration, confinement, and entrainment. Many authors incorporate variables to approach the phenomenon representation, such as Wang

and Sassa (2000a) that incorporate the pore pressure and Hutchinson (1986) developing a model for cohesionless and loose materials, considering debris spreads out as a uniform sheet.

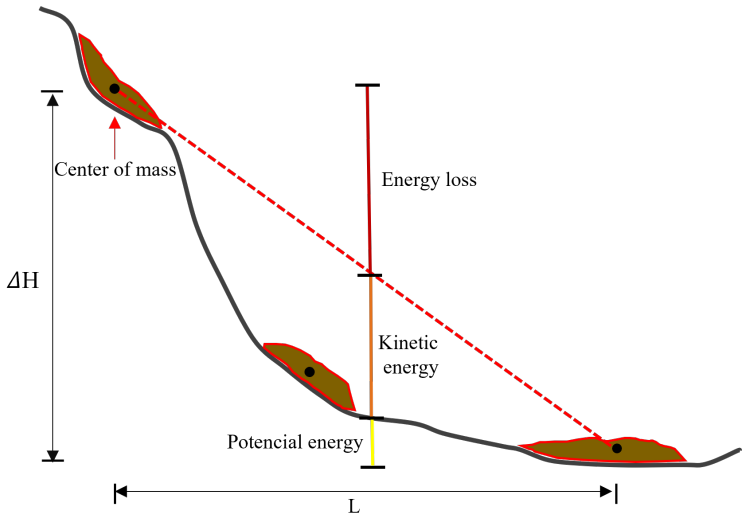

Figure 2.4: Energy analysis in lumped mass approach. Modified from Pirulli (2005) and Sassa (1988)

2.3.2 Empirical-statistical methods

According to Hungr et al. (2005) there are three empirical methods for estimating runout path: (i) geomorphologically based, where photo interpretation and fieldwork are used to determine landslide travel distance which is the basis for defining the runout of future landslides, with the difficulty that the results cannot be applied to other sites due to the conditions of each area; (ii) geometrical approaches employing the angle of reach, used by many authors who determine relationships through regressions considering parameters like volume, height difference, and slope to determine the travel distance; (iii) volume change methods, such as the one implemented by Cannon (1993) who analyzed the potential travel distance using twenty-six debris flows, considering the behavior in the change of volume during downslope propagation, considering the slope and the degree of confinement. Fannin and Wise (2001) use the same principle but deal separately with entrainment and deposition, considering movement in open and confined areas.

Among the first works carried out on runout prediction is Heim (1932) who introduced the *fahrböschung* also known as the angle of reach and travel distance angle (Corominas, 1996). The angle of reach α is an empirical index for relative mobility of landslides, it is the angle that connect the points between scar of source area and the end of the deposition area. So, the mobility is expressed in equation 2.1 as the ratio between the vertical height H, that is the elevation difference between points and L the horizontal distance (Corominas, 1996; Hungr et al., 2005; Hunter and Fell, 2003).

$$\tan\alpha = \frac{H}{L} \tag{2.1}$$

Authors have addressed the runout through relationships between landslide volume, height, and runout distance (Corominas, 1996; Hungr et al., 2005; Hunter and Fell, 2003; Li, 1983; Scheidegger, 1973). For e.g. Scheidegger (1973), from what was done by Heim (1932), establishes a correlation between volume and the coefficient of friction ($f = \tan\phi$) by performing a regression with 33 landslides (eq. 2.2)

$$logf = -0.15666 \cdot logV + 0.62419 \tag{2.2}$$

Other authors estimate correlations in different study areas, Rickenmann (1999) developed an empirical relationship for debris flows in the Swiss Alps and Devoli et al. (2009) in Central America using several landslide types. Corominas (1996) used 204 landslides from some countries in his research and showed not only the influence of volume in the determination of the angle of reach but also that of other factors such as the type of movement, obstacles, and topography. Benda and Cundy (1990) determined travel distance and volume and employed two criteria for the prediction of deposition of coarse-textured debris flows in confined mountain channels, considering (i) deposition in channels with a slope less than 3.5° and (ii) deposition in tributary junctions with angles above 70° between channels.

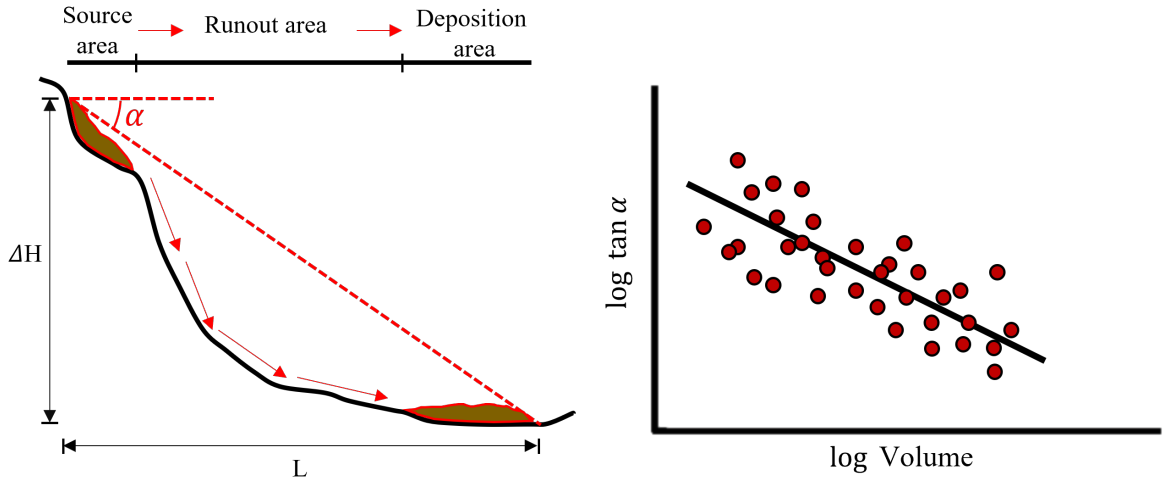

Figure 2.5: a) Schematic illustrations of landslide area and angle of reach; b) empirical correlation $\log\tan\alpha$ vs $\log Volume$

Among the most relevant empirical-statistical methods is that of Iverson et al. (1998), with data of 27 lahar paths at 9 volcanoes, estimates cross-sectional flow area (A, constant) and inundated planimetric area (B) as a function of volume, to predict the deposition area through two semi-empirical equations 2.3 and 2.4.

$$A = K_A V^{2/3} \tag{2.3}$$

$$B = K_B V^{2/3} \tag{2.4}$$

where K_A and K_B are dimensionless mobility coefficients, according to flow type. Some estimations are performed. Schilling (1998) incorporated LAHARZ as a computational tool on Geographic Information System (GIS); this program estimates the possible inundated areas, considering the drainage and established volumes, given (i) A is constant along the depositional reach and (ii) the flow is confined within a valley. Berti and Simoni (2007, 2014) modified LAHARZ and included unconfined flow conditions on the fan with the DFLOWZ model, using 27 Alpine debris flows, computing mobility coefficients ($K_A = 0.08$ and $K_B = 0.17$) through regressions considering factors of uncertainty in the prediction of A and B.
Some authors have developed models based on rules considering propagation routines cell by cell. Scheidl and Rickenmann (2010) present TopRunDF as an empirical method for predicting the runout of debris flows with data from Austria, Switzerland, and northern Italy, tested with 14 debris flows. Flow paths and spreading probabilities are a combination of a Monte Carlo simulation and the flow routing algorithm of Hürlimann et al. (2008), based on the D8 algorithm, for the distribution of volume in the deposition area. Later, Mergili et al. (2015) followed the same principle with r.randomwalk using a Monte Carlo approach, considering multiples break criteria that consist in the definition of thresholds for empirical parameters like travel distance and angle of reach; for each source-point, the flow is routed down through the digital terrain model (DTM) using random walks (paths), until the mass leaves the study area or all break criteria is fulfilled. Horton et al. (2013) implemented Flow-R, a software that allows propagation from previously defined source areas on a regional scale, considering as basic input a DTM. The analysis is bounded by user-defined constraints based on several algorithms; (i) directional algorithms for path and propagation control and (ii) frictional laws for propagation distances; mass and volume are not considered. The use of these algorithms is not recommended for modeling individual events, since the propagation may trigger other events. Furthermore, it is recommended to model different types of processes separately (e.g., debris flow and mudflow). Guthrie and Befus (2021) developed DebrisFlow Predictor, which is a semi-empirical model, based on the mathematical model of cellular automata developed by Von Neumann (1966). They use rules for erosion, deposition, path, and propagation, employing a DTM (5mx5m) for their study.

2.3.3 Numerical methods

Empirical methods allow for suitable estimates of travel distance and deposition areas. However, to obtain more information about flow heights, velocities, and impact pressures, the use of numerical models is necessary (McDougall, 2017). The analysis of runout behavior by numerical methods includes continuum and discontinuum models. Continuum models are

based on the conservation of mass, energy, momentum, and physical laws (rheology) (Quan Luna et al., 2012). In discontinuum models, the displaced material (downslope) is represented by a group of particles of different geometric shapes (discs/cylinders and spheres) that can represent more complex shapes when combined; the movement is governed by laws that describe the contact forces between interacting particles (Pastor et al., 2014; Poisel et al., 2008). Pastor et al. (2014) mentions that continuum models can be applied to many problems, while discontinuum (discrete) models are generally applied for the analysis of rock mass movements with limitations associated with the number of particles and do not recommend their use in other types of landslides.
The internal deformation of the flowing mass is described by the rheology. Several rheological models have been used in mass flow propagation modeling, according to the characteristics of the anisotropic material assumptions (elasticity, plasticity, and viscosity). The Bingham model considers a two-phase behavior (visco-plastic): in the initial phase, the flow material behaves like a solid, and in the second phase like a fluid. The model considers two parameters, (i) initial shear stress required to move, this point is called critical shear stress (yield stress), and (ii) viscosity which is the slope between shear stress and shear rate (Maros and Juniar, 2019; Quan Luna, 2012). In the frictional Coulomb model, the basal shear stress is not dependent on velocity, but on the effective normal stress and is proportional to it (Pirulli, 2005). The frictional-turbulent model of Voellmy 1955 considers a mixture of solid and fluid where the main variables are the coefficient of turbulence of the mass and the coefficient of friction. O'brien et al. (1993) incorporate turbulent and dispersive functions into the Bingham model, thus developing the Quadratic model.
Pastor et al. (2014) consider four subgroups of continuum models. (i) 3D models based on mixture theory are highly complex due to numerous unknowns and equations to the material that flows in all its phases (fluid, solid, and gas). They are relevant when analyzing mudflows and rock-debris avalanches with complex geometry and physics. (ii) Velocity-pressure models are usually used in geotechnical engineering to describe the behavior of foundations, geostructures, slope failures, etc. They are based on the velocity of solid particles and interstitial pressure, since the water movement in the soil is not significant. (iii) Depth-integrated models consider the fact that many flow-type landslides propagate as shallow bodies, with the thickness being much less than the length and width. They reduce the analysis from 3D to 2D, as in work presented by Savage and Hutter (1989). (iv) Depth-averaged (St. Venant) shallow-water equations (SWE) must be mentioned, too. Savage and Hutter (1989, 1991) present a Lagrangian frictional model for the description of the movement of flow-type landslides and snow avalanches, which are modeled as a finite mass of cohesionless granular material. The material moves downslope on a rough curved rigid bed, considering shallow flow and employing depth-averaged mass and momentum conservation equations along with the Coulomb model (incompressible continuum).

According to McDougall (2017) many models are based on depth-averaged equations, like DAN (Dynamic ANalysis) numerical model of unsteady flow introduced by Hungr (1995),

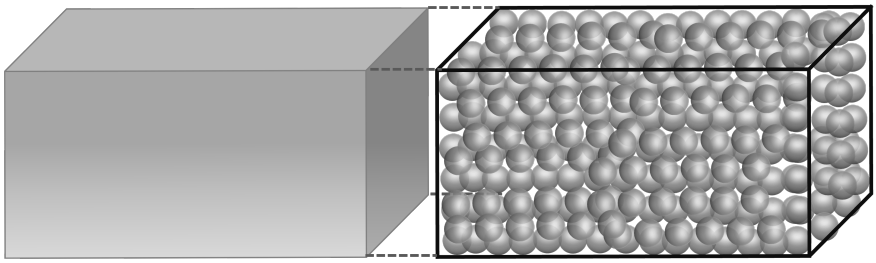

Figure 2.6: Continuum and discontinuum (or discrete) methods of numerical modeling (e.g., discretization in spheres)

where the heterogeneous and complex landslide is modeled as a hypothetical material governed by simple rheological relationships. DAN was modified by McDougall and Hungr (2004, 2005) considering 3D analysis with a discretization method adapted from smoothed particle hydrodynamics (SPH) of Gingold and Monaghan (1977), considering constant density. The mass is discretized in particles with finite volume, that only can increase due to entrainment, and the rheology can change along the flow path. Pastor et al. (2009) presented the GeoFlow-SPH model based on SPH, applied by Cuomo (2020) considering several source areas. The Geotechnical Engineering Office of the Government of the Hong Kong Special Administrative Region (GEO) developed a debris mobility model (DMM) based on DAN. GEO implemented some enhancements, like considering a trapezoidal cross-section rather than a rectangular cross-section and considering resistance in the entire wetted perimeter of the section. DMM was calibrated with Hong Kong's landslides and implemented by Kwan and Sun (2006) in its 2D version and Kwan et al. (2007) as 3dDMM.

Medina et al. (2008) present FLATModel for the propagation of debris flows, using the depth-averaged mathematical model SWE. It includes many basal resistance laws and incorporates simplifications related to the constitutive relations and mixture phases, and dimension (monophasic 2D model). This model also uses a "stop and go" mechanism to establish the repose of the particle through 3 conditions (previous motion, velocity, and slope). It was tested with a debris flow of one source, whereas Papa et al. (2018) simulated an event considering two source areas. Quan Luna et al. (2012) proposed AschFlow (2D), a one-phase continuum model developed in the open-source GIS software PCRaster as a medium-scale model (1:10000 to 1:50000). It simulates the spreading, entrainment, and deposition process, distributing the material based on rheology and flow routing. They tested, considering several source areas in three levels of susceptibility to debris flow initiation, where the initiation area increases in each level, minor, moderate, and major level.
Some mass flow simulation tools were implemented as raster modules of the free and open-source software GRASS GIS or PCRaster . Molinari et al. (2014) showed r.massmov, a reimplementation of the non-commercial model MassMov2D of Beguería et al. (2009). The original model was developed in PCRaster based on SWE. It includes four rheological laws

and builds on mass, and momentum balance in a monophasic fluid model. Restrictions regarding code modification, interfaces, and advanced parameter modification were applied, so it was implemented in GRASS GIS as r.massmov with some changes to make it ready for use with early warning systems and to improve computational efficiency. It incorporates a fluidization algorithm, parallel computing and a new stopping criterion. In early works, Mergili (2008); Mergili et al. (2012) presented r.debrisflow. Later, presented r.avaflow 2017, designed to simulate different types of mass flows and geomorphological process chains. r.avaflow propagates mass from pre-defined source areas through the DTM by redistribution of mass and momentum. It allows the user to choose between a Voellmy 1955 type mixture model and the multi-phase model of Pudasaini and Mergili (2019), which allows considering solid, fine-solid, and fluid materials and can be applied with one to three phases. Erosion and entrainment from the basal surface can be simulated using a simple empirical model. Christen et al. (2010) developed RAMMS for the analysis of snow avalanches using a Voellmy rheological model, modified by Salm (1993), and implemented it in Swiss guidelines for the analysis of this type of phenomenon. In addition, they incorporate the methodology to consider the entrainment proposed by Sovilla et al. (2006). Currently, RAMMS has a module for debris flows that uses depth-averaged equations, implemented by Zimmermann et al. (2020) in Switzerland.

2.4 Propagation analyses in Colombia – Background

Few models have been applied in Colombia for the propagation of landslides, especially those occurring in cluster events. Llano Serna et al. (2015) analyse the propagation of a single landslide that occurred in the Alto Verde urbanization in the city of Medellín (2008), which caused 12 fatalities and significant economic losses. The analysis was done using the material point method, based on particles with a double discretization (Lagrangian-Eulerian) to simulate the distortion inside the sliding mass. In addition, an algorithm of contact between material and topography was considered, obtaining velocity, kinetic energy, and reach of the mass. Castro López (2018) simulated the behavior of granular flows in two small basins of the Doña Juana volcanic complex in the department of Nariño. The analysis was carried out with r.avaflow considering the Voellmy-type mixture model, with two sets of parameters in 10 simulations. A velocity between 6 $km\ h^{-1}$ and 50 $km\ h^{-1}$ and a travel distance between 100 m and 1200 m were estimated. Moncayo (2021), using a database of 199 landslides that occurred in the Andean region, developed an empirical-statistical multiple regression model to estimate the mobility of landslides, considering as dependent variables the travel distance, angle of reach, and the affected planimetric area.
Palacio et al. (2021b) simulated the cluster event occurred in the catchment of La Arenosa in 1991 (San Carlos, Antioquia). The hillslope landslide propagation was estimated with r.avaflow, using as source areas those determined with the model r.slope.stability (Mergili et al., 2014; Palacio et al., 2020). In the same catchment; Carmona Arango et al. (2021)

analyzed a series of connected events, evaluating the occurrence with TRIGRS (Baum et al., 2008). The propagation over the hillslope was modeled with Flow-R and the flash flood with IBER (Bladé et al., 2014). Palacio et al. (2021a, 2022) simulated 94 hillslope landslides triggered on March 31 (2017) in the basin area of the San Antonio Creek (Mocoa), using the semi-empirical model DebrisFlow Predictor, based on cellular automata and Flow-R. Many other studies have been developed by public entities as part of risk management in land use planning. Among them was carried out in Mocoa by the National Unit for Risk and Disaster Management (UNGRD, by its Spanish acronym), in which they report the simulation of the event that occurred on March 31, 2017, using r.avaflow (UNGRD and Universidad Pontificia Javeriana, 2017).

2.5 Risk management

According to UNGRD and Fundación Instituto Geofísico Universidad Javeriana (2016), 23256 events associated with disasters were recorded in Colombia between 2005 and 2014, including landslides, hurricanes, forest fires, flash floods, and droughts, among others. These events resulted in 3436 fatalities, affected 14.2 million people, and destroyed nearly, 58600 homes. Therefore, the government in its national plan for risk and disaster management (2015-2030) established objectives aimed mainly at improving and reinforcing knowledge in risk management, ensuring timely and adequate attention to disasters, and reducing the conditioning factors, all supported by existing legislation.

In 1989, Colombia through Law 9 began to introduce regulations for territorial administration and risk management. In the same year, Decree 919 organized the national system for disaster prevention and response; then Law 9 was modified by Law 388 of 1997 which established that all the country's municipalities must develop their respective land management planning. Through laws and decrees, regulations regarding land use planning were established over the years, but it was not until 2012, that Law 1523 established new provisions for risk management. Decree 1807 from 2014 regulates the incorporation of technical studies for risk management in land use planning, which is a relevant step for risk reduction for the population and infrastructure. In 2011 the Colombian government by decree 4131 changed the nature of the Colombian Institute of Geology and Mining giving origin to the current Colombian Geological Survey (SGC, by its Spanish acronym). Among the reasons for the reorganization of the entity is to deepen the basic scientific research and monitoring of geological hazards (unico de informacion normativa, 2011). As a part of its responsibilities, the SGC has developed to date three handbooks associated with risk management in land use planning to support Law 1523 from 2012, decree 1807 from 2014, and decree 1077 from 2015 (Division urban, city, and territory). The manuals generated are the guide for landslide hazard zoning at a scale of 1:25000 (2017), the guide for landslide hazard, vulnerability, and risk studies at a scale of 1:5000 (2016), and the most recent guide for debris flows hazard zoning at a scale of 1:2000 (detailed scale) and 1:25000 (basic scale) (2021).

Risk reduction measures and regulations for territorial development have advanced in the incorporation of empirical and physical mass flow propagation models. However, hillslope landslides remain considered mainly as a contribution of material for other processes, e.g., debris flows and flash floods. The SGC debris flow guide mentions different methodologies to determine the source zones and volumes of solids from hillslope landslides by modeling or geoenvironmental characterization but concerning the contribution of solids to debris flows it mentions, that is possible to propagate from points considered as source areas to the channel with hydrodynamic models or establishing points of solids contribution according to delimited areas. The SGC guidelines for the assessment of landslide hazard, vulnerability, and risk mention that the analysis should determine not only the areas of occurrence but also the areas that are potentially affected during propagation and deposition. That guide also recommends, in studies scale of 1:25000, geomorphological mapping, empirical methods, and the use of tools such as Flow-R for the calibration and validation of results obtained through landslide propagation modeling. In addition, it mentions that zones categorized with high susceptibility can be considered source areas in a propagation analysis. For hazard characterization, the analysis of the exposure of elements at risk, the guide for mass movements suggests estimating the travel distance by mainly geometric methods from regressions, derived from data from different locations worldwide. The correct selection of equations is complicated by considering factors such as the type of landslide, topographic conditions (obstruction), and confinement of the path. It is evident that propagation analyses depend on the information available and the scale of work, so it is necessary to improve and establish detailed and clear methodologies for the different scales. An important point in this respect is the suggestion of specific models and tools that support the simulation of hillslope landslide propagation, as was done in the recent hazard guide for debris flows. Considering both empirical and physical models, to reduce uncertainty regarding the delimitation of areas of hazard and risk.

This paper aims to provide an overview of some relevant models and the current state in the simulation of the propagation of flow-type landslides in Colombia, and their usefulness to predict the mobilization of SL – whether as single events or in clusters – that result in debris flows.

Acknowledgments

This review was developed within the framework of the project “Evaluación de amenaza por movimientos en masa y flujos torrenciales en ambientes tropicales y montañosos” (202010030246). Universidad Nacional de Colombia, campus Medellín. Geohazards research group

3 Empirical Modeling

This chapter was written with support of Edier Aristizábal, Martin Mergili and, Oscar Echeverrí.

Exploring best-fit parameters for propagation modeling of shallow landslides, using Flow-R

Abstract

Almost one-fifth of the Earth's surface is considered vulnerable to at least one natural hazard such as cyclones, droughts, floods, earthquakes, volcanoes, and landslides. Colombia, in terms of landslide risk level, is classified as medium to high. Historical records of landslide occurrence in the country between 1900 and 2018 found that rainfall was responsible for 87 percent of them. This research focuses on propagation of landslides of the shallow type triggered by heavy or prolonged rainfall. In the post-failure stage, Shallow Landslides (SL) can mobilize similar to other types of landslides, the mass accelerates, internal deformation occurs, and the change from slide to avalanche or flow tends to happen, and their mobilization changes from very rapid to extremely rapid, without response capacity. The majority of studies in the country focus on estimating the areas most susceptible to the occurrence of SL. But what happens when an SL propagates? This research focuses on empirical parameters for modelling SL using data from Clustered Shallow Landslides (CSL). Specifically, from SL occurred on March 31, 2017, in Mocoa, which resulted in approximately 306 fatalities. The modeling is carried out through the use of the empirical tool Flow-R, it requires little input information, the propagation is performed using different algorithms and friction laws, fundamental factors like the travel distance angle, velocity, and dispersion. Among the key achievements of this study is the identification of optimal parameters of modeling, including a maximum velocity of $10ms^{-1}$, a minimum travel distance angle of 15 degrees, and exponents "x" of 2 and 4. These parameters enhance our understanding of landslide propagation in tropical and mountainous contexts, which is essential for risk management in these areas. Additionally, the study highlights the relevance of impact probability thresholds, such as the 25% threshold, in risk management in tropical and mountainous environments. These

thresholds play a crucial role in delineating affected areas and are essential for land planning, balancing economic and social aspects in decision-making.

3.1 Introduction

Almost one-fifth of the Earth's surface is considered vulnerable to at least one natural hazard such as cyclones, droughts, floods, earthquakes, volcanoes, and landslides (Dilley et al., 2005). Landslides caused deaths, injuries, and damages each year around the world (Dai et al., 2002; Schuster, 1996; Kjekstad and Highland, 2009; Schuster and Highland, 2003). According to Nadim and Kjekstad (2009), Colombia is one of the countries with the highest landslide risk level, classified as medium to high, with an annual occurrence of $0.0125\% - 0.050\%$ per km^2. The Colombian Andean region is mountainous with steep terrain and corresponds to the northern part of the Andes mountain range. It is divided into three mountain ranges that rise in the south and cover one-third of the territory. Additionally, the region has a seasonal rainfall regime that is influenced by macro-climatic phenomena such as the Chocó jet, which transports a stream of moisture from the Pacific Ocean to the interior (Poveda, 2004). And by the intertropical convergence zone, where cloudiness and concentrated rainfall oscillate from south to north, causing rain in the March-May and September-November (Mesa et al., 2000; Guzmán et al., 2014). Furthermore, rainfall becomes more frequent and intense during the cold phase (*La Niña*) of the *El Niño*/Southern Oscillation (ENSO) (Poveda, 2004). These linked conditions; mountainous environments, and rainfall, contribute to the occurrence of landslides in the country.

Gómez et al. (2023) constructed the Unified Global Landslide Database (UGLD) unifying information between 1903-2020, by combining data from the disaster inventory system, the international disaster database, the global landslide catalog, and the global fatal landslide database. They indicated that in 37946 records, rainfall was responsible for 61.3% of landslides. According to the UGLD, Colombia has the highest number of landslides causing 1 to 10 fatalities (~ 1600), and ~ 150 landslides causing 11–100 fatalities. Furthermore, it has a landslide incidence of 10 per 1000 km^2. Aristizábal and Sánchez (2019) reviewed historical records of landslide occurrence in the country between 1900 and 2018 and found that rainfall was responsible for 87% of them.

The term "landslide" is defined as a movement of material mainly downward and outward, influenced by gravity (Cruden, 1991). It includes a broad variety of mass movements according to two characteristics; material (rock, earth, or debris) and movement (flow, topple, fall, slide, or spread) (Cruden and Varnes, 1996).This research focuses on propagation (runout) of landslides of the shallow type (depths less than 3 m), this type is triggered by heavy or prolonged rainfall events and occur on steep slopes (Moser and Hohensinn, 1983; Engelen, 1967; Campbell, 1974; Anderson and Sitar, 1995). These are describes by Varnes (1978) as a translational slide type of debris, rock, or soil occurring on shallow planar/undulated failure surfaces; their occurrence is often controlled by discontinuities, joints, or material changes –

between layers – on steep slopes.

In Colombia and worldwide, these landslides triggered by rainfall occasionally occur in clusters. According, to Crozier (2005) in these events, hundreds to thousands of landslides can be distributed over tens to thousands of square kilometers. They might occur in relative short time, ranging from minutes to days (Witt et al., 2010). The multiple occurrence of Shallow Landslides (SL), referred to in this study as Clustered Shallow Landslides (CSL), often results in loss of life, injuries, and damage to infrastructure. According, to historical records reviewed from 1990s in Colombia, CSL events occurred in San Carlos (1990), Fraile River basin (1994), La Estrella (2000), Tarazá (2007), Salgar (2015), Mocoa (2017), Anorí, Yalí, Suaza and Dabeiba (2020), Santo Domingo (2021), and Anorí (2023) (See Section 2).

In terms of spatial analysis, most studies in the country focus on estimating the areas most susceptible to the occurrence of SL. But what happens when a SL propagates? In the post-failure stage, SL can mobilize like other types of landslides, the mass accelerates, internal deformation occurs, and the change from slide to avalanche or flow tends to happen. Their mobilization changes from very rapid to extremely rapid, without response capacity (Hungr et al., 2001, 2014; Cascini et al., 2010; Cuomo, 2020). It is generally the propagation that causes the most damage, hence the need of estimating the potential areas affected by the moving masses, which is helpful in the hazard estimation.

Numerous methods and approaches have been developed to runout analysis of the failed mass. Hungr et al. (2005) split the runout methods in three main groups: (i) Analytical methods, that focus in the center mass of the sliding mass, this is concentrate in a single point without internal deformation, and motion is based on energy loss due to friction. (Dai et al., 2002; Quan Luna, 2012; Pirulli, 2005; Wang and Sassa, 2000b; Hutchinson, 1986). (ii) Empirical–statistical methods, to determine the travel distance, subgrouped by Hungr et al. (2005) in geomorphologically based on photo interpretation and fieldwork; geometrical approaches employing the travel distance angle and relationships; and volume change methods. (iii) Numerical methods perform more advanced analyses to learn about flow heights, velocities, and impact pressures. However, extensive geotechnical and rheological information is required (McDougall, 2017). This category is divided into two subgroups: continuum models based on the conservation of mass, energy, momentum, and physical laws (Quan Luna, 2012). And discontinuum models, where the material is represented by particles and motion is controlled by contact forces (Pastor et al., 2014).

This study is based on the modeling of CSL occurred due to heavy rainfall on March 31, 2017, in 3 basins of southwestern Colombia. Located in mountainous areas under a tropical environment. The most relevant aspect of using data from CSL is the possibility of having hundreds of landslides that occurred under the same triggering conditions and with geoenvironmental variability. Risk management studies generally delimit the areas susceptible to landslide occurrence, covering large areas. CSL propagation can be considered as the realistic representation of propagating all those areas simultaneously, thus delimiting the possible areas affected by landslide propagation from susceptibility data occurrence. The goal is

to present a more comprehensive view of the parameters that influence in SL propagation modeling and to explore the empirical parameters that best fit them. Through the use of the empirical model Flow-R, which requires little input information and fundamental factors are the travel distance angle, velocity, and dispersion. It estimates the propagation from predefined source areas using algorithms and frictional laws.
In order to build on this research. Initially, the length and height difference between the source area and the deposition zone were assessed for 178 of 233 landslides. They were also classified according to the average slope of the path in the direction of flow; to explore whether the observation of well-defined differences in travel distance angle parameter, may be properly represented in a grouped way. The analysis values are taken from the first and third quartiles, for velocity and travel distance angle, for each group in each basin. The collected data allow a set of simulations that are then compared and evaluated by validation metrics regarding the existing inventory.
The results provide values for the most relevant parameters in the empirical methodologies for propagation modeling of rainfall-triggered landslide in basins such as the one studied, characterized by rugged topography in a tropical environment. Also, establish the minimum probability of damage that can be considered in future studies

3.2 Study area

Mocoa is a Colombian municipality in the department of Putumayo, located in the southwest. It has a total area of 1263 km^2, of which 580 km^2 is urban. The research zone covers an area of 30.5 km^2 and includes the Mulato River, Sangoyaco River, and Taruca Creek basins. These streams are Mocoa River tributaries that flow mostly west-east from the eastern mountain range at 2344 $masl$ to plains located at 550 $masl$ (See Figure 3.1). In addition, these tributaries have the biggest impact on the urban area concerning to natural hazards.

3.2.1 Geological settings

Mocoa is located on the eastern flank of the northern Andes mountain range. To the east, it extends into the Amazonian foothills. As a result, its geological and geomorphological environment is diversified, ranging from high hills and steep V-shaped valleys in the west to fans, terraces, and plains in the east. The area features an active mountain front with a network of faults crossing north-south and east-west (SGC, 2017b). Locally, are present the Mulato, Campucama, Mocoa - La Tebaida, and Cantayaco faults. In addition, there are also the lineaments of the Taruca Creek and the Sangoyaco River.
The Campucama fault crosses through the northwest sector of the study area. However, the Mocoa - La Tebaida and Cantayaco faults are the most significant. They structurally split the area into three key zones. According to SGC (2017b, 2018b) the zones can be described as: (i) The transition zone between the eastern mountain range and the Amazonian foothills,

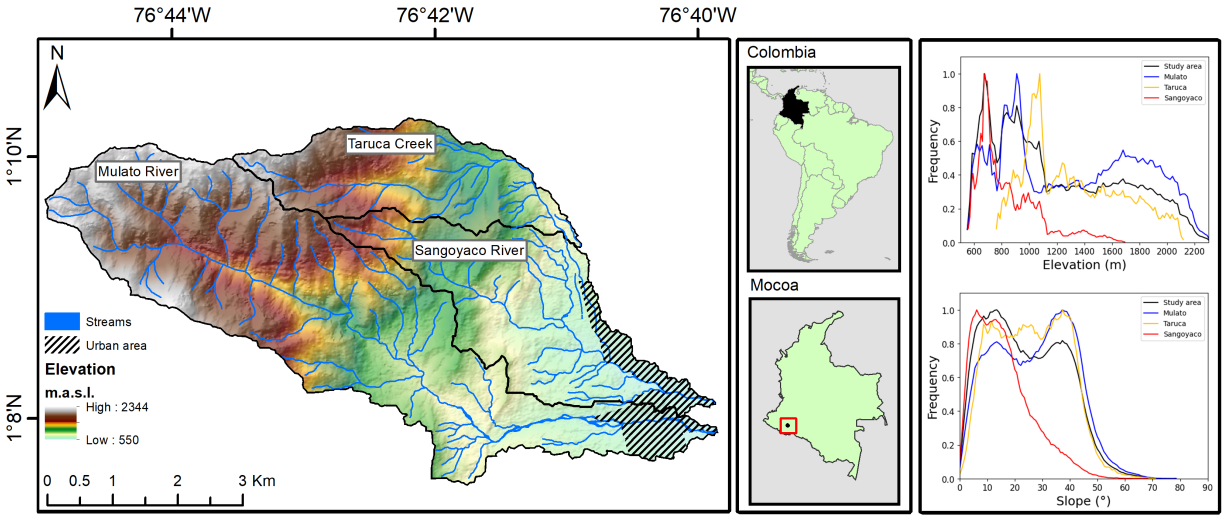

Figure 3.1: Location of the study area – Elevation and slope frequency of the study basins

where the highest slopes are found. The Mocoa Monzogranite igneous unit is found here. To the east, it evolves in a sequence of subunits of heavily fractured rocks of moderate to very low quality, up to the Mocoa - La Tebaida fault. Lower-quality zones present residual soils with up to 2 m thick and severely weathered blocks. (ii) The middle zone is located between the Mocoa - La Tebaida and Cantayaco faults. It is formed by a sequence of Cretaceous sedimentary rocks, where the Pepino and Orito group formations rise above the Rumiyaco formation. The Orito group consists primarily of mudstone and siltstone strata and may produce soils up to 1.5 m thick. The Pepino formation includes three layers, the upper is dominated by resistance to erosion and weathering conglomerates that generate sandy soils, mudstone dominate the middle. The Rumiyaco formation contains claystone with intercalations of fine conglomerates and sandstones, resulting in soils up to 2.5 m thick. (iii) The Rumiyaco formation rises above the Villeta formation in the lower zone due to the Cantayaco fault, and it is composed of mudstone that produce coarse-textured soils up to 1.5 m thick. This zone is generally covered with deposits and fans of the Mocoa tributaries and terraces of the Mocoa River (See Figure 3.2a).

3.2.2 Debris flow records

There have been approximately fifteen important natural hazard events, including floods, debris flows, mudflows and landslides, between 1947 and 2018. Table 3.1 show events related to debris flows that affected the urban area of the municipality. A representative event occurred in 1960. This was an event on the Taruca Creek, which had a slight impact where the urban area is currently located. Given the low population at the time, the loss of life and damage was minimum. It affected an area of about 30 ha, this is an event precursor of

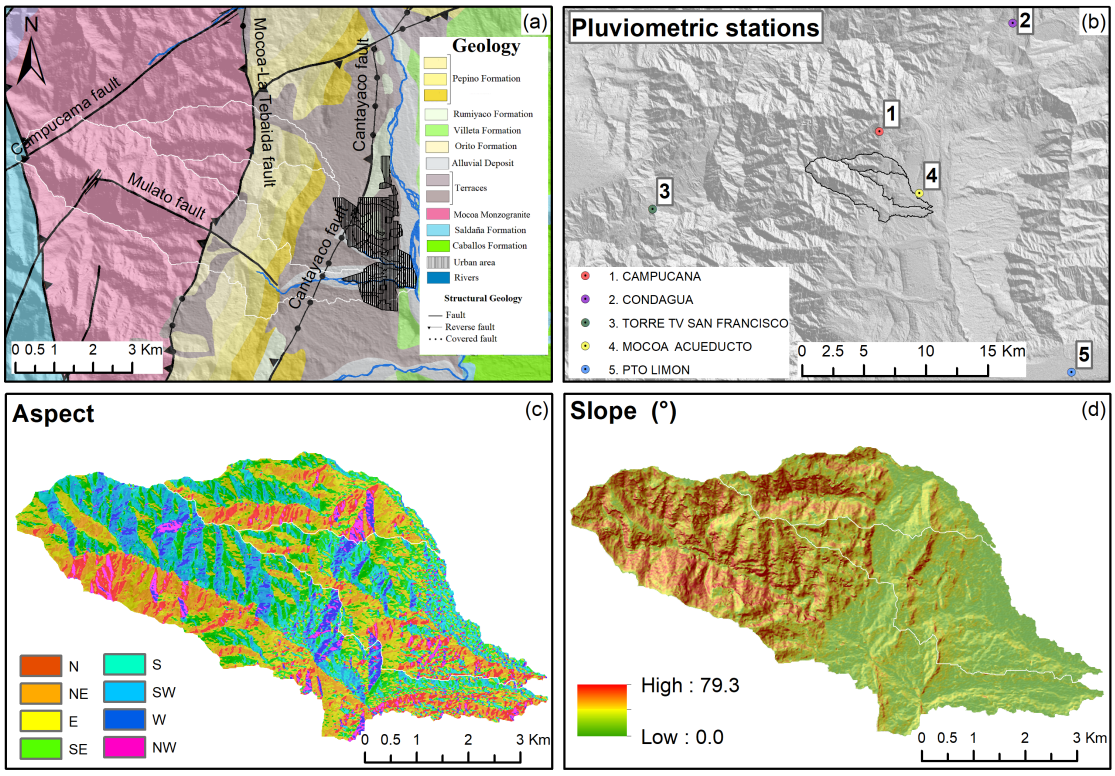

Figure 3.2: (a) Overall geological setting modified from Núñez Tello (2003), (b) pluviometric stations, (c) aspect and (d) slope

2017 event that cover ~ 50 *ha* in the same zone (SGC, 2017).

3.2.3 Rainfall characteristics

Mocoa has not defined dry season, and rainfall persists all year. However, has a highlighted rainy season from April to August, with up to 25 rainy days in May, June, and July (www.ideam.gov.co). Figure 3.2b shows the pluviometric stations of The Institute of Hydrology, Meteorology and Environmental Studies (IDEAM, by its Spanish acronym). The San Francisco (3000 masl) and acueducto (650 masl) stations represent the weather conditions on the eastern mountain range and lower zone in the Amazonian foothills, respectively. IDEAM records from 1985 to 2016. show that San Francisco station had a higher multiannual accumulated rainfall than Acueducto station, it has an average of 4673.7 *mm* respect to 3813.1 *mm* of Acueducto station. The monthly multiannual records also show higher accumulated rainfall for San Francisco station during the rainy season. Data indicate nonuniform rainfall distribution in the study area, since San Francisco station has fewer rainy days but most accumulated rainfall per day or event (See Figure.3.3).

Type	Year	Basin	Observations
Debris flow	1947	Mulato River	Landslides and damming
Mud flow and debris flow	1960	Taruca Creek	Pre-event 2017
Debris flow	1995	Taruca Creek	Landslides and damming
Debris flow	1998	Mulato, Sangoyaco and Mocoa rivers	Landslides and prolonged rainfalls
Debris flow	2014	Taruca Creek	Landslides
Mud flow and debris flow	2017	*	Landslides
Debris flow	2018	**	Landslides
*Taruca, El Carmen and San Antonio Creek - Mulato, Sangoyaco and Mocoa rivers			
**Taruca Creek - lower basin of Mulato and Sangoyaco rivers (Medina Bello et al., 2018)			

Table 3.1: Historical records of cascade events related to rainfall-triggered landslides in Mocoa. Modified from SGC (2017b)

3.3 31 March 2017 Debris flow

In 2017 between the night of March 31 and dawn on April 1, hours of rainfall triggered hundreds of landslides and chain processes over the urban area and nearby villages. Reports from the National Institute of Legal Medicine and Forensic Sciences 2017, up to April 6 (2017), about 306 dead people were identified. However, the press mentioned 322 deaths, more than 100 missing, and about 330 injured (RCN Radio, 2017). It was the propagation of biggest possesses like debris flow that caused the highest amount of damage over the population and infrastructure.

Figure 3.4 shows landslides occurrence distribution and debris flow impacted area. The event caused $\sim$ 276 hillslopes landslides,$\sim$ 70% of them supplied sediments to the drainage system directly (See Figure 3.5). According to Prada-Sarmiento et al. (2019) the processess presented were a debris flow along Taruca Creek, which was then converted into a hyperconcentrated flow in the Sangoyaco River and a mud flow in the Mulato River.

Records of Acueducto station on March 31^{st} show a peak precipitation at 23:00h of 62.8 mm. Hours later on the next day (1:00h) chain processes impacted the urban area. Accumulated rainfall during the event was $\sim$ 130 mm in three hours, Figure 3.3b shows how 130 mm only was exceeded 3 times according to the Acueducto station and 6 times in the San Francisco station. SGC (2018b) indicates that accumulated rainfall of 600 mm (38 days) in Acueducto station linked to accumulated rainfall during the event (130 mm) represents a return period of 25 years (SGC, 2017b). Figure 3.3d shows multiannual mean monthly precipitation. On March, 2017 pluviometric record exceeds 2016 record.

3.3.1 Landslide characteristics

Landslides triggered by rainfall generally presented planar failure surfaces and shallow depths, section 3.2.1 describes the thickness of some soils in the study area, which do not exceed 3 m. These shallow landslides can mobilize as other landslides-type (Iverson et al., 1998;

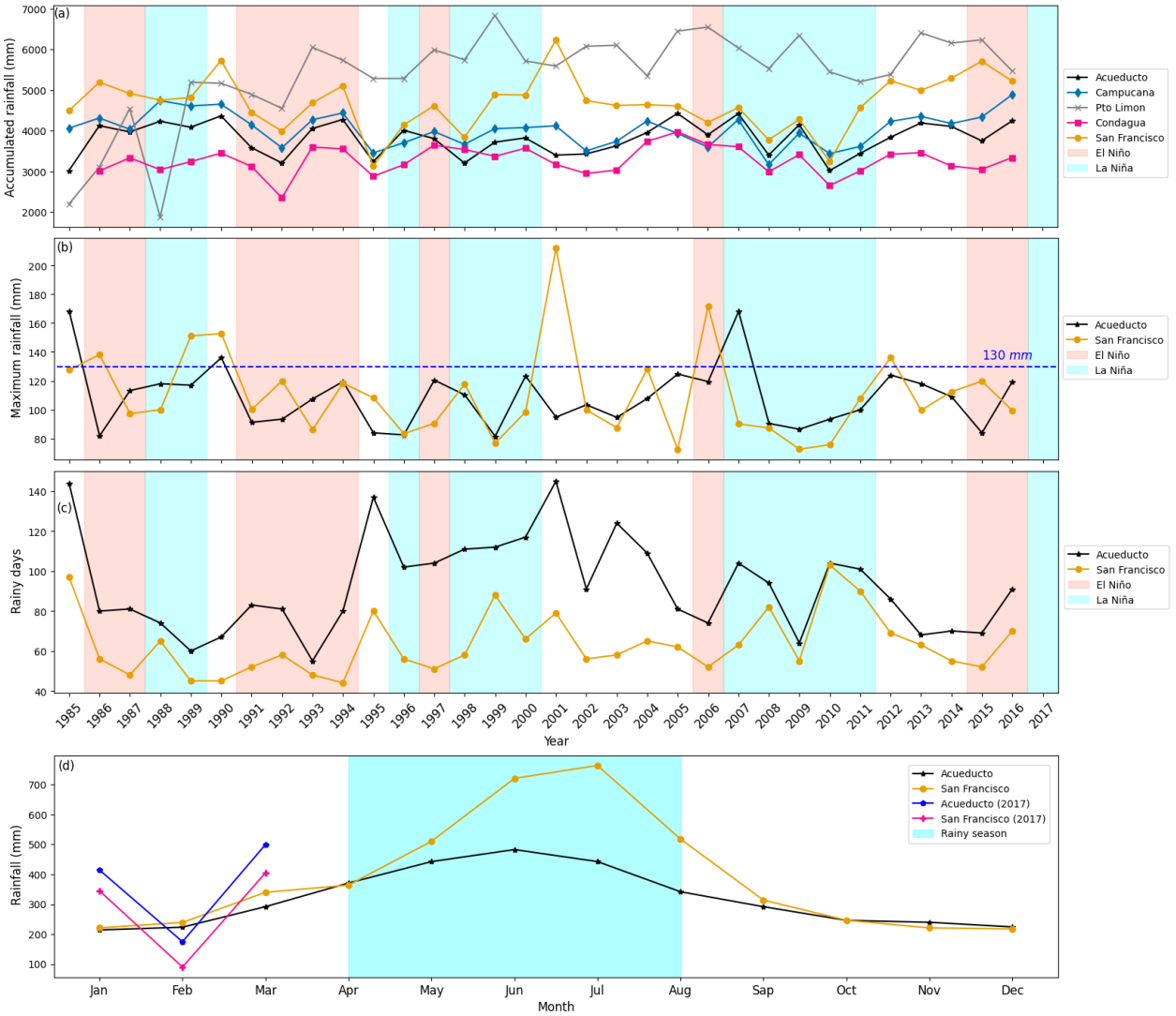

Figure 3.3: (a) Multiannual rainfall distribution from five pluviometric stations, showing ENSO seasons. (b) Maximum multiannual daily rainfall. (c) Multiannual rainy days. (d) Monthly multiannual rainfall distribution showing rainy season. Modified from SGC (2018a). Data provided by IDEAM

Caine, 1980; Mergili et al., 2012). Therefore, can be classified as a complex landslide and is difficult to predict its propagation. The inventory of $\sim$ 276 landslides (source areas) was carried out by SGC (2017b), of which 90% are classified as a debris flow. However, this research considers 233 landslides – not reactivated – detonated during the March 31 event. In the study area predominates slopes between 0° and 25° ; however, the occurrence of landslides is concentrated between 20° and 40°, in convex-convex areas and smaller concave-concave areas (See Figure 3.6).

In this section, we initially estimate and describe various characteristics related to terrain of

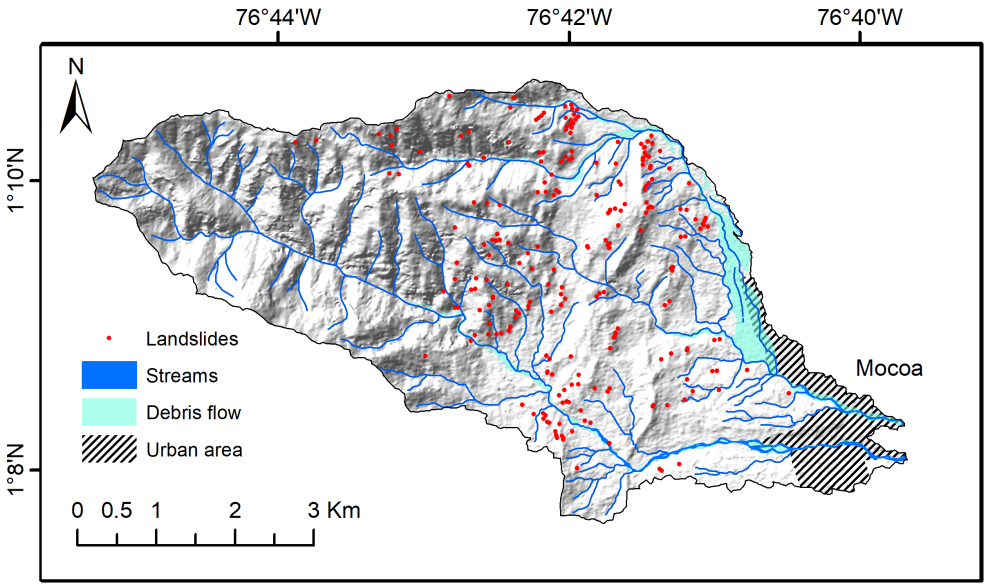

Figure 3.4: Landslide distribution and debris flow impacted area

Figure 3.5: Landslides and debris flow in study area. From Corpoamazonia.

the affected areas, as well as their distribution within each of the basins. Using the collected and processed information, we estimate and explore geometric parameters for a total of 178 landslides in the study area. The parameters include velocity and travel distance angle, which

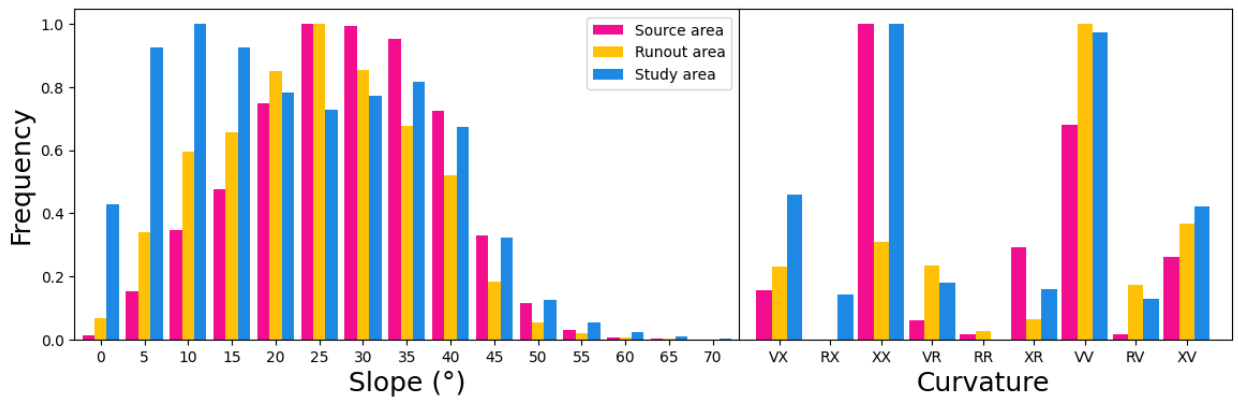

Figure 3.6: Frequency slope and curvature for source, runout, and study area. Convex (X), concave (V) and Planar (R)

are significant factors in landslide modeling using empirical approaches. These analyses have provided us with initial and notable findings concerning the parameterization of this type of landslides in high mountain basins within tropical regions.

Despite being the smallest basin, Taruca Creek accounts for 39% of all landslides, followed by the Mulato River (36%), and the Sangoyaco River (24%). Seventy percent of the landslides occur between 800 and 1200 *masl*, which corresponds to the central band of the Pepino Formation, Orito Group, and Mocoa Monzogranite. 37% of the landslides occurred in the Mocoa monzogranite, with 27% occurring in an adjacent subunit of the Mocoa - La Tebaida fault; this subunit consists of relatively low-quality rocks that are heavily weathered and fractured. This zone is also characterized by an abrupt change in slope at the transition between the eastern cordillera and the Amazonian foothills. In the upper Pepino Formation, 18% of the landslides occurred; this unit presents slopes with cuts of up to 90 degrees in medium-quality, weather-resistant conglomerates; in the entire formation, 30% of landslides occurred. In the Orito group, 19% of the landslides occurred. Figure 3.7) illustrates the estimated correlation between volume and area, as well as height and length, for 178 of the 233 included in the inventory. To calculate volume, we considered the area covered by the source area and the depth of the geological unit. Additionally, we estimated the height and horizontal length from the source to the deposit area for each SL. The majority (54%) have a length of less than 100 m. When classified according to Fell (1994) criteria, 60.5% of the landslides are extremely small with a volume of less than 500 m^3. Another 36.4% are classified as very small, with volumes ranging from 500 m^3 to 5000 m^3, while 3.1% are considered small, with volumes ranging from 5000 m^3 to 50000 m^3.

Travel distance angle

In 1932, Heim introduced the concept of *fahrböschung* also known as the angle of reach or travel distance angle (Corominas, 1996). This angle, as defined by Hungr et al. (2005), is a

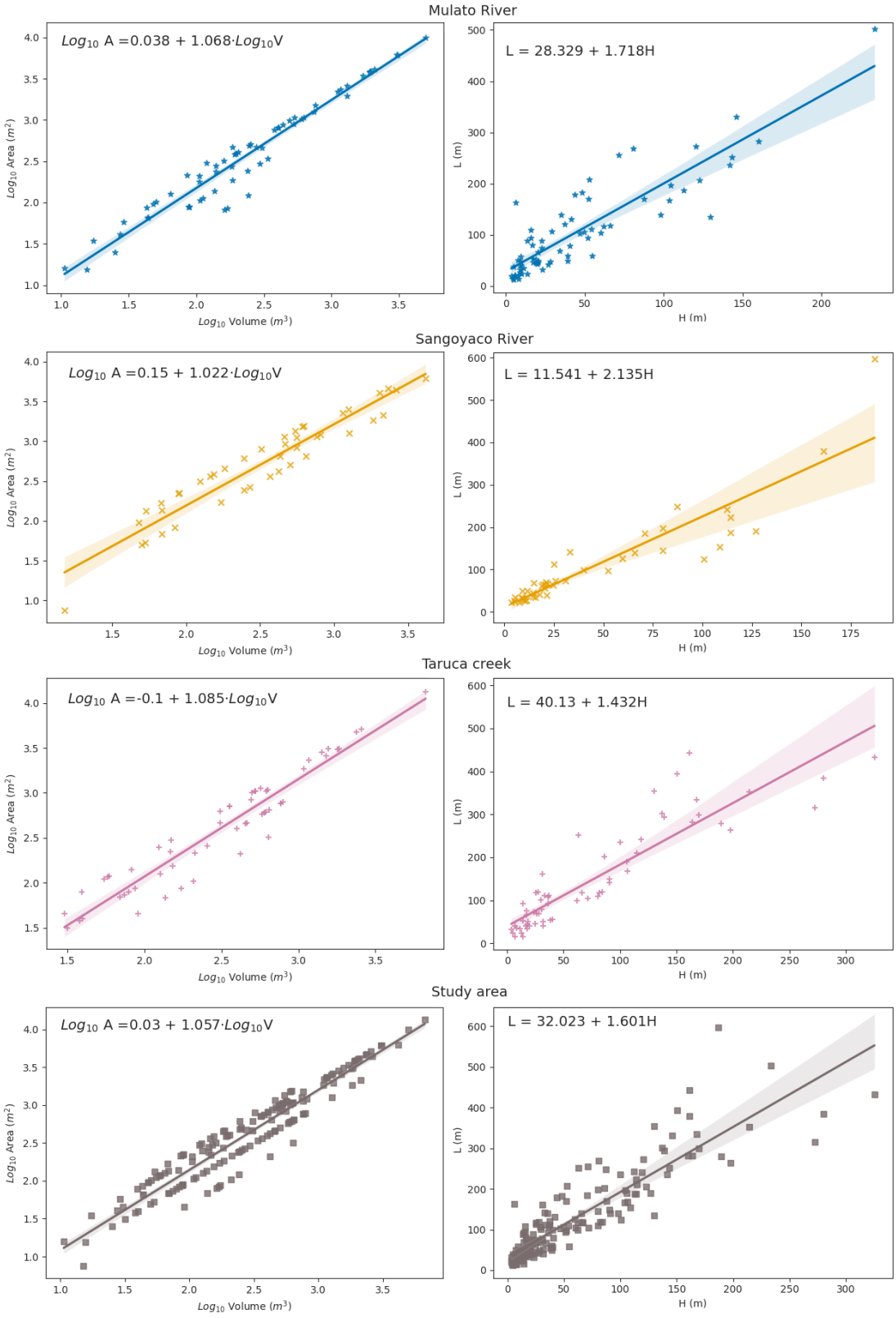

Figure 3.7: Correlations, volume – area (left) and height – length (right)

key parameter in many empirical methods used for estimating runout path. It is calculated as the angle connecting the points from the source area to the endpoint of the deposition area. Mobility, on the other hand, is expressed as the ratio between the vertical height (H), which represents the elevation difference between these points, and the horizontal distance (L) (Corominas, 1996; Hungr et al., 2005; Hunter and Fell, 2003). See equation 3.1 for travel distance angle and graphical representation in Figure 3.8.

$$\tan \alpha = \frac{H}{L} \tag{3.1}$$

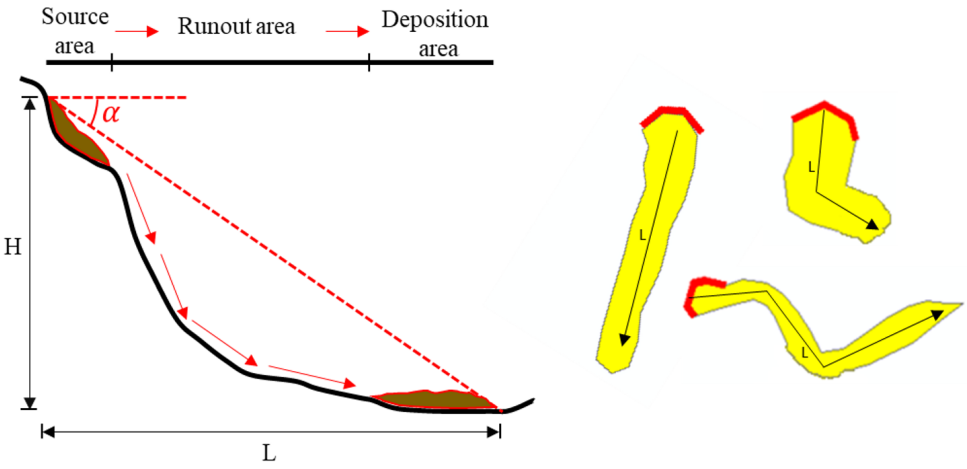

Figure 3.8: Schematic illustrations of travel distance angle and path lenght of landslides

For 178 source areas, which are part of the total 233 in the inventory, we determined the trajectory, length, and elevation of both the scar and the deposit at their lowest points. The estimated travel distance angles for these areas exhibit a wide distribution of data. In the Mulato River Basin, the travel distance angles range from 2.1° to 43.9°, and an average of 21.8°. Taruca Creek has the highest average travel distance angle, which is 24.7°, with data distributed between 6.4° and 41.8°. In the Sangoyaco River, the range is from 8.9° to 38.9° and a mean of 20.7°. It's important to note that higher values in the H/L ratio indicate a larger travel distance angle. For instance, a landslide with an elevation difference of 50 m and a horizontal runout length of 100 m would result in a travel distance angle of 26.6°. When L greatly exceeds H, it is associated with low travel distance angles, whereas when H significantly exceeds L, it is related to larger travel distance angles.

Velocity

The velocity of a landslide plays a significant role in its destructive power, estimating it accurately can be challenging. The velocity classification presented by International Union of Geological Sciences Working Group on Landslides (1995) is based on damage, exposed

elements, and loss of life, with typical velocities ranging from 16 $mm\ year^{-1}$ to 5 $m\ s^{-1}$ for extremely rapid movements. Debris flows, as described by Hungr et al. (2014) fall into the category of very rapid to extremely rapid movements, characterized by zero response capacity. For indirect estimation of debris flow velocity, various equations have been proposed. In this study, using the same dataset mentioned in section 3.3.1. We use the equation by Te Chow (1959), which calculates the velocity v, based on the height difference between the source and deposit (Δh) and the gravity g. (See equation 3.2).

$$v = \sqrt{2g\Delta h} \tag{3.2}$$

The equation, 3.2 indicates that landslides with greater values of Δh tend to exhibit higher velocities. For landslides, modelling similar to SL, Horton et al. (2013) suggests a limiting velocity of 15 $m\ s^{-1}$ for modeling in Flow-R. On the other hand, there are higher velocities that reach up to 70 $m\ s^{-1}$, observed in several events and reported by International Union of Geological Sciences Working Group on Landslides (1995). Based on the results obtained, the Taruca Creek basin has the highest recorded velocity at 80 $m\ s^{-1}$. In comparison, the Mulato and Sangoyaco rivers have maximum velocities of 68 $m\ s^{-1}$ and 61 $m\ s^{-1}$, respectively. On average, landslides in these basins tend to have velocities of approximately 27 $m\ s^{-1}$. Notably, the Taruca Creek basin stands out with an average velocity of 34 $m\ s^{-1}$, suggesting that the landslides in this basin typically involve the highest values of Δh.

3.4 Data and methods

Predicting the propagation of mass flows is a complex process. Generally, approaches to modeling mass flow propagation are based on empirical methods and complex physically based models. The latter, which are more advanced but also more data-intensive, require detailed information about the unstable mass, geotechnical (soil properties) parameters and sometimes rheological information (flow behavior). CSL data provide valuable insights into the occurrence and propagation of many landslides, representing a useful inventory of individual SL that occur under similar conditions within the same basin. The methodological steps follow, in this research for identifying runout, start with collecting the input data. This includes utilizing a digital terrain model (DTM) derived from a 5 m spatial resolution GEOSAR image, which has been processed and adjusted by SGC (2017b) for investigations of the event occurred on March 31 in Mocoa. The inventory of landslides (source areas) was carried out by SGC (2017b).

Section 3.3.1 provides a comprehensive description of various landslide features. Additionally, sections 3.3.1 and 3.3.1 focus on estimating the travel distance angle and velocity, based on the data collected. These parameters play a crucial role in governing the empirical model's simulations. In the section 3.4.1 the landslide inventory is categorized into four groups based on average flow path slope. These groups are denoted as G1: $0°-20°$, G2: $20°-30°$, G3: $> 30°$

and G4: comprising all data. The modeling process in each basin includes simulations for these individual groups as well as for the total inventory. Section 3.4.2 explains in detail the theoretical foundations and requirements for modeling using the Flow-R model. Finally, Section 3.4.3 establishes the parameters necessary for modeling, setting the stage for the presentation of results in Section 3.5. This latter section also outlines the validation criteria applied to assess the accuracy and reliability of the modeling outcomes.

3.4.1 Data groups

In this study, the modeling of SL propagation is carried out using four distinct data groups within each basin. One group includes "All data", while the other groups classify landslides based on average slope of the flow path in the direction of movement. Exactly, the classifications are as follows: G1: $0° - 20°$, G2: $20° - 30°$, G3: $> 30°$, representing low, medium, and high slopes, respectively.

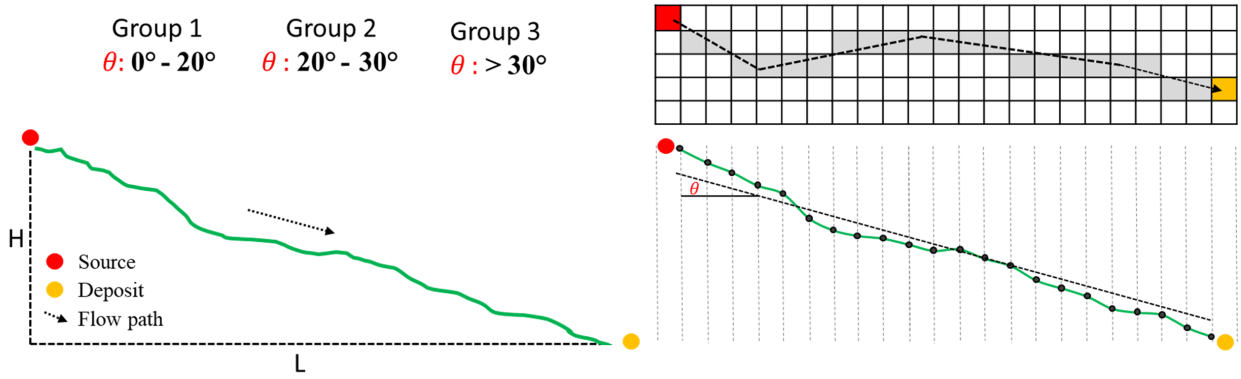

Figure 3.9: Schematic average flow path slope – angle θ

The purpose of inventory grouping is to investigate whether distinct differences in the travel distance angle parameter can be appropriately represented through classification. Table 3.2 shows the mean and first and third quartile values for travel distance angle and velocity within each of the groups. These values are utilized in Section 3.4.3 to establish the parameterization range.

3.4.2 Flow-R model

Flow-R is an empirical spatial distribution model introduced by Horton et al. (2013) for flow path assessment of gravitational hazards at a regional scale without dependency on many inputs for modeling. The latest free version 1.0.0 runs under MATLAB® compiler runtime 2022a. The fundamental inputs include DTM. From this DTM, numerous morphometric features can be computed to initially identify source areas and subsequently estimate the propagation.

Basin	Data	Count	Travel distance angle(°)			Velocity ($m\ s^{-1}$)		
			mean	Q1	Q3	mean	Q1	Q3
Mulato	All	71	22	15	29	27	16	34
	G1	16	12	9	16	14	11	17
	G2	23	20	15	23	20	14	24
	G3	32	28	25	31	38	29	47
Taruca	All	63	25	19	32	34	19	47
	G1	12	13	11	14	20	12	24
	G2	16	21	18	23	24	18	27
	G3	35	30	26	35	44	28	56
Sangoyaco	All	44	21	17	25	27	16	38
	G1	8	14	10	16	14	10	17
	G2	20	19	17	22	23	17	22
	G3	16	27	22	29	38	31	47

Table 3.2: Travel distance angle and velocity statistics per group

The model is essentially split into two modules that can be employed separately. (i) Susceptibility analysis to identify source areas primarily based on geomorphological features like curvature, accumulated flow, geology, slope, land cover, and other factors chosen by the user. It takes into consideration whether conditions are favorable or unfavorable for initiation. (ii) The propagation from the source areas, it uses various algorithms and friction laws. This study concentrates on the propagation aspect.

Flow direction algorithms

The model implements several directional algorithms, and their advantages and disadvantages are discussed by Horton et al. (2008). These include D8 (O'Callaghan and Mark, 1984), D∞ (Tarboton, 1997) , Rho8 (Fairfield and Leymarie, 1991) , and multidirectional flow algorithms of Quinn et al. (1991), Freeman (1991) and Holmgren (1994). Nevertheless, due to its capability to provide a more realistic downslope flow distribution, Holgrem's algorithm is the preferred choice (Kappes et al., 2011). In addition, the algorithm includes an exponent "x" that enables control over the propagation process. This allows parameterization of the modeling, which is not possible with the other algorithms. A value of $x = 1$ represents multidirectional spreading, while a value of $x \to \infty$ tends to unidirectional flow, see Equation 3.3.

$$p_i^{fd} = \frac{(\tan\beta_i)^x}{\sum_{j=1}^{8}(\tan\beta_j)^x} \qquad \forall \begin{cases} \tan\beta > 0 \\ x \,\epsilon\, [1, +\infty) \end{cases} \tag{3.3}$$

Where i, j are the flow directions, P_i^{fd} is the susceptibility flow proportion in direction

i, $\tan\beta_i$ is the slope gradient between the central cell and the cell in direction i, and the variable exponent "x". Horton et al. (2013) proposes a variation to Holgrem's algorithm that considers a correction factor "dh", this changes the height (m) of the central cell, so the flow can reach the neighboring cells. This is especially useful in high-resolution DTM where elevation differences between cells in the 3×3 array are small.

Persistence function

The model does not consider the mass of the source areas, and thus, it does not require information about height and density. The persistence function seeks to reflect the inertial behavior of the material based on changes in direction from the previous direction, see Equation 3.4.

$$p_i^p = w_{\alpha(i)} \tag{3.4}$$

Where p_i^p is the flow proportion in the direction i, and $w_{\alpha(i)}$ is the weight proportions considering the angle α between the previous direction and the direction from the central cell to next cell i. Weights are assigned according to direction and persistence functions, that they are Cosines that consider $w_{0,45}$, proportional with $w_{0,45,90}$ and a third one based on Gamma (2000) that considers $w_{0,45,90,135}$, in all function $w_{180} = 0$ because is the opposite direction of flow and it is not possible.
Horton et al. (2013) presents in the Equation 3.5 the general spreading algorithm that combines flow direction and persistence function.

$$p_i = \frac{p_i^{fd} p_i^p}{\sum_{j=1}^{8} p_j^{fd} p_j^p} p_0 \tag{3.5}$$

Where i, j are the flow directions, p_i is the susceptibility value in direction i, p_i^{fd} is the susceptibility flow proportion in direction, p_i^p i the flow proportion according to the persistence, and p_0 the previously determined susceptibility value of the central cell.

Runout distance assessment

Since the mass of the source area is unknown, the runout distance is controlled for frictional laws (energy loss function) in a unitary energy balance. Furthermore, lateral spreading is limited; if there is no sufficient energy, the neighboring cell cannot be reached (Equation 3.6).

$$E_{kin}^i = E_{kin}^0 + \Delta E_{pot}^i - E_f^i \tag{3.6}$$

Where E_{kin}^i is the kinetic energy of the cell in direction i, E_{kin}^0 is the kinetic energy of the central cell, ΔE_{pot}^i is the change in potential energy to the cell in direction i, and E_f^i is the energy lost in friction to the cell in direction i.

Two models are used by Flow-R to calculate friction loss. (i) Perla et al. (1980), similar to Voellmy (1955), based on a coefficient of friction and mass-to-drag-ratio, and (ii) a simplified friction-limited model that calculates the maximum distance reached based on the minimum travel distance angle and maximum velocity as an energy limitation (Equation 3.7).

$$E_f^i = g\Delta x \tan\varphi \tag{3.7}$$

where E_f^i is the energy lost in friction from the central cell i to the cell in direction i, Δx the increment of horizontal displacement, $\tan\varphi$ the gradient of the energy line, and g the acceleration due to gravity.

Propagation process

Explaining briefly the process used by Horton et al. (2013). The spreading of one active cell is estimated, and if other cells are reached are added to the active cells list. The active cells list is an array of cells that are considered with energy not null and will continue to propagate. The evolution of the propagation from the source area is saved and, other cells become inactive as a result. Some active cells will be overlaid, and the sum of susceptibility values and the maximum energy values will be saved in this case. After completion of the propagation process from a specific source area, the results are stored. The final output is a composite of all these individual propagations originating from various source areas.

3.4.3 Modeling parameters

The parameter selection for modeling is shown in Table 3.3. In all tests, the direction algorithm has a correction factor of $dh = 2$. Horton et al. (2013) contrasts different dh values and DTM resolutions; in the test using $dh = 2$, the propagation covers slightly more susceptibility area than with $dh = 0$ or 1, particularly in the inner zones. For the exponent "x", Holmgren (1994) proposes values between 4 and 6. Considering that, the propagation is multidirectional for $x \sim 1$ and unidirectional for $x \to \infty$. The values $x = 2, 4$, and 8 are selected.

Rule	Selection	Value
Direction algorithm	Holmgren (1994) modified	dh= 2, exponents x = 2, 4 and 8
Inertial algorithm	Weights	Gamma (2000)
Friction loss function	Minimum travel distance angle, SFLM	See table 3.4
Energy limitation	Maximum velocity	See table 3.4

Table 3.3: Parameters used to modeling with Flow-R

For energy limitation, Horton et al. (2013) recommends setting a maximum velocity of 15 $m\ s^{-1}$. Some researchers have implemented a minimum travel angle of $\sim 7°$ (Zimmer-

mann et al., 1997) and $\sim 11°$ (Huggel et al., 2002; Rickenmann and Zimmermann, 1993; Haeberli, 1984; Zimmermann et al., 1997). However, the specific range of values employed in this study is derived from the estimates provided in section 3.3.1 and 3.3.1. Table 3.4 summarizes the values chosen for the minimum travel distance angle and maximum velocity, which were determined for each group based on the first and third quartiles.

Data	**Parameter**	
	Minimum travel distance angle (°)	Maximum velocity ($m\ s^{-1}$)
All	9, 11, 15, 19, 24, 27	10, 15, 20, 25, 30
G1	9, 11, 13, 15	10,15,20
G2	15, 17, 19, 22	15, 20, 25
G3	24, 27, 30, 33	30, 35, 40

Table 3.4: Values of parameters used in modeling

Validation metrics

The chosen validation metrics for identifying the best-fit parameters are outlined in Table 3.6. As described by Fawcett (2005), the metrics for assessing model performance consider four possible scenarios, reflecting the comparison between model predictions and actual observations. In our case, these scenarios can be defined as follows:

- True Positive (TP): Areas that were impacted and correctly identified as impacted in the simulation
- True Negative (TN): Areas that were not impacted and correctly identified as non-impacted in the simulation
- False Positive (FP): Areas that were not impacted but incorrectly identified as impacted in the simulation
- False Negative (FN): Areas that were impacted but incorrectly identified as non-impacted in the simulation.

These parameters together constitute the confusion matrix, which forms the basis for evaluating performance.

The imbalance between impacted and non-impacted areas presents a notable challenge, with non-impacted areas significantly outnumbering the impacted ones, as is reflected in the simulation results where TN >> TP. Some validation metrics, that take TN into account, tend to skew the evaluation toward the prediction of non-impacted areas rather than assessing

Parameter	Definition	Range	Optimum
Factor of conservativeness (FoC)	$\frac{TP+FP}{TP+FN}$	$[0, \infty]$	1.0
Recall (TPr)	$\frac{TP}{TP+FN}$	[0,1]	1.0
Precision (PPV)	$\frac{TP}{TP+FP}$	[0,1]	1.0
F1-Score	$2 \cdot \frac{precision+recall}{precision \cdot recall}$	[0,1]	1.0

TPr: True positive rate **PPV**: Positive predictive value
TP: True positive **FP**: False positive **FN**: False negative

Table 3.5: Validation criteria

the prediction of impacted areas accurately. Consequently, we have selected metrics that are not influenced by the TN (See Table 3.5). One of the key metrics chosen is the Factor of Conservativeness (FoC), which indicates the degree of conservatism in the obtained results, FoC values less than 1 suggest non-conservative results, while values greater than 1 indicate conservative results. An FoC value close to 1 is considered optimal. Additionally, we use metrics like Recall or True Positive rate (TPr), which measures the predictive accuracy of positive cases, and Precision also known as Predictive Positive Value (PPV), which represent the proportion of correctly identified impacted areas among the total number of identified positives. The F1-Score, another important metric, combines the assessment of precision and recall to provide an overall accuracy measurement.

3.5 Results

Multiple simulations were conducted based on the parameter configurations presented in Table 3.4. These parameter settings were determined in accordance with the criteria delineated in sections 3.4.1 and 3.4.3. The propagation results stemming from these Flow-R simulations, conducted for each group within every basin, manifest as a array of impact probabilities spanning the range of 0 to 1. For each simulation, metrics were systematically evaluated in increments of 0.05. The process of selecting best-fit parameters involved identifying combinations of high F1-Score values, indicative of precision and predictive capabilities, and a FoC value hovering around 1. The final parameter selection corresponds to the probability of impact, wherein the best-fit parameters were selected.
Table 3.6 presents the consolidated results obtained; the results for each of the basins are described below. Figure 3.10 shows the simulation results related with the best fit parameters as determined by validation metrics for the Mulato basin. The cut-off probability of impact

Basin	Data	Parameters x, Min angle, Max vel	Cut-off Probability (%)	Recall	Precision	FoC	F1-Score
Mulato	All	4, 15, 10	25	0.466	0.477	0.98	0.47
	G1	4, 19, 20	30	0.261	0.253	1.03	0.26
	G2	2, 19, 15	20	0.356	0.333	1.07	0.34
	G3	8, 24, 30	25	0.480	0.433	1.11	0.46
Taruca	All	2, 15, 10	25	0.438	0.439	1.00	0.44
	G1	4, 15, 10	15	0.228	0.221	1.03	0.22
	G2	2, 19, 15	25	0.328	0.320	1.03	0.32
	G3	4, 30, 30	25	0.449	0.440	1.02	0.44
Sangoyaco	All	2, 15, 10	25	0.489	0.477	1.03	0.48
	G1	4, 9, 10	40	0.450	0.350	1.29	0.39
	G2	8, 19, 20	25	0.385	0.374	1.03	0.38
	G3	4, 24, 30	25	0.413	0.418	0.99	0.42

Table 3.6: Best fit parameters

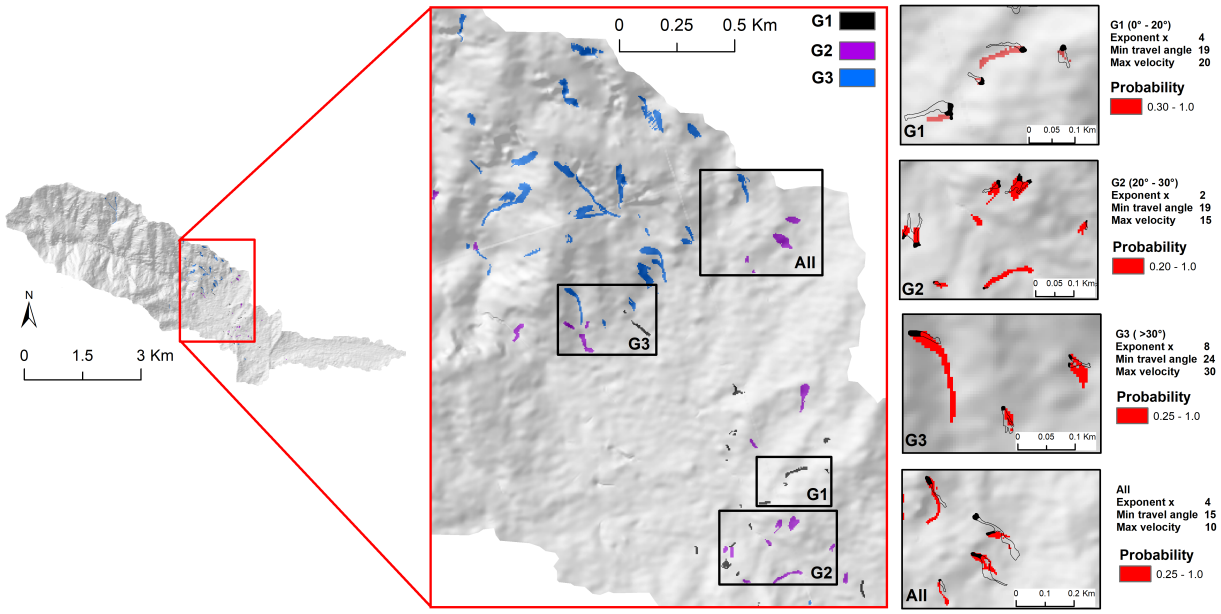

Figure 3.10: Modeling and best-fit parameters - Mulato River

is consistent across different groups, ranging between 20% and 30%. The group with the highest validation criterion achieved an F1-Score of 0.47, which corresponded to modeling all source areas in a single simulation, This is followed closely by a score of 0.46 for the G3; While these two groups exhibit similar metric values, the best-fit parameters differ.

The simulation encompassing all source areas is characterized by a maximum velocity of 10 $m\ s^{-1}$ and a minimum travel distance angle of 15°; these parameters are close to values found in the first quartile (15 $m\ s^{-1}$ and 16°) and those propose by Horton et al. (15 $m\ s^{-1}$ and 11°). The exponent "x" varies across all groups, for all source area propagations, this

value falls within the range suggested by Holmgren, which spans from 4 to 6. In the case of G3, where the average slopes of the propagation trajectories exceed 30°, $x = 8$ provide better a best-fit, indicating unidirectional flows patterns. Meanwhile, $x = 2$ corresponds to the G2 group, reflecting a multidirectional flow trend. In summary, modeling all source areas within a single simulation for the Mulato River basin not only yields the best metrics, but also results that closely align with values documented in the reviewing literature.

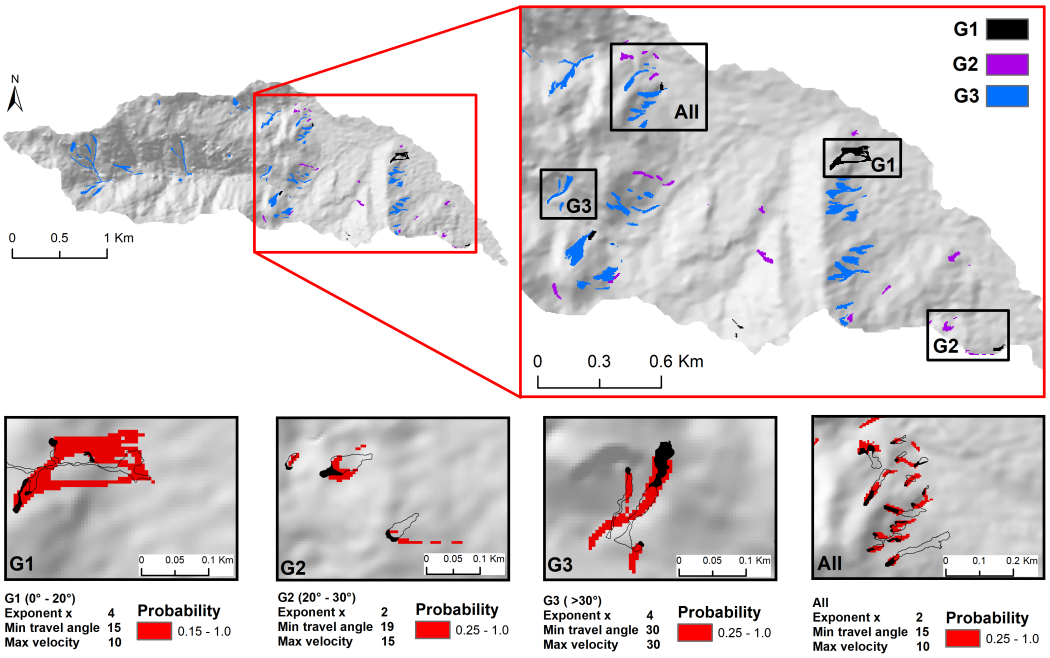

Figure 3.11: Modeling and best-fit parameters - Taruca Creek

For Taruca Creek, as shown in Figure 3.11, an F1-Score value of 0.44 was determined for the simulations involving all 65 source areas in the inventory, as well as for the G3, which is composed of 35 source areas, while G1 group has the lower F1-Score of 0.22. The cut-off probability is set at 25% for all groups, except for G1 group set at 0.22. The exponent "x" takes values on 2 and 4, with multidirectional flow represented by $x = 2$ in the simulation involving all source areas. The maximum velocity and minimum travel distance angle parameters are both set at 10 $m\ s^{-1}$ and 15°. It's worth noting that these parameter values differ from those in the first quartile.

In the case of Sangoyaco River, as shown in Figure 3.12, the best-fit parameters exhibit greater variability. Overall, the F1-Score is high for all simulated groups compared to the other basins. However, the "All" group achieves the highest F1-Score of 0.48 with a probability of 25%. G2, which includes 20 of the 44 source areas in the basin, shows a considerably different cutoff probability of 40%.

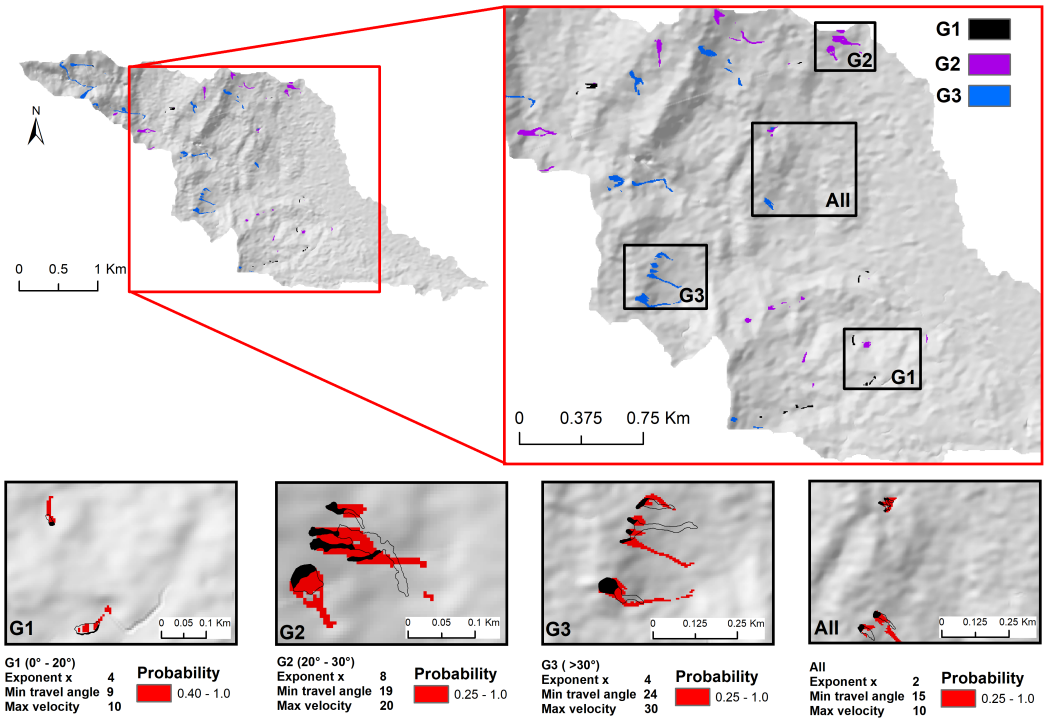

Figure 3.12: Modeling and best-fit parameters - Sangoyaco River

3.6 Discussion

Models based on empirical methodologies offer practical advantages in terms of the required data and the scale of analysis. The Flow-R model, which primarily relies on geometric approaches and empirical rules, facilitates landslide runout simulations. However, it's crucial to emphasize that the modeling parameters used in this study underwent thorough exploration and parameterization in an area with distinct geoenvironmental characteristics in the Colombian Andes. This underscores the need for adapting and fine-tuning modeling parameters to suit specific geoenvironmental conditions.

The estimated travel distance angles for modeling, when considering grouped data, differ to the values indicated in the literature, which typically range from around $\sim 7°$ and $\sim 11°$ (Huggel et al., 2002; Rickenmann and Zimmermann, 1993; Haeberli, 1984; Zimmermann et al., 1997). In the study area, the mean travel distance angle exceeds 20°. Among the six values tested within the range of 9° to 27°, the best results were obtained with a travel distance angle of 15°, which was slightly lower than the established mean, and near to literature values

Regarding maximum velocity, Horton et al. (2013) suggests a limiting velocity of 15 $m\ s^{-1}$; the velocities taken into account for modeling were estimated based on the elevation difference between the source and the deposit, and estimated velocities exceeded the suggested. On the other hand, the modeling results indicated that the velocity that best fits the simu-

lations is 10 $m\ s^{-1}$, which is slightly lower than the suggested velocity.
According to the validation criteria, the most suitable approach is to model all source areas in a – "All" group – single simulation. When data is grouped, especially in basins like Taruca Creek, it leads to lower F1-Score values, with values as low as 0.22. Numerous factors influence landslide propagation. Initially, grouping data may appear to be a well approach to modeling. However, this approach does not effectively capture the complexities of actual landslide propagations. It is evident that grouping data based on the average slope of the flow path is not a relevant criterion. Additionally, the best-fit parameters in these groups (G1, G2, and G3) vary significantly across different basins
The study area encompasses a diverse terrain, ranging from mountains in the west to plains in the east. Topography plays a crucial role in influencing the runout of landslides, as discussed by Corominas (1996). In this investigation, a DTM with a resolution of 5 m x 5 m was employed in this investigation. It's important to note that since the landslide modeling process heavily relies on algorithms that consider topography for mobility, the quality of the DTM used significantly impacts the accuracy of the results. To enhance the precision of the modeling results, a correction factor dh was applied. However, it's worth mentioning that the impacted areas may not always match perfectly with the estimated ones, due to quality in the available DTM data. Furthermore, various factors such as cover and the presence of obstructions, which can change relatively over time, also influence landslide mobility. For instance, the vegetation in the study area experienced a significant reduction in 2016, can be attributed to the effects of *El Niño* (Qiu et al., 2007). In future studies conducted in the Colombian Andes, using a more precise and up-to-date DTM will help reduce uncertainty in the established modeling parameters and improve the accuracy of landslide propagation simulations
The analysis considered three different values for the exponent "x" proposed by Holmgren (1994) to study landslide propagation. The values $x = 2,\ 4$ and 8 were explored to understand the dynamics of propagation. The results indicated that for accurate modeling of landslide propagation, it is important to consider relative variations in direction, with reference to the fact that values close to $x \sim 1$ indicate multidirectional flow and $x \to \infty$ represents unidirectional flow. In areas such as the Taruca Creek and Sangoyaco River, landslides propagation is characterized by constant change of direction, $x = 2$ represents the data. On the other hand, in the Mulato River basin, many landslides occurred in areas with smoother topography, an "x" value of 4 provided a better fit to the data. Additionally, the results revealed that short propagations, especially those closer to riverbeds, tended to exhibit unidirectional flow characteristics. This analysis highlights the significance of selecting an appropriate "x" value to effectively model landslide propagation, considering the local topographical conditions and the nature of the terrain in the study area.
The results obtained from Flow-R modeling are reported in the form of probability values. In the context of risk assessment, it is crucial to emphasize the significance of probability of impact thresholds and how these thresholds influence risk management studies. To es-

tablish the correct thresholds is essential to ensure that effective preventive and corrective measures. Besides, overestimating the risk can have significant economic implications, while underestimating it can impact the social aspect. A crucial finding is the determination of a cut-off probability of impact, which is set at 25%. This threshold represents the minimum probability required for zoning areas as potentially impacted during landslides propagation.

3.7 Conclusion

In this comprehensive study on landslide propagation modeling. We have explored the critical factors that influencing the accuracy of simulations using the empirical tool Flow-R and their relevance in risk management and land use decision-making, particularly in tropical and mountainous environments. The extensive dataset collected underlines on the careful parameter selection in landslide propagation modeling. Furthermore, it highlights the importance of considering local conditions when adapting modeling parameters, and emphasizes the influence of topography and data quality on simulation accuracy in these challenging settings. Among the key achievements of this study is the identification of optimal parameters for these environments, including a maximum velocity of $10ms^{-1}$, a minimum travel distance angle of 15 degrees, and exponents "x" of 2 and 4. These parameters enhance our understanding of landslide propagation in tropical and mountainous contexts, which is essential for risk management in these areas. Additionally, the study highlights the relevance of impact probability thresholds, such as the 25% threshold, in risk management in tropical and mountainous environments. These thresholds play a crucial role in delineating affected areas and are essential for land planning, balancing economic and social aspects in decision-making. It is crucial to recognize that there is no one-size-fits-all approach to modeling landslide propagation. It is essential to adapt modeling parameters to local conditions and consider area-specific factors. Nonetheless, the findings of this study provide a valuable foundation for future research and risk management practices in tropical and mountainous environments, significantly contributing to safety and effective land use planning in these regions.

4 Physical modeling

This chapter was written with support of Martin Mergili, Edier Aristizábal, and, Oscar Echeverrí.

Exploration of basal friction parameter in shallow landslide propagation modeling using r.avaflow

Abstract

Landslides pose a significant natural hazard around the world, with several triggering factors. In the Colombian Andes, rainfall is the primary triggering factor. These landslides are typically shallow and can evolve into more rapid movements such as flows or avalanches. According to recent records, debris flows have caused some of the most severe damage and some of them happened as a result of the occurrence of Clustered Shallow Landslides (CSL). Many investigations focus on the occurrence of landslides, and the areas affected by their propagation (runout) should also be considered. Landslide runout is influenced by different variables, the mass propagates with some cohesion, and variable density, and in most cases loses and gains material according to the rate of erosion and entrainment, where basal friction plays an important role. This investigation focuses on the influence of basal friction variation in modelling of SL using the r.avaflow tool that incorporates various physics-based models. The model is implemented in Mocoa, it is in the Colombian southwestern, occupies two completely different environments. To the west, it is located on the eastern Colombian mountain range. To the east, it is in the Amazonian foothills. As a result, it has geomorphological and geological diversity. Between the night of March 31 and early April 1, hours of rain triggered CSL and chain processes over the city and surrounding villages, with approximately 306 dead people. Some results from modeling SL under or overestimate the affected areas according to basal friction used. However, analysis indicates that basal friction equal to the internal friction of the material has better results. As well, they indicate that the minimum heights estimated ranging from 0.51 m to 0.61 m offer conservative results to perform hazard zoning of the possible affected areas.

4.1 Introduction

Landslides are one of the most destructive natural hazards around the world, causing thousands of deaths, injuries, and damages each year (Petley, 2012; Froude and Petley, 2018; Dilley et al., 2005; Schuster and Highland, 2001; Kjekstad and Highland, 2009; Schuster and Highland, 2003; Dai et al., 2002; Kirschbaum et al., 2009). Rainfall, earthquakes, volcanic activity, and anthropical activity are factors that can cause them. However, rainfall is the primary triggering factor in tropical and high mountain settings such as the Colombian Andes (Froude and Petley, 2018; Gómez et al., 2023).

The occurrence of landslides in the country is common due to two environmental factors, specially in the central zone known as the Andean region. (i) Mountains and steep slopes cover one-third of the country as the result of the subduction of the Nazca Plate beneath the South American Plate along the western margin. (ii) The central zone has seasonal rains from March to May and September to November. Which, during the cold phase of the *El Niño*/Southern Oscillation (*La Niña*) become more frequent and strong (Poveda, 2004), so landslides occurrences increase. Aristizábal and Sánchez (2019) estimates that rains caused 87 percent of the landslides that occurred in the country between 1900 – 2018, and the Andean region contributes about 93 percent of all landslides occurred. Gómez et al. (2023) reports that Colombia has the highest amount of landslides in the world that caused 1 to 10 deaths (~ 1600), and a landslide frequency of 10 per 1000 km^2.

Landslides, according to Cruden and Varnes (1996), encompass a broad range of mass movements, and their classification is based on material – rock, earth, or debris – and movement type (flow, topple, fall, slide, or spread). Landslides triggered by rainfall are typically translational slide types, with – shallow – thicknesses not exceeding 3 m (Moser and Hohensinn, 1983; Engelen, 1967; Campbell, 1974; Anderson and Sitar, 1995). Shallow Landslides (SL) usually occur on steep slopes with a planar or slightly undulating failure surface, controlled primarily by joints, discontinuities, or material changes (Varnes, 1978). The updated classification by Hungr et al. (2014) illustrates, how following failure, a shallow slide can evolve into more rapid movements such as flows or avalanches depending on water content, material, entrainment, and topography. According to recent records, debris flows have caused some of the most severe damage to the inhabitants and infrastructure, such as occurred in Tarazá (2007), Salgar (2015), Mocoa (2017) and Dabeiba (2020). Many of them happened as a result of the occurrence of Clustered Shallow Landslides (CSL), tens to hundreds of landslides were triggered by intense and/or prolonged rainfalls in a short period (hours) in a defined area. Some landslides were deposited in drainages and contributed sediments to the formation of more damaging events in chain processes.

Many investigations focus on the occurrence of landslides, and the areas affected by their propagation should also be considered. There are several approaches for analyzing landslide mass propagation (runout). They can be mainly grouped into (i) empirical-statistical methods, based mainly on geometric estimations of volume, area, height difference, length, and

travel angle (Hungr et al., 2005). (ii) analytical methods, which neglect the internal deformation, and the mass is reduced to a point representing of the center of mass (Dai et al., 2002; Quan Luna et al., 2012). And (iii) Numerical methods that include discontinuum models that represent the mass by a group of particles and continuum models, as the physical models that, which model in major detail the composition and mobilization mass (Pastor et al., 2014). Many of these methods are applied based on available data, i.e., empirical methods require basic information such as source location (point or area) and topography of the terrain to determine the potential travel distance and area of deposition. While physically based models require additional detailed information as unstable mass composition, geotechnical parameters, and volume.

Landslide runout is influenced by different variables and parameters, including acceleration, velocity, terrain, material composition, internal deformation, saturation degree, rheological settings and basal friction. Deepen in the rheology, the mixture of soil, vegetation and/or debris with a certain degree of saturation does not behave as a Newtonian fluid after failure. The mass propagates with internal deformation and no linear behavior. This mixture sometimes also has some cohesion, and variable density, and in most cases loses and gains material according to the rate of erosion and entrainment, where basal friction plays an important role. Pudasaini and Krautblatter (2021) contrast between erosion and entrainment. Erosion is described as the procedure of loose material separating from the bed surface, whereas entrainment is defined as the incorporation of the removed material into the mass being mobilized. These two phenomena are significant in the propagation of landslides, specifically in the increase of mass or volume and destructive potential. This research focuses on the analysis of SL propagation and the influence of basal friction variation in modelling using the r.avaflow tool that incorporates several physics-based models and phase interaction. We use single phase analysis, since the velocity change between phases is negligible. The basic geotechnical parameter required is the internal friction of the materials, which is the starting point to establish the range of values for the basal friction. In this research, It's ranging from 80% to 100% of the internal friction. In each basin, the modeling corresponds to a 5 percent increase in the defined range. The validation criteria reflect the value of the basal friction, i.e., the proportion of internal friction with which the best results were produced. In addition to the minimum flow height for zoning the areas affected by shallow landslide propagation.

4.2 Study area

Mocoa is located in the Colombian southwestern, it is the capital of the department of Putumayo. It has 683 km^2 of rural and 580 km^2 of urban area. The study area covers 30.5 km^2. It includes the basins of the Mulato River, Sangoyaco River and Taruca Creek. These tributaries of Mocoa River flow mainly in a W-E direction from the eastern mountain range, where the maximum elevation of the study area is 2344 $masl$ and slopes close to 79°,

to plains located at 550 *masl*. They flow into the Mocoa River in the urban area of the municipality (See Figure 4.1). Therefore, in terms of natural hazards such as debris flows, especially in concatenated events, these tributaries are the most influential.

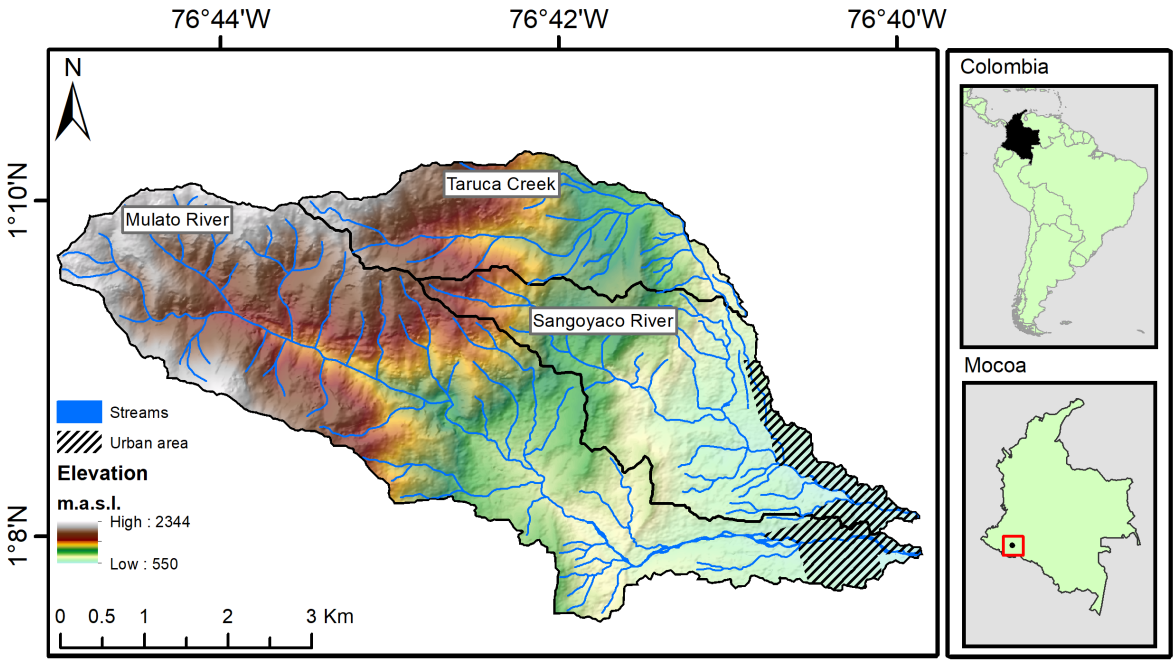

Figure 4.1: Location of the study area – Elevation and slope frequency of the study basins

4.2.1 Geological settings

Mocoa occupies two completely different environments. To the west, it is located on the eastern Colombian mountain range. To the east, it is in the Amazonian foothills. As a result, it has geomorphological and geological diversity. From a geomorphological point of view there are steep terrains and steep V-shaped valleys in the west and fans, terraces and plains to the east. There is a system of faults crossing the study area in a N-S, NE-SW direction. The Mulato, Campucama, Mocoa - La Tebaida and Cantayaco faults and the lineaments of the Taruca Creek and the Sangoyaco River are in (SGC, 2017b).
The most important faults are Mocoa - La Tebaida and Cantayaco. These structurally divide the study area into 3 zones. According to SGC (2017b, 2018b) the zones can be described as: (i) It is a high slope zone that represents the transition between the eastern mountain range and the Amazonian foothills, bounded by the Mocoa - La Tebaida fault. In this zone, the Mocoa monzogranite outcrops (igneous unit), which in turn is divided into a series of subunits of highly fractured rocks of intermediate quality in the west to very low quality in the east, with residual soils up to 2 m thick. (ii) The middle zone is formed by a sequence of sedimentary rocks of the Pepino and Orito Group formations, which overlay the Rumiyaco

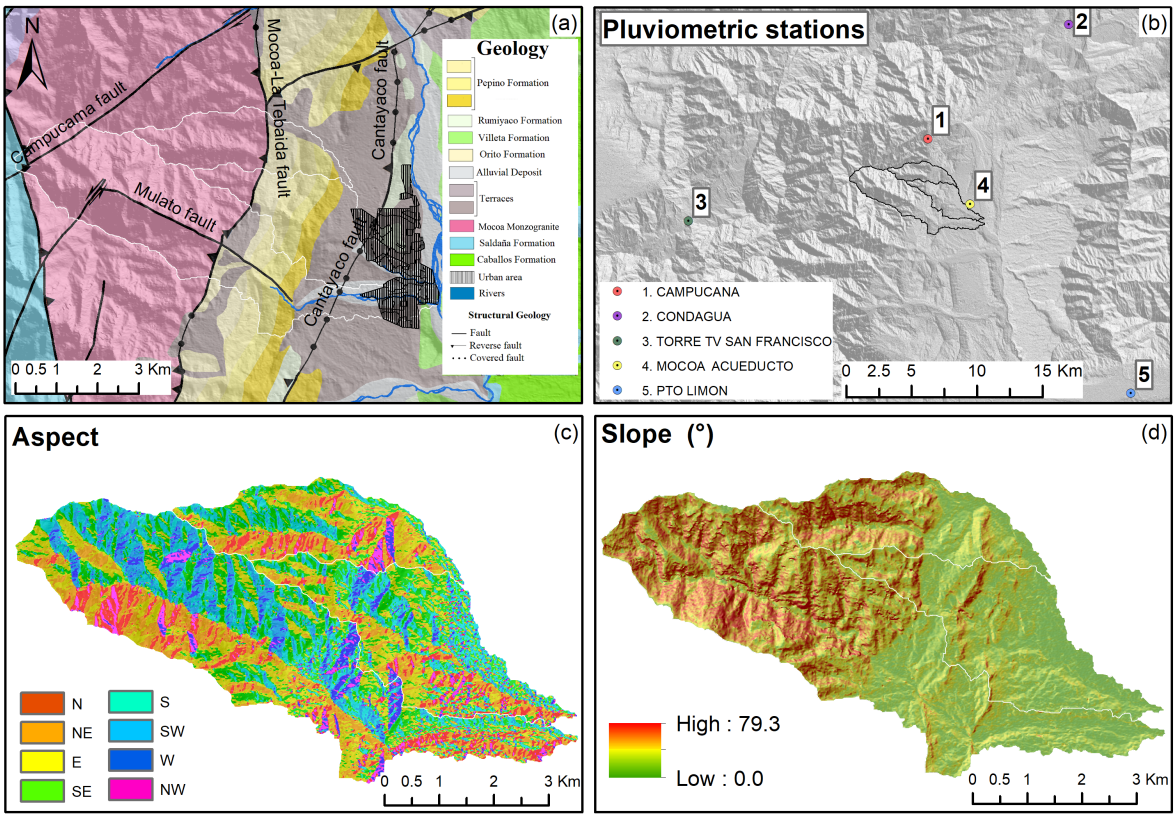

Figure 4.2: (a) Geological setting modified from Núñez Tello (2003), (b) pluviometric stations, (c) aspect and (d) slope

Formation. The zone is bounded by the Mocoa - La Tebaida and Cantayaco faults. The Orito Group develops soils up to 1.5 m thick in mudstone and siltstone beds. The Pepino Formation is dominated by weathering resistant conglomerates that develop sandy soils in their upper member. (iii) In the Amazonian foothills, the Rumiyaco Formation rises above the Villeta Formation due to the Cantayaco fault and develops soils up to 1.5 m thick, which are generally covered by deposits and terraces of the Mocoa River and its tributaries (See Figure 4.2a).

4.2.2 Debris flow records

Mocoa urban area is located on several fans, including the alluvial fan of Taruca Creek, which extends around 15 km^2 SGC (2018a). Between 1947 and 2018, there were approximately 15 significant natural hazards that included floods, debris flows, mudflows, and landslides. Table 4.1 highlights the occurrences related to debris flows that have impacted the urban area, with the occurrence of landslides that produced damming and/or contributed sediments to the event. In 1960, there was an event on Taruca Creek, it had a slight impact on the area where the urban area is now located. Due to the low occupancy at the time, the loss of

life and damage was minor. It impacted an area of about 30 *ha*, whereas the deposits from the 2017 event covered about 50 *ha* in the same location (SGC, 2017).

Type	Year	Basin	Observations
Debris flow	1947	Mulato River	Landslides and damming
Mud flow and debris flow	1960	Taruca Creek	Pre-event 2017
Debris flow	1995	Taruca Creek	Landslides and damming
Debris flow	1998	Mulato, Sangoyaco and Mocoa rivers	Landslides and prolonged rainfalls
Debris flow	2014	Taruca Creek	Landslides
Mud flow and debris flow	2017	*	Landslides
Debris flow	2018	**	Landslides
*Taruca, El Carmen and San Antonio Creek - Mulato, Sangoyaco and Mocoa rivers			
**Taruca Creek - lower basin of Mulato and Sangoyaco rivers (Medina Bello et al., 2018)			

Table 4.1: Historical records of cascade events related to rainfall-triggered landslides in Mocoa. Modified from SGC (2017b)

4.2.3 Climate

Mocoa has a humid warm climate with an average temperature of $\sim$ 23 °C, and it does not have a well-defined dry season. Rainfall occurs throughout the year, with the heaviest rainy season occurring between April and August, with a maximum number of rainy days in May, June, and July (www.ideam.gov.co). The Institute of Hydrology, Meteorology, and Environmental Studies (IDEAM, by its Spanish acronym) has several pluviometric stations in the area, two of them represent the geoenvironmental diversity. The San Francisco station represents the climatic conditions of the upper zone of the study basins on the eastern mountain range at an altitude of 3000 masl, while the Acueducto station is located in the urban area representing the conditions of the lower zone in the Amazonian foothills at 650 masl, the horizontal distance between stations is $\sim$ 21.6 km (See Figure 4.3).
The San Francisco station has an average accumulated rainfall record of 4673.7 mm during a multiannual period between 1985 and 2016, the Acueducto station registered 3813.1 mm. During the rainy season, the monthly multiannual records reveal that San Francisco station had more accumulated rainfall, which indicates heavier rains in fewer days, and nonuniform rainfall distribution in the study zone.

4.3 The event

The night of March 31 and early April 1 (2017), hours of rain triggered hundreds of landslides clustered and chain processes over urban area and surrounding countryside places. According to the National Institute of Legal Medicine and Forensic Sciences, approximately 306 dead people were identified 2017. News reported 322 dead, approximately 330 people injured and,

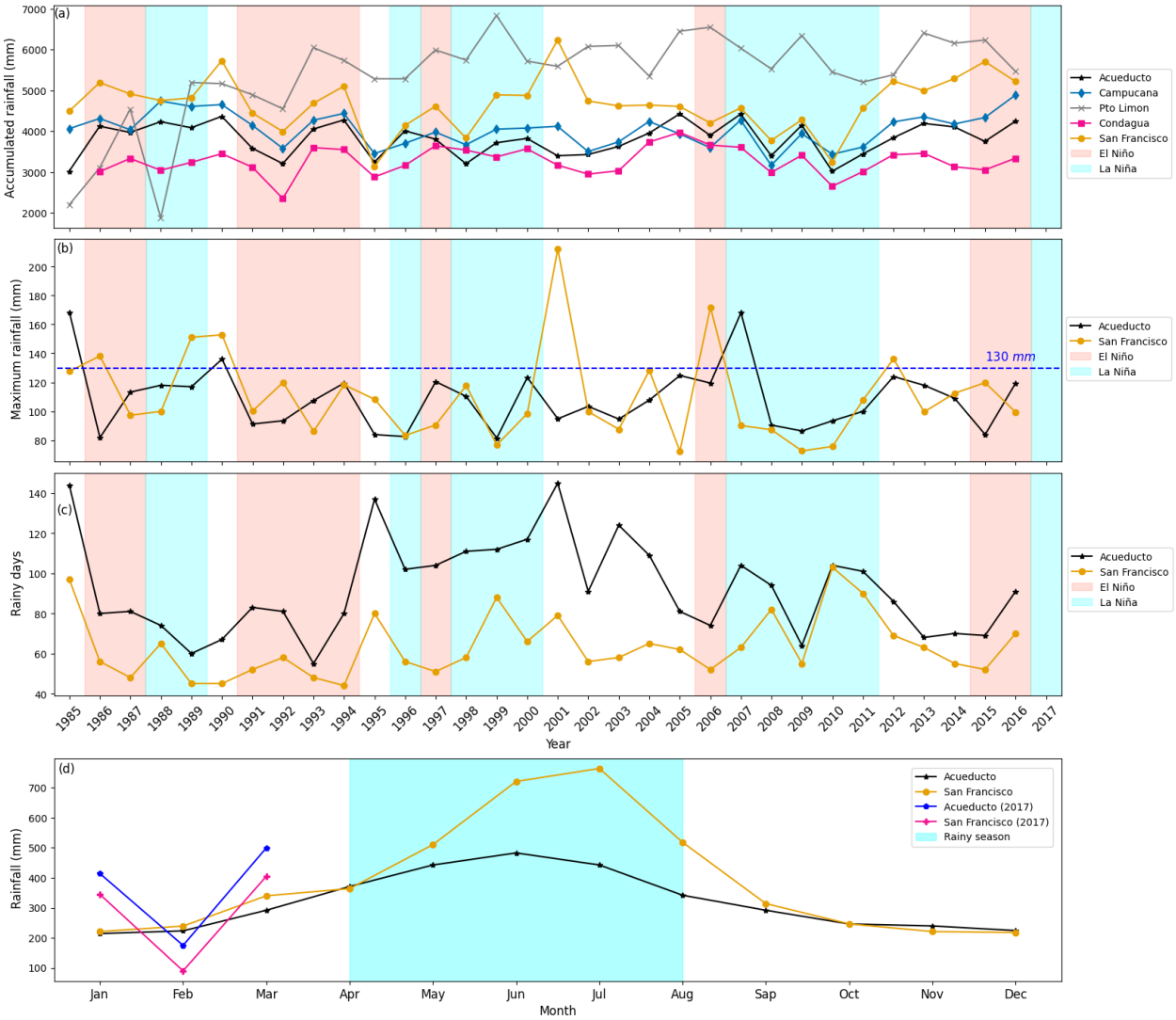

Figure 4.3: (a) Multiannual rainfall distribution from five pluviometric stations, showing ENSO seasons. (b) Maximum multiannual daily rainfall. (c) Multiannual rainy days. (d) Monthly multiannual rainfall distribution showing rainy season. Modified from SGC (2018a). Data provided by IDEAM

more than 100 people missing (RCN Radio, 2017). The propagation of the largest possesses, such as debris flow, caused the most damage to the population and infrastructure.

Slopes between 0° and 25° predominate in the study area; however, the occurrence of landslides is concentrated between 20° and 40°, in convex-convex areas and smaller concave-concave areas. Figure 4.4 depicts landslides distribution and debris flow damage area. Rainfall triggered $\sim$ 276 landslides, 90% of them were classified as a debris flow (SGC, 2017b). 190 landslides supplied sediments to the drainage system directly (See Figure 4.5).
The contribution in the Sangoyaco River basin was estimated to be 76940 m^3 of solids; in

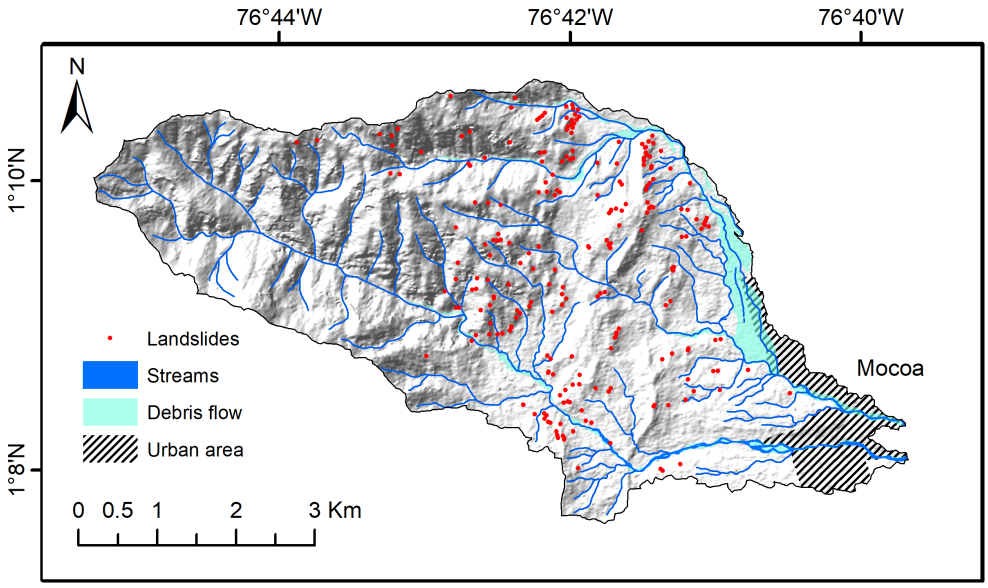

Figure 4.4: Landslide distribution and debris flow impacted area

the Mulato River 34009 m^3; and in Taruca Creek, 187831 m^3 (SGC, 2017b). According to Prada-Sarmiento et al. (2019), the materials deposited, studied and tested by SGC (2017b, 2018a, 2017,a, 2018b) indicate that the chain processes formed were a debris flow along Taruca Creek, which was then converted into a hyper-concentrated flow in the Sangoyaco River and a mud flow in the Mulato River.

4.3.1 Triggering rainfall

Records of Acueducto station on March 31^{st} show light rainfall at, 20:00h with peak precipitation at 23:00h of 62.8 mm. At 1:00h on April, 1^{st} chain processes impacted the urban area of the municipality. Registered accumulated rainfall was $\sim$ 130 mm in three hours. According to the maximum daily multiannual precipitation records for Acueducto and San Francisco stations shown in Figure 4.3b. The 130 mm precipitation has been exceeded 3 and 6 times for each station respectively. However, the 130 mm precipitation accumulated in a short time represents almost half of the March monthly average for the Acueducto station. SGC (2018b) indicates that this precipitation corresponds to a return period of 5–10 years for the Acueducto station and 5 years for the San Francisco station. On the other hand, the accumulated rainfall 38 days before the event for Acueducto station was 600 mm and is repeated more than once a year. However, this accumulated rainfall linked to 130 mm precipitation represents a condition with a return period of 25 years (SGC, 2017b).
Figure 4.3d shows multiannual mean monthly precipitation. On March, 2017 pluviometric record exceeds 2016 record.

Figure 4.5: Landslides and debris flow in study area. From Corpoamazonia and ibtimes

4.4 Data and methods

SL propagation estimation is a difficult task, CSL data provide the occurrence and propagation of numerous individual landslides, this information builds up a useful inventory of SL that occur in similar conditions in a defined area. For modeling, authors have developed models based generally on empirical, analytical, and physical methodologies. The latter is who requires more detailed information. This research employs a physics-based numerical tool r.avaflow, this requires basic inputs such as the digital terrain model (DTM), height of the source areas (volume), spatial distribution of the internal friction of the materials, and basal friction. The DTM is derived from a 5 m spatial resolution GEOSAR image processed and adjusted by SGC (2017b) for investigations of the event occurred on March 31 in Mocoa. The inventory of $\sim$ 276 landslides (source areas) was carried out by SGC (2017b). However, this research considers 233 landslides – not reactivated – detonated during the March 31 event. The geotechnical information comes from studies carried out by the SGC at a scale of 1:25000. The Section 4.4.1 explains in detail the theoretical foundations and requirements for modeling with the r.avaflow. Sections 4.4.2 establish the parameters for modeling and Section 4.4.3 presents the validation metrics used. Section 4.5 and 4.6 present the results and discuss.

4.4.1 r.avaflow

r.avaflow is an open-source computational tool developed as a raster module in GRASS GIS to simulate mass flows and complex process chains. The model computes the propagation from previous defined masses, release masses are input to the model as heights in raster map and/or hydrographs, which are then simulated over the terrain from source area up to deposition zone. Depending on the basic information given and the type of analysis executed, the tool produces different results. It provides hydrographs, ROC plots, 3D animation, height, velocity, pressure of the flow, and other raster maps. The first version of r.avaflow (2017) considers the mixture solid-fluid model of Pudasaini (2012). This study uses r.avaflow 2.3, it is feasible for single-phase and multi-phase modeling, it considers the interaction between phases in a redistribution of mass and momentum using a numerical scheme of Wang et al. (2004) linked to dynamic flow model of Pudasaini and Mergili (2019). Recent versions include changes in the basal topography, deposition, dispersion, and phase transformations. Follows are described as the phases taken into account by Pudasaini and Mergili (2019).

- The fluid phase is a mixture of water and very fine particles ranging from colloids to silt, which can be represented using a fluid shear-rate-dependent viscoplastic rheology; the material can behave like a common viscous fluid if the particle concentration is zero.
- The fine-solid phase is a fine granular material composed of bigger clay particles up to fine gravels, and it is governed by shear- and pressure-dependent Coulomb-viscoplastic rheology, where particle interaction influences energy dissipation.
- The solid phase considers coarse material modeling by shear-rate-independent Mohr-Coulomb plastic rheology. With frictional, no viscous behavior.

3-Dimensional three-phase mass flow model is given by balance for mass (4.1)–(4.3) and momentum (4.4)–(4.6) conservation differential equations for the solid, fine-solid, and fluid phases respectively. Where solid, fine-solid, and fluid phases are denoted by the suffix s, fs, and f, respectively. ρ is density, δ the basal friction angle, and ϕ the internal friction angle in solid and fine-solid phase and n viscosity is considered in fluid phase.

$$\frac{\partial \alpha_s}{\partial t} + \bigtriangledown \cdot (\alpha_s \mathbf{u}_s) = 0 \tag{4.1}$$

$$\frac{\partial \alpha_{fs}}{\partial t} + \bigtriangledown \cdot (\alpha_{fs} \mathbf{u}_{fs}) = 0 \tag{4.2}$$

$$\frac{\partial \alpha_f}{\partial t} + \bigtriangledown \cdot (\alpha_f \mathbf{u}_f) = 0 \tag{4.3}$$

$$\frac{\partial}{\partial t}(\alpha_s \rho_s \mathbf{u}_s) + \bigtriangledown \cdot (\alpha_s \rho_s \mathbf{u}_s \otimes \mathbf{u}_s) = \alpha_s \rho_s \mathbf{f} - \bigtriangledown \cdot \alpha_s \mathbf{T}_s + p_s \bigtriangledown \alpha_s + \mathbf{C}^{s,f}_{DG} + \mathbf{C}^{s,fs}_{DG} + \mathbf{C}^{s,f}_{vm} + \mathbf{C}^{s,fs}_{vm} \tag{4.4}$$

$$\frac{\partial}{\partial t}(\alpha_{fs}\rho_{fs}\mathbf{u}_{fs})+\bigtriangledown\cdot(\alpha_{fs}\rho_{fs}\mathbf{u}_{fs}\otimes\mathbf{u}_{fs}) = \alpha_{fs}\rho_{fs}\mathbf{f}-\alpha_{fs}\bigtriangledown p_{sf}+\bigtriangledown\cdot\alpha_{fs}\tau_{fs}-\mathbf{C}_{DG}^{s,fs}+\mathbf{C}_{DG}^{fs,f}-\mathbf{C}_{vm}^{s,fs}+\mathbf{C}_{vm}^{fs,f} \quad (4.5)$$

$$\frac{\partial}{\partial t}(\alpha_f\rho_f\mathbf{u}_f) + \bigtriangledown\cdot(\alpha_f\rho_f\mathbf{u}_f\otimes\mathbf{u}_f) = \alpha_f\rho_f\mathbf{f} - \alpha_f\bigtriangledown p_s + \bigtriangledown\cdot\alpha_f\tau_f - \mathbf{C}_{DG}^{s,f} - \mathbf{C}_{DG}^{fs,f} - \mathbf{C}_{vm}^{s,f} - \mathbf{C}_{vm}^{fs,f} \quad (4.6)$$

Where $\mathbf{u} = (u, v, w)$ denote the velocities along the flow directions (x, y, z), and α volume fractions with $\alpha_s + \alpha_{fs} + \alpha_f = 1$. $\mathbf{C}_{DG}$ and $\mathbf{C}_{vm}$ constitute the interfacial force densities, the drags and the virtual mass forces respectively. $\mathbf{T}$ is the negative Cauchy stress tensor, τ is the extra stress, and $\mathbf{p}$ the pressure. The complete mathematical and physic framework is explained by Pudasaini and Mergili (2019).

4.4.2 Modeling parameters

The simulations are computed considering a solid one-phase model. Although the mass is saturated to some degree, the flow of water within it is considered to be minimal, as are the changes in acceleration (Pastor et al., 2014; Tayyebi et al., 2022). So, the contact between the solid and fluid phases is insignificant, and the motion is the same, where the rheology of the solid phase prevails.

Symbol	Parameter	Value	Unit
ρ_s	Solid material density (grain density)	2700	$kg\ m^{-3}$
ρ_f	Fluid density	1000	$kg\ m^{-3}$
ϕ	Internal friction angle	See Fig. 4.6	Degree
δ	Basal friction angle	$0.8\ \phi - 1.0\ \phi$	Degree

Table 4.2: Parameters used to modeling in r.avaflow

r.avaflow being a physically based tool demands detailed information. However, the input data for a single-phase analysis – solid – are minimal. The main input is the volume, considering the soil thickness from the source areas identified at the field ($< 2.5\ m$); shown in Figures 4.4 and 4.6. The parameters utilized in the modeling are shown in Table 4.2. Basal friction describes the contact between the propagating mass and the ground surface and corresponds to the variation of the internal friction of the material in 5% increments from 80% to 100% of the internal friction, shown in Figure 4.6.
Spatially every zone is characterized by an angle of internal friction, r.avaflow specifies that the basal friction cannot be higher than the internal friction and in case the user increases it to a higher value, both frictions will be set equal to the given value. For this reason, the modeling is performed considering a basal friction range of 0.8 to 1.0 of the internal friction.

4.4.3 Validation metrics

The best-fit parameters can be assessed through the use of validation metrics to explore and analyze the results obtained concerning the existing inventory. Fawcett (2005) proposes four variables,

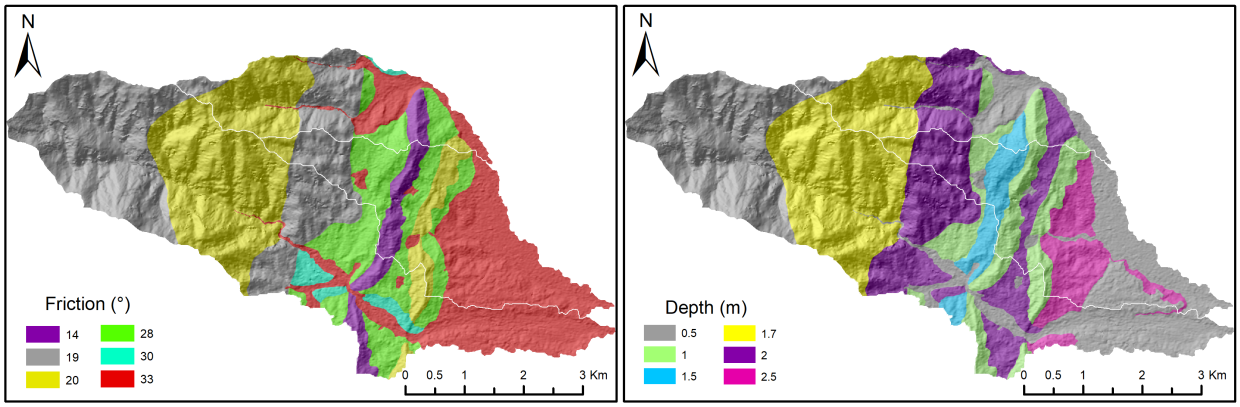

Figure 4.6: Internal friction angle and depth distribution

considering model prediction and actual inventory observations. Applied to this study, they can be defined as a set of four scenarios, as follows. True Positive (TP) observed areas that were correctly identified as impacted in the simulation; True Negative (TN) non-impact areas that were correctly identified as non-impacted in the simulation; False Positive (FP) non-impacted area that was incorrectly identified as impacted; False Negative (FN) impacted area that was incorrectly identified as non-impacted. Since both the inventory and the results show an imbalance between impacted and non-impacted areas, with TN exceeding TP. The validation metrics selected do not take TN value into account. If this variable is included, for this specific case the metric would be more a measure of effectiveness of the model by estimating the non-impacted areas rather than the impacted ones. As a result, measures unaffected by the TN were selected (See Table 4.3).

Parameter	Definition	Range	Optimum
Factor of conservativeness (FoC)	$\frac{TP+FP}{TP+FN}$	$[0, \infty]$	1.0
F1-Score	$2 \cdot \frac{precision+recall}{precision \cdot recall}$	[0,1]	1.0
Recall (TPr)	$\frac{TP}{TP+FN}$	[0,1]	1.0
Precision (PPV)	$\frac{TP}{TP+FP}$	[0,1]	1.0

TPr: True positive rate **PPV**: Positive predictive value
TP: True positive **FP**: False positive **FN**: False negative

Table 4.3: Validation criteria

The Factor of Conservativeness (FoC) denotes how conservative the results obtained are, FoC$<$ 1 means that the results are not conservative, while FoC$>$ 1, indicates that they are conservative, and FoC$=$ 1 is the optimal.The predictive accuracy of positive cases is measured by recall or True Positive rate (TPr). Precision, also known as Predictive Positive Value (PPV), is the percentage of

impacted areas relating to the total number of positives identified. The F1-Score combines precision and recall as an accuracy metric.

4.5 Results

The results provided by r.avaflow correspond to the height of the flow deposit for each basal friction value in every basin, following the simulation of propagation within a 300 second interval. The Figure 4.7 illustrates the variation of TPr and F1-Score relating to FoC for each basal friction that is proportionate to the internal friction. When the FoC approaches one, assuming that the basal friction equals the internal friction ($\delta = 1.00\ \phi$) yields the most accurate model results. As FoC increases, F1-Score decrease, while TPr rises, showing a loss of accuracy in the positive predictions due to an increase of FP.

Simulations with $\delta = 1.00\ \phi$, which produced the highest metrics, are summarized in Table 4.4, and the metrics for the various minimum – cut-off – flow heights and FoC are presented. In general, the flow height with the best F1-Score in the three basins is close to FoC$\sim$ 2. In addition, a similar cut-off flow height from 0.51 m to 0.61 m is observed, differing by 10 cm between them. In second place are the heights associated with FoC$\sim$ 3 and the optimal value for FoC$\sim$ 1 is in third place with a cut-off flow height greater than 1 m. For all cases, the lowest F1-Score corresponds to the most conservative results, FoC$\sim$ 6.

Figures 4.8, 4.9, and 4.10 show the result achieved considering $\delta = 1.00\ \phi$. Each subfigure depicts the area covered by the deposit with the minimum height from which the area of affectation is considered, with increases in the FoC of approximately one. In general, as the FoC increases, the area covered by the deposit increases too since the minimum height considered decreases. So, conservative values of FoC indicate a very low flow height cut-off, from which the affectation will occur, reflecting deposits with more area, whereas non-conservative values have higher minimum flow height cutoffs, representing deposits with less area.
Figure 4.8 presents the results for the Mulato River basin. Figure 4.8a shows the area covered by the depositional area associated with the optimum FoC$\sim$ 1, considering a minimum deposition height of 1.48 m up to a maximum of 10.24 m; some impacted areas (inventory) are not covered due to a relatively high minimum flow height of 1.48 m. However, in Figure 4.8g, a more conservative result not only covers the impacted areas but also significantly increases it, with a minimum flow height of 5 cm; thus increasing the FP.

For Taruca Creek the result is shown in Figure 4.9. Figure 4.9a shows how the deposit areas are minor in the targeted zone concerning the inventoried ones, with a minimum cut-off height of 1.06 m. For FoC$\sim$ 2 a larger area is covered and although visually it is not representative; it is more accurate than the results for FoC$>$ 2 as these cover too many areas that were not impacted.

The results for the Sangoyaco River basin reveal similarities in the areas covered by the deposits associated with FoC$>$ 2, which are elongated deposits that differ little from the most conservative result with a minimum flow height of 0.10 m. Although the result linked with the FoC$\sim$ 1 fits the impacted areas, it does not cover all of them.

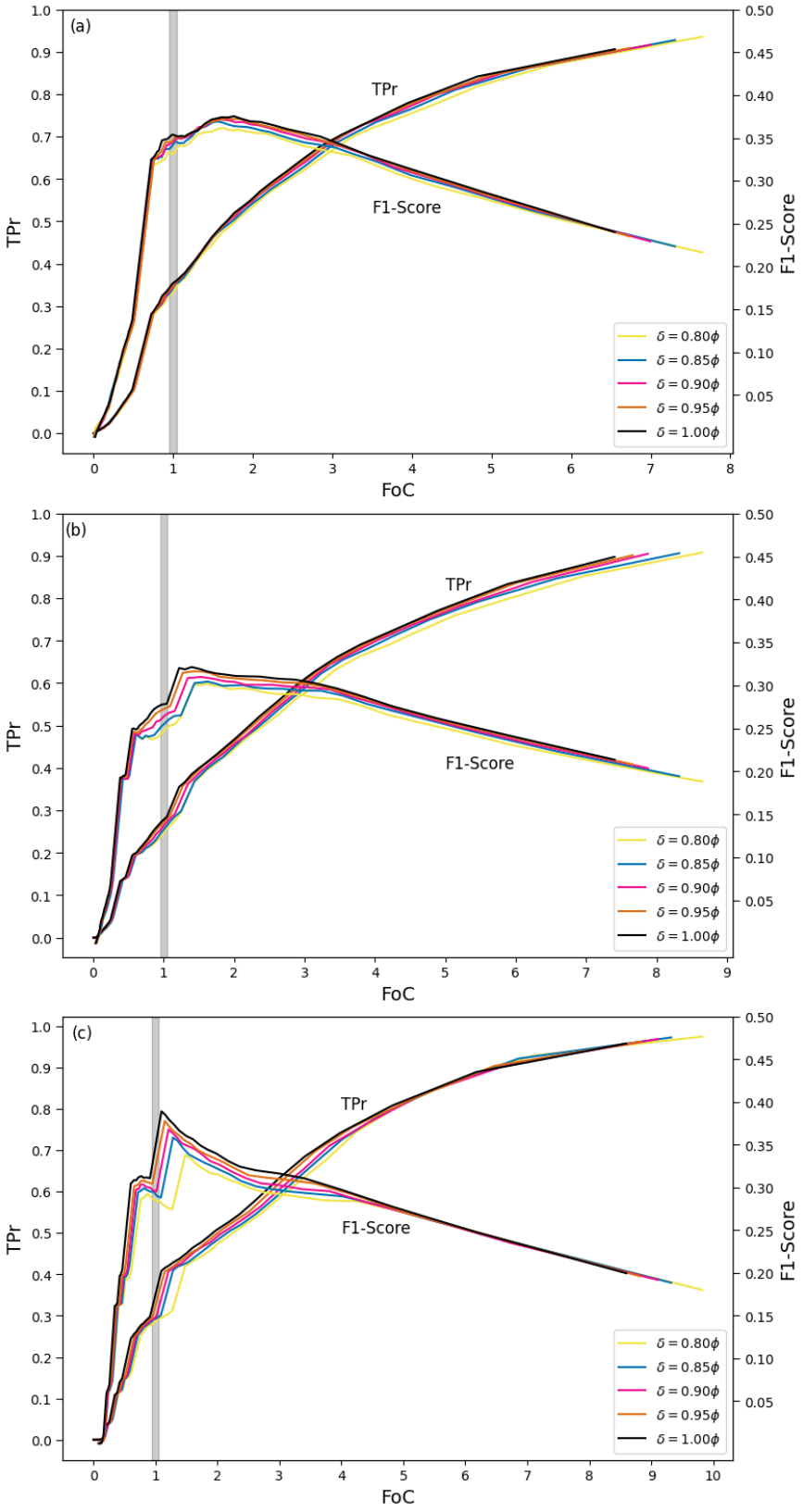

Figure 4.7: Variation of TPr and F1-Score depending on FoC for each basal friction. (a) Mulato River, (b) Taruca Creek and (c) Sangoyaco River

Basin	**Cut-off flow height** (m)	**Recall**	**FoC**	**F1-Score**
Mulato $\delta = 1.00\ \phi$	1.48	0.35	0.99	0.35
	0.51	0.57	2.10	0.37
	0.26	0.71	3.13	0.34
	0.15	0.78	3.95	0.31
	0.10	0.84	4.83	0.29
	0.05	0.91	6.55	0.24
Taruca $\delta = 1.00\ \phi$	1.06	0.27	0.97	0.28
	0.61	0.47	2.02	0.31
	0.35	0.63	3.15	0.30
	0.20	0.72	4.26	0.28
	0.15	0.77	4.88	0.26
	0.10	0.83	5.89	0.24
Sangoyaco $\delta = 1.00\ \phi$	1.03	0.30	0.91	0.31
	0.51	0.51	1.98	0.34
	0.31	0.63	2.99	0.32
	0.21	0.74	3.98	0.30
	0.15	0.81	4.82	0.28
	0.10	0.89	6.18	0.25

Table 4.4: Cut-off flow height and metrics variation for $\delta = 1.00\ \phi$

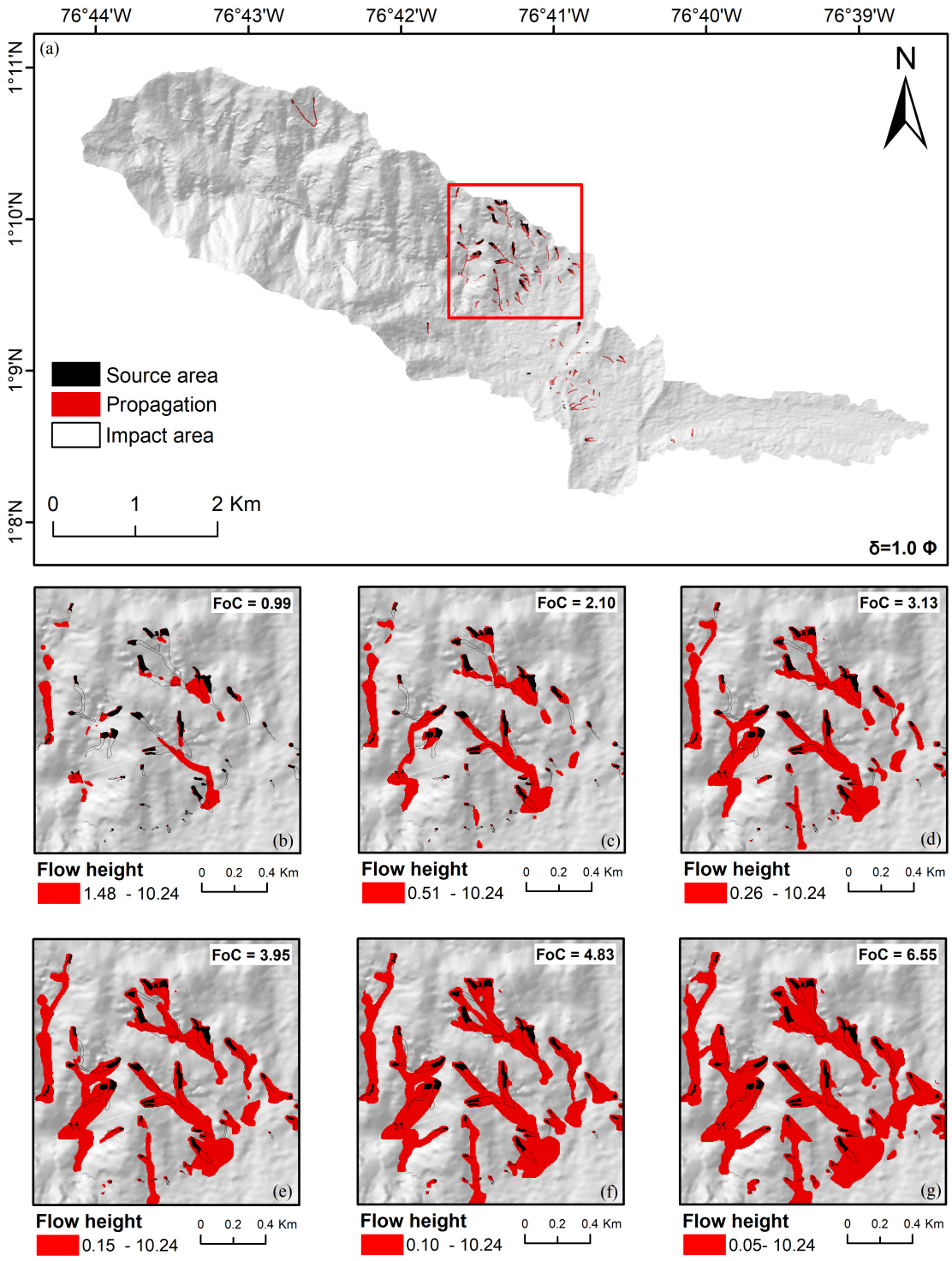

Figure 4.8: Modeling FoC and flow height (m) - Mulato River

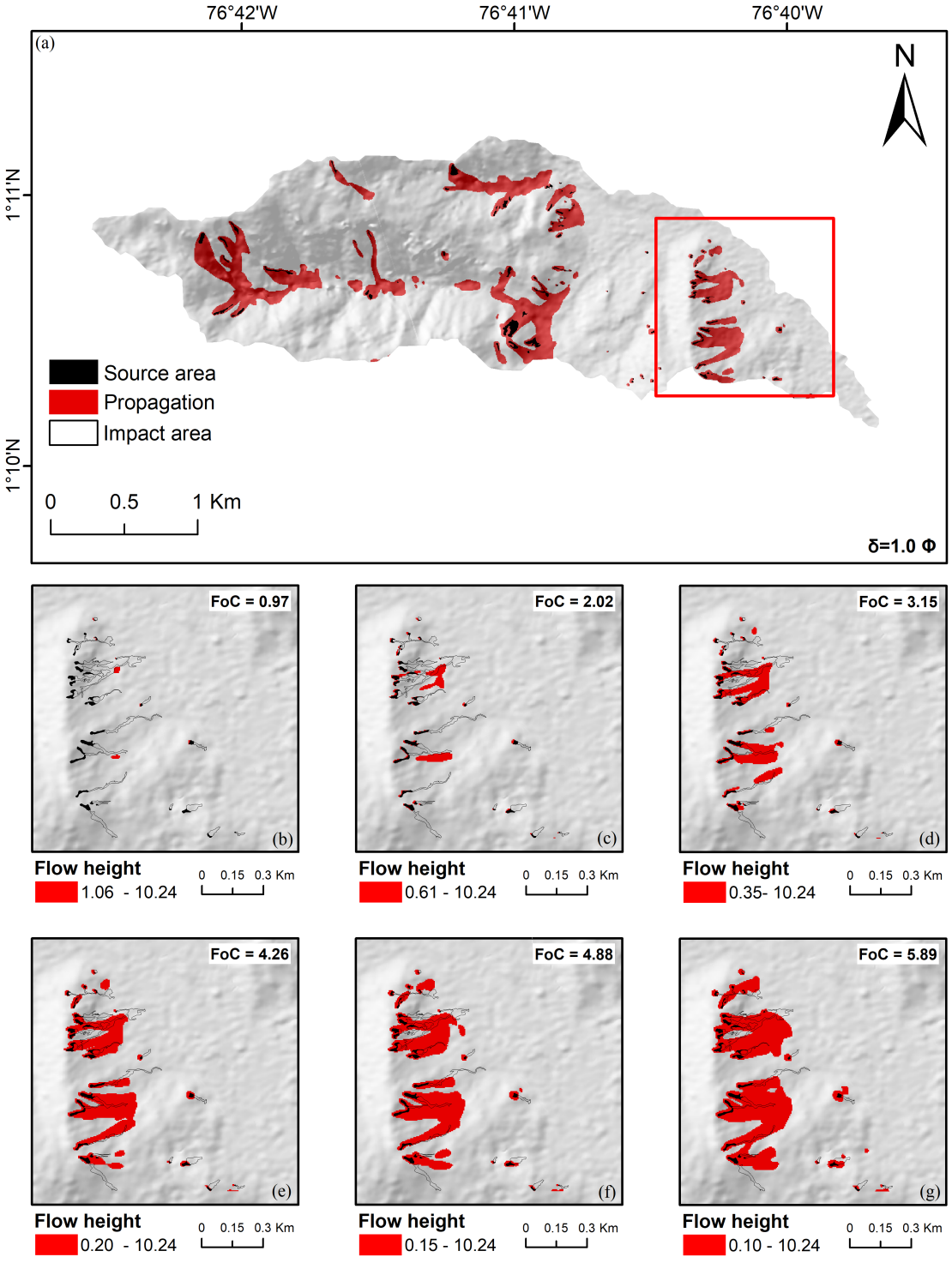

Figure 4.9: Modeling FoC and flow height (m) - Taruca creek

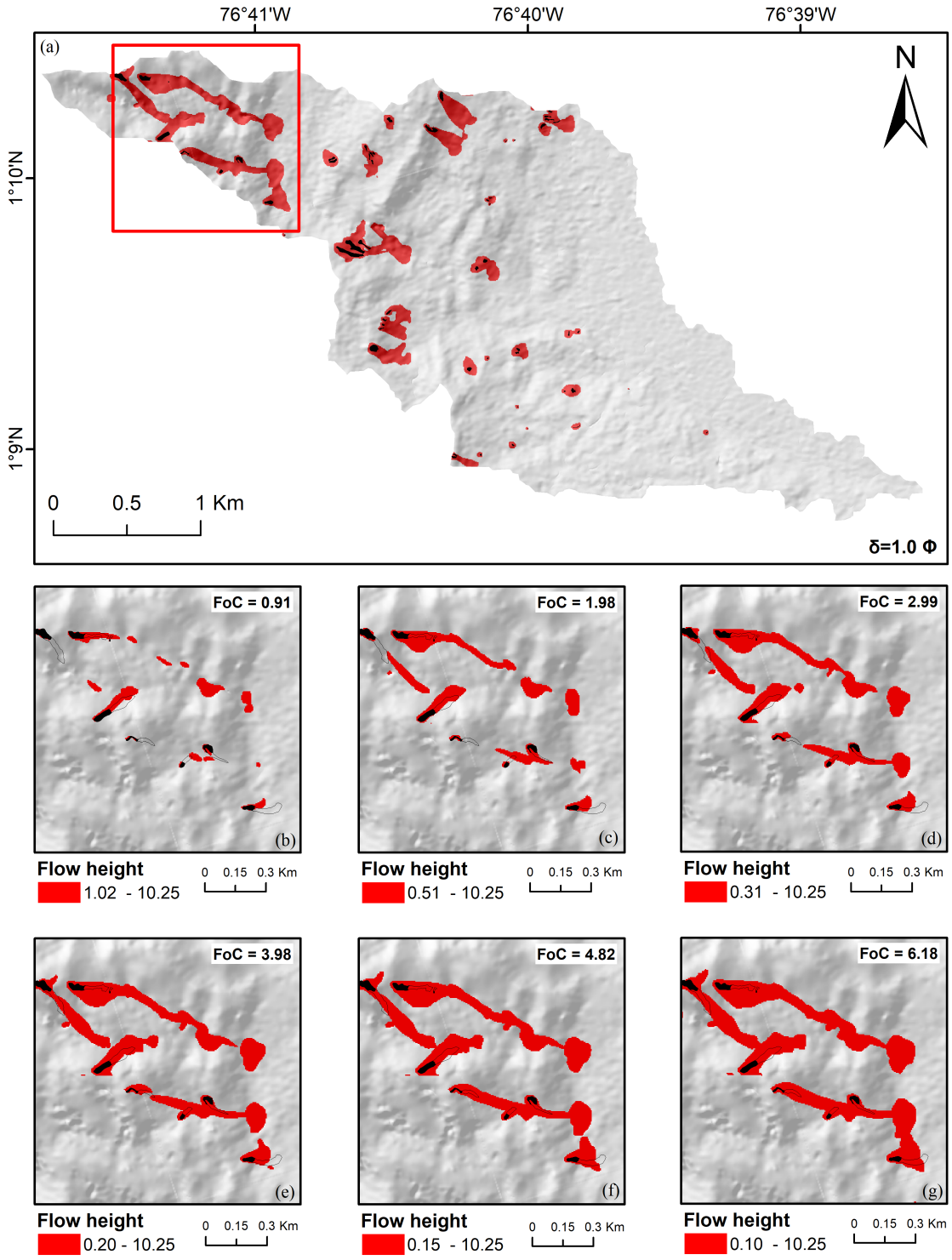

Figure 4.10: Modeling FoC and flow height (m) - Sangoyaco River

4.6 Discussion

r.avaflow is a tool based on physical models, the approaches to landslide runout modeling struggle to incorporate material physical features, composition, and interaction with the environment. Landslides are natural phenomena, therefore modeling them is challenging, with many elements affecting their downslope mobility. According to Varnes (1984), hazard implies the assessment of the spatial probability of affectation, hence the importance of determining the possible areas affected not only during the occurrence but also during the propagation. In runout process, the contact force between the moving mass and the terrain is represented by basal friction, which is one of the variables that determines the evolution of the nature of the phenomenon and thus the modeling. As a result, being a part of the erosion and entrainment processes. According to Hungr et al. (2014), the initial volume in many landslides is low in comparison to the volume from erosion and entrainment, particularly in channelized landslides. The availability of material to raise the volume of the mass as it moves is significant in humid tropical and high mountain environments like the research location. It has many low and medium-quality rocks, heavily weathered and fractured, mainly in an adjacent zones of the Mocoa - La Tebaida fault. in the abrupt change of the transition between the eastern cordillera and the Amazonian foothills. Besides, In the 2016-2007 period, according to Qiu et al. (2007), vegetation cover changed considerably in the upper zone of the basin due to *El Niño*, leaving bare erodible soils exposed.

This study investigates the effect of basal friction variation on SL propagation modeling. Low basal friction angles allow the mass to move at high velocity, resulting in longer travel distances; higher values result in lower velocities due to ground-material friction. Besides, the mass is constantly evolving due to the entrainment of the eroded material or deposition.

Based on the results obtained and presented above, none of the simulations ran got better validation metrics than the consideration of basal friction equal to internal friction. Although it better reflects the inventory of impacted areas, various basal friction produced comparable results, as shown in Figure 4.7. Table 4.5 also shows the second-best performance in terms of FoC$\sim$ 1 and F1-Score.

Basin	**Basal friction**	**FoC**	**Flow height**	**F1-Score**
Mulato River	1.00 ϕ	0.99	1.48	0.354
	0.90 ϕ	1.00	1.51	0.345
Taruca Creek	1.00 ϕ	0.97	1.06	0.278
	0.85 ϕ	1.01	1.16	0.255
Sangoyaco River	1.00 ϕ	0.91	1.03	0.31
	0.90 ϕ	1.02	1.04	0.295

Table 4.5: Second-best performance in terms of FoC$\sim$ 1 and F1-Score

In the modeling of the Mulato River basin, the simulation with $\delta = 0.90\ \phi$ produces an F1-Score of 0.345, values associated with a minimum flow height of 1.51 m. Therefore, it covers less area concerning the area affected and a height of 1.48 m of $\delta = 1.00\ \phi$. In the Taruca Creek basin, the second-best simulation was obtained with $\delta = 0.85\ \phi$, with a minimum flow height of 1.16 m and an F1-Score of 0.255; the height is 0.1 m higher than the obtained for $\delta = 1.00\ \phi$. The Sangoyaco River

basin presents a slight variation between the heights associated with $\delta = 1.00\ \phi$ and $\delta = 0.90\ \phi$. However, its F1-Score varies significantly, as does the FoC.

4.7 Conclusion

According to the results, FoC$\sim$ 2 has the highest F1-Score in the three basins. The minimum height from which the region affected for the simulated SL propagations should be regarded is estimated from there, and it varies between 0.51 m and 0.61 m. In terms of modeling parameters for modeling SL in r.avaflow, results suggest: (i) consider the basal friction equal to the internal friction of the material as the starting value; (ii) use minimum heights in the range of 0.51 m to 0.61 m to perform hazard zoning of the possible affected areas.

5 Summary and conclusions

5.1 Summary

This research studied numerous landslides – clustered – triggered by rainfall in Mocoa (2017). It focuses on features and modeling parameters, applying two approaches to landslides propagation.
Section 2 covers the basic principles and most significant definitions of shallow landslides, shallow landslides clustered, and the relevance of propagation in risk management. It explores the foundations, models, and tools employed in each of the major approaches applied for the analysis and determination of landslide propagation. Furthermore, it briefly discusses the cluster-type events recorded in the country since the 1990s and shows some researches carried out on landslide propagation. Finally, it looks into the timeline in the Colombian risk management regulation, from its origins to the most recent guidelines developed to support the implementation of studies of susceptibility, vulnerability, hazard, and risk due to landslides.
Section 3 explores the values for the best-fit parameters for the use of the empirical tool of spatial distribution, Flow-R that estimates the propagation from predefined source locations using algorithms and frictional laws. The basic modeling parameters that govern mobility are maximum velocity, minimum travel distance angle, and the Holmgren's exponent, which limits flow diffusion taking into account values close to the recommended. Initially, the length and height difference between the source area and the deposition zone were assessed for 178 of 233 landslides. They were also classified according to the average slope of the path in the direction of flow; to explore whether the observation of well-defined differences in travel distance angle parameter, may be properly represented in a grouped way. The analysis values are taken from the first and third quartiles, for velocity and travel distance angle, for each group in each of the basins. The collected data allow a set of simulations that are then compared and evaluated by validation metrics regarding the existing inventory. The results allow for defining the most appropriate values for the modeling of shallow landslides in basins, such as the one studied, characterized by rugged topography in a tropical environment. In addition to establishing the minimum probability of damage that can be considered in future studies.
Section 4 implements the physical modeling using r.avaflow. Although it uses a phase interaction model; the modeling is carried out considering a single phase. Since the velocity change between materials is negligible. The basic geotechnical parameter required is the internal friction of the materials, which is the starting point to establish the range of values for the basal friction, ranging from 80% to 100% of the internal friction. In each basin, the modeling corresponds to a 5 percent increase in the defined range. The validation criteria findings reflect the value of the basal friction, i.e., the proportion of internal friction with which the best results were produced. In addition to the minimum flow height for zoning the areas affected by shallow landslide propagation.

5.2 Conclusions

In this research, it was presented two useful tools for propagation modeling of SL. It was established for each tool the best-fit parameters for modeling with minimal requirements. Results indicated a maximum velocity of 10 $m\ s^{-1}$, minimum travel distance angle of 15°, and x value of 2 and 4 for modeling in Flow-R. In addition, the cut-off for the probability of impact was set to 25% as the minimal threshold for zoning. The results concerning to the parameters to modeling SL in r.avaflow suggest; to consider the basal friction equal to the internal friction of the material as the starting value. And to use the minimum heights in the range of 0.51 m to 0.61 m to perform hazard zoning of the possible affected areas.
It is key in future research using Flow-R, the variation of Holmgren's exponent and modelling over topography at different resolutions should be investigated in detail. In this way, the influence of cover land and obstructions on the propagation of landslides in tropical mountainous regions could also be taken into account and analyzed. Regarding r.avaflow, it is necessary to explore not only the variation of the basal friction, but also the internal friction of the material as a consequence of the incorporation of materials by erosion and entrainment. To explore in detail the height of the deposit and the FoC, thus determining thickness thresholds to support risk management for hazard zoning.

5.3 Future research

Climate change has become an important factor, that influences rainfall patterns, extreme events will be more common. However, estimates of rainfall threshold remain a complex topic. Overall, under climate-change scenarios, the current Colombian regulations, and growing people exposure. It's necessary more detailed research focus on linked landslide occurrence, propagation, and mitigation measures; specially entire hazard chains. Specifically, current legislation stipulates that intervention – mitigation – measures must be proposed according to the hazards identified in a given study area. Countermeasures may be structural or non-structural, to prevent, mitigate, and reduce the hazards over the elements exposed. Non-structural measures focus on establishing restrictions and a viable occupation model, implementing measures such as early warning systems, and adopting responsibility and precautionary principles. Structural-physical measures mainly involve the construction of engineering structures to reduce or eliminate the impact of hazardous conditions on the population. Mitigation measures, particularly structural measures, have received little attention. Education, prevention, and mitigation are largely absent in the scope of the torrential flow guide, this issue requires more attention in hazard chains specially. In this context, the case study of Mocoa is highly instructive and requires special attention. Towns need solutions that allow people to live with the problem of landslides in the context of recognition and reduced risk. This research can be used as a guide – step – in future projects in a long process of risk management, to support decision-making.

6 Bibliography

(2017). INMLCF identifica 191 cuerpos en Mocoa.

Anderson, S. A. and Sitar, N. (1995). Analysis of Rainfall-Induced Debris Flows. *Journal of Geotechnical Engineering*, 121(12):544–552.

Aristizábal, E. (2013). *SHIA – Landslide: Developing a physically based model to predict shallow landslides triggered by rainfall in tropical environments.* PhD thesis, Universidad Nacional de Colombia.

Aristizábal, E., Carmona, M. I. A., and López, I. K. G. (2020). Definición y clasificación de las avenidas torrenciales y su impacto en los Andes colombianos. *Cuadernos de Geografia: Revista Colombiana de Geografia*, 29(1):242–258.

Aristizábal, E., Martínez, E., and Vélez-Upegui, J. I. (2017). Influencia de la lluvia antecedente y la conductivdad hidraulica en la ocurrencia de deslizamientos detonados por lluvias utilizando el modelo SHIA$_l$*andslide.EIA*, 13(*January*) : 31 − −46.

Aristizábal, E. and Sánchez, O. (2019). Spatial and temporal patterns and the socioeconomic impacts of landslides in the tropical and mountainous Colombian Andes. *Disasters*.

Baum, R. L., Savage, W. Z., and Godt, J. W. (2008). TRIGRS — A Fortran Program for Transient Rainfall Infiltration and Grid-Based Regional Slope-Stability Analysis, Version 2.0. *U.S. Geological Survey*, (2008-1159):75.

Beguería, S., W. J. Van Asch, T., Malet, J. P., and Gröndahl, S. (2009). A GIS-based numerical model for simulating the kinematics of mud and debris flows over complex terrain. *Natural Hazards and Earth System Science*, 9(6):1897–1909.

Benda, L. E. and Cundy, T. W. (1990). Predicting deposition of debris flows in mountain channels. *Canadian Geotechnical Journal*, 27(4):409–417.

Berti, M. and Simoni, A. (2007). Prediction of debris flow inundation areas using empirical mobility relationships. *Geomorphology*, 90(1-2):144–161.

Berti, M. and Simoni, A. (2014). DFLOWZ: A free program to evaluate the area potentially inundated by a debris flow. *Computers and Geosciences*, 67:14–23.

Bladé, E., Cea, L., Corestein, G., Escolano, E., Puertas, J., Vázquez-Cendón, E., Dolz, J., and Coll, A. (2014). Iber: herramienta de simulación numérica del flujo en ríos. *Revista Internacional de Metodos Numericos para Calculo y Diseno en Ingenieria*, 30(1):1–10.

Borga, M., Dalla Fontana, G., Daros, D., and Marchi, L. (1998). Shallow landslide hazard assessment using a physically based model and digital elevation data. *Environ Geol*, 28:81–88.

Caine, N. (1980). The Rainfall Intensity: Duration Control of Shallow Landslides and Debris Flows. *Geografiska Annaler. Series A, Physical Geography*, 62:23–27.

Campbell, R. H. (1974). Debris flows originating from soil slips during rainstorms in southern california. *Journal of Engineering Geology and Hydrogeology*, 7(4):339–349.

Cannon, S. H. (1993). Empirical model for the volume-change behavior of debris flows. In *Proceedings - National Conference on Hydraulic Engineering*, pages 1768–1773, San Francisco, CA, USA.

Caracol Radio (2007). Terrible calamidad enfrenta Antioquia por lluvias y derrumbes.

Caracol Radio (2020a). 438 afectados por deslizamiento en Dabeiba permanecen en albergues.

Caracol Radio (2020b). Un muerto y quince municipios afectados por lluvias en Antioquia.

Carmona Arango, M. I., Aristizábal, E., Jaboyedoff, M., and McArdell, B. (2021). Assessing torrential flow susceptibility using triggering and propagation models for tropical mountainous regions, a case study of the northern Andes, Colombia. In Cabrera, M. A., Prada-Sarmiento, L. F., and Montero, J., editors, *SCG-XIII INTERNATIONAL SYMPOSIUM ON LANDSLIDES*, number June 2020, page 9, Cartagena. International Society for Soil Mechanics and Geotechnical Engineering (ISSMGE).

Cascini, L., Cuomo, S., Pastor, M., and Sorbino, G. (2010). Modeling of rainfall-induced shallow landslides of the flow-type. *Journal of Geotechnical and Geoenvironmental Engineering*, 136(1):85–98.

Castro López, F. R. (2018). *Simulación de flujos granulares detonados desde el Cerro Montoso (Nariño, Colombia) e implicaciones para amenazas por remoción en masa*. PhD thesis, Universidad de los Andes.

Christen, M., Kowalski, J., and Bartelt, P. (2010). RAMMS: Numerical simulation of dense snow avalanches in three-dimensional terrain. *Cold Regions Science and Technology*, 63(1-2):1–14.

Corominas, J. (1996). The angle of reach as a mobility index for small and large landslides. *Canadian Geotechnical Journal*, 2(33):260–271.

Crosta, G. (1998). Regionalization of rainfall thresholds: an aid to landslide hazard evaluation. *Environmental Geology*, 35(2-3):131–145.

Crosta, G. and Frattini, P. (2001). Rainfall thresholds for soil slip and debris flow triggering. *Proceedings of the 2nd EGS Plinius Conference on Mediterranean Storms*, (January 2001):463–487.

Crosta, G., Imposimato, S., and Roddeman, D. G. (2003). Numerical modelling of large landslides stability and runout. *Natural Hazards and Earth System Science*, 3(6):523–538.

Crozier, M. J. (2005). Multiple-occurrence regional landslide events in New Zealand: Hazard management issues. *Landslides*, 2(4):247–256.

Crozier, M. J. (2017). A proposed cell model for multiple-occurrence regional landslide events: Implications for landslide susceptibility mapping. *Geomorphology*, 295(July):480–488.

Cruden, D. M. (1991). A simple definition of a landslide. *Bulletin of the International Association of Engineering Geology*, 43:27–29.

Cruden, D. M. and Varnes, D. J. (1996). Landslide types and processes. pages 36–75.

Cuomo, S. (2020). Modelling of flowslides and debris avalanches in natural and engineered slopes: a review. *Geoenvironmental Disasters*, 7(1):1–25.

Dai, F. C., Lee, C. F., and Ngai, Y. Y. (2002). Landslide risk assessment and management: An overview. *Engineering Geology*, 64(1):65–87.

Dai, L., Scaringi, G., Fan, X., Yunus, A. P., Liu-Zeng, J., Xu, Q., and Huang, R. (2021). Coseismic Debris Remains in the Orogen Despite a Decade of Enhanced Landsliding. *Geophysical Research Letters*, 48(19).

Devoli, G., De Blasio, F. V., Elverhøi, A., and Høeg, K. (2009). Statistical analysis of landslide events in Central America and their run-out distance. *Geotechnical and Geological Engineering*, 27(1):23–42.

Dilley, M., Chen, R. S., Deichmann, U., Lener-Lam, A. L., Arnold, M., Agwe, J., Buys, P., Kjekstad, O., Lyon, B., Yetman, G., Lerner-Lam, A. L., Arnold, M., Agwe, J., Buys, P., Kjekstad, O., Lyon, B., and Yetman, G. (2005). *Natural Disaster Hotspots A Global Risk Analysis*.

El Tiempo (2007). Tarazá (Bajo Cauca antioqueño) fue declarado en estado de emergencia.

Engelen, G. (1967). Landslides in the metamorphic northern border of the dolomites (north italy). *Engineering Geology*, 2(3):135–147.

Fairfield, J. and Leymarie, P. (1991). Drainage Networks From Grid Digital Elevation Models. *Water Resources Research*, 27(5):709–717.

Fannin, R. J. and Wise, M. P. (2001). An empirical-statistical model for debris flow travel distance. *Canadian Geotechnical Journal*, 38(5):982–994.

Fawcett, T. (2005). An introduction to ROC analysis. 35(6):299–309.

Fell, R. (1994). Landslide risk assessment and acceptable risk. *Canadian Geotechnical Journal*, 31(2):261–272.

Freeman, T. G. (1991). Calculating catchment area with divergent flow based on a regular grid. *Computers 6eosciences*, 17(3):413–422.

Froude, M. J. and Petley, D. N. (2018). Global fatal landslide occurrence from 2004 to 2016. *Nat. Hazards Earth Syst. Sci.*, (18):2161–2181.

Gamma, P. (2000). *Ein Murgang-Simulationsprogramm zur Gefahrenzonierung*. PhD thesis, Geographisches Institut der Universität Bern.

Gingold, R. and Monaghan, J. (1977). Smoothed particles hydrodynam ics: theory and application to non-spherical stars. *Mon Not R Astron Soc*, 181:375–389.

Gómez, D., García, E. F., and Aristizábal, E. (2023). *Spatial and temporal landslide distributions using global and open landslide databases*, volume 117. Springer Netherlands.

González, J. L., Chavez, O. A., and Hermelin, M. (2005). Aspectos geomorfológicos de la avenida torrencial del 31 de enero de 1994 en la cuenca del río Fraile y sus fenómenos asociados. In Hermelin, M., editor, *Desastres de origen natural en colombia 1979-2004*, chapter 11, pages 135–150. Fondo Editorial Universidad EAFIT, Medellín.

Guthrie, R. and Befus, A. (2021). DebrisFlow Predictor : an agent-based runout program for shallow landslides. *Nat. Hazards Earth Syst. Sci.*, 21:1029–1049.

Guzmán, F., Ruíz, J., and Cadena, M. (2014). Regionalización de Colombia segun la estacionalidad de la precipitacion media mensual, a través de análisis de componentes principales (ACP). pages 1–55.

Haeberli, W. (1984). Permafrost glacier relationships in the Swiss Alps: today and in the past. In *Fourth International Conference on Permafrost*, pages 415–420, Fairbanks, Alaska. Versuchsanst. für Wasserbau, Hydrologie u. Glaziologie an d. Eidg. Techn. Hochsch.

Heim, A. (1932). *Bergsturz und Menschenleben.* Zürich.

Hermelin, M. and Hoyos, N. (2010a). Convulsive Events , a Widespread Hazard in the Colombian Andes. In Latrubesse, E. M., editor, *Natural hazards and human-exacerbated disasters in Latin-America : special volumes of geomorphology*, volume 13, chapter 7, pages 131–148. Earth Surface Processes.

Hermelin, M. and Hoyos, N. (2010b). Convulsive Events , a Widespread Hazard in the Colombian Andes. In Latrubesse, E. M., editor, *Natural hazards and human-exacerbated disasters in Latin-America : special volumes of geomorphology*, volume 13, chapter 7, pages 131–148. Earth Surface Processes.

Hernández, A. F. (2015). Avenida Torrencial en Salgar, Antioquia (Colombia).

Holmgren, P. (1994). Multiple flow direction algorithms for runoff modelling in grid based elevation models: An empirical evaluation. *Hydrological Processes*, 8(4):327–334.

Horton, P., Jaboyedoff, M., and Bardou, E. (2008). Debris flow susceptibility mapping at a regional scale. In *4th Canadian Conference on Geohazards*, Québec, Canada, 20–24 May 2008.

Horton, P., Jaboyedoff, M., Rudaz, B., and Zimmermann, M. (2013). Flow-R, a model for susceptibility mapping of debris flows and other gravitational hazards at a regional scale. *Natural Hazards and Earth System Sciences*, 13(4):869–885.

Huggel, C., Kääb, A., Haeberli, W., Teysseire, P., and Paul, F. (2002). Remote sensing based assessment of hazards from glacier lake outbursts: a case study in the Swiss Alps. *Canadian Geotechnical Journal*, 39(2):316–330.

Hungr, O. (1995). A model for the runout analysis of rapid flow slides, debris flows, and avalanches. *Canadian Geotechnical Journal*, 32(4):610–623.

Hungr, O., Corominas, J., and Eberhardt, E. (2005). Estimating landslide motion mechanism, travel distance and velocity. pages 99–128.

Hungr, O., Evans, S. G., Bovis, M. J., and Hutchinson, J. N. (2001). A review of the classification of landslides of the flow type. *Environmental and Engineering Geoscience*, 7(3):221–238.

Hungr, O., Leroueil, S., and Picarelli, L. (2014). The Varnes classification of landslide types, an update. *Landslides*, 11(2):167–194.

Hunter, G. and Fell, R. (2003). Travel distance angle for "rapid" landslides in constructed and natural soil slopes. *Canadian Geotechnical Journal*, 40(6):1123–1141.

Hürlimann, M., Rickenmann, D., Medina, V., and Bateman, A. (2008). Evaluation of approaches to calculate debris-flow parameters for hazard assessment. *Engineering Geology*, 102(3-4):152–163.

Hutchinson, J. N. (1986). A sliding–consolidation model for flow slides. *Canadian Geotechnical Journal*, 23(2):115–126.

International Union of Geological Sciences Working Group on Landslides (1995). A suggested method for describing the rate of movement of a landslide. *Bulletin of the International Association of Engineering Geology*, 52(1):75–78.

Iverson, R. M., Schilling, S. P., and Vallance, J. W. (1998). Objective delineation of lahar-inundation hazard zones. *GSA Bulletin*, 110(8):972–984.

Kappes, M. S., Malet, J. P., Remaître, A., Horton, P., Jaboyedoff, M., and Bell, R. (2011). Assessment of debris-flow susceptibility at medium-scale in the Barcelonnette Basin, France. *Natural Hazards and Earth System Science*, 11(2):627–641.

Kirschbaum, D., Stanley, T., and Zhou, Y. (2015). Spatial and temporal analysis of a global landslide catalog. *Geomorphology*, 249:4–15.

Kirschbaum, D. B., Adler, R., Hong, Y., Hill, S., and Lerner-Lam, A. (2009). A global landslide catalog for hazard applications: method, results, and limitations. pages 561–575.

Kjekstad, O. and Highland, L. (2009). *Economic and Social Impacts of Landslides*. Springer, Berlin, Heidelberg.

Kwan, J. S. and Sun, H. W. (2006). An improved landslide mobility model. *Canadian Geotechnical Journal*, 43(5):531–539.

Kwan, J. S. H., Sun, H. W., and of Engineers, H. K. I. (2007). Benchmarking exercise on landslide mobility modelling - runout analyses using 3dDMM. In *International Forum, Landslide disaster management*, Hong Kong, Hong Kong, China. Geotechnical Division, Hong Kong Institution of Engineers;.

Li, T. (1983). A mathematical model for predicting the extent of a major rockfall. *Zeitschrift fur Geomorphologie*, 27:473–482.

Llano Serna, M. A., Muniz-de Farias, M., and Martínez-Carvajal, H. E. (2015). Numerical modelling of Alto Verde landslide using the material point method. *Dyna*, 82(194):150–159.

Maros, H. and Juniar, S. (2019). *Modelación de flujos de escombros con DAN3D en quebradas susceptiblesdel sector norte del AMSS*. PhD thesis, Universidad del Salvador.

McDougall, S. (2017). 2014 canadian geotechnical colloquium: Landslide runout analysis — current practice and challenges. *Canadian Geotechnical Journal*, 54(5):605–620.

McDougall, S. and Hungr, O. (2004). A model for the analysis of rapid landslide motion across three-dimensional terrain. *Canadian Geotechnical Journal*, 41(6):1084–1097.

McDougall, S. and Hungr, O. (2005). Dynamic modelling of entrainment in rapid landslides. *Canadian Geotechnical Journal*, 42(5):1437–1448.

Medina, V., Hürlimann, M., and Bateman, A. (2008). Application of FLATModel, a 2D finite volume code, to debris flows in the northeastern part of the Iberian Peninsula. *Landslides*, 5(1):127–142.

Medina Bello, E., Reyes Merchan, A. A., Castro, J. A., Sandoval Martínez, A., Torres, J., and Pérez Moreno, M. A. (2018). Observaciones de campo de la avenida torrencial del 12 de agosto de 2018 en el municipio de Mocoa - Putumayo. Technical report.

Mergili, M. (2008). *Integrated modelling of debris flows with Open Source GIS*. PhD thesis, University of Innsbruck, Austria.

Mergili, M., Fellin, W., Moreiras, S. M., and Stötter, J. (2012). Simulation of debris flows in the Central Andes based on Open Source GIS: Possibilities, limitations, and parameter sensitivity. *Natural Hazards*, 61(3):1051–1081.

Mergili, M., Fischer, J. T., Krenn, J., and Pudasaini, S. P. (2017). r.avaflow v1, an advanced open-source computational framework for the propagation and interaction of two-phase mass flows. *Geoscientific Model Development*, 10(2):553–569.

Mergili, M., Krenn, J., and Chu, H. J. (2015). r.randomwalk v1, a multi-functional conceptual tool for mass movement routing. *Geoscientific Model Development*, 8(12):4027–4043.

Mergili, M., Marchesini, I., Alvioli, M., Metz, M., Schneider-muntau, B., Rossi, M., and Guzzetti, F. (2014). A strategy for GIS-based 3-D slope stability modelling over large areas. *Geoscientific Model Development*, 7(6):2969–2982.

Mesa, Ó., Poveda, G., Vélez-Upegui, J. I., Mejía Valencia, J. F., Hoyos Ortiz, C. D., Mantilla Gutiérrez, R., Barco Mejía, O. J., Cuartas Pineda, L. A., Botero Hernández, B., and Montoya, M. (2000). Distribución espacial y ciclos anual y semianual de la precipitación en Colombia. *XIV Seminario de Hidráulica e Hidrología*, (1):1–9.

Molinari, M. E., Cannata, M., and Meisina, C. (2014). r.massmov: An open-source landslide model for dynamic early warning systems. *Natural Hazards*, 70(2):1153–1179.

Moncayo, C. (2021). *Evaluación de la distancia de viaje de movimientos en masa en Colombia a partir de registros históricos*. PhD thesis, Universidad Nacional de Colombia (Bogotá).

Moser, M. and Hohensinn, F. (1983). Geotechnical aspects of soil slips in Alpine regions. *Engineering Geology*, 19(3):185–211.

Nadim, F. and Kjekstad, O. (2009). *Assessment of global high-risk landslide disaster hotspots*.

Noticias RCN (2020). Cinco muertos y 16 heridos por deslizamientos en Dabeiba, Antioquia.

Núñez Tello, A. (2003). Reconocmiemiento geolócico regional de la Planchas 411 La Cruz, 412 San Juan de Villalobos, 430 Mocoa, 431 Piamonte, 448 Monopamba, 449 Orito y 465 Churuyaco departamentos de Caquetá, Cauca, Huila, Nariño y Putumayo. Technical report, INSTITUTO DE INVESTIGACIÓN E INFORMACIÓN GEOCIENTÍFICA MINERO AMBIENTAL Y NUCLEAR INGEOMINAS, Bogotá, D. C.

O'brien, J. S., Julien, P. Y., and Fullerton, W. T. (1993). Two-Dimensional Water Flood and Mudflow Simulation. *Journal of Hydraulic Engineering*, 119:244–261.

O'Callaghan, J. F. and Mark, D. M. (1984). The Extraction of Drainage Networks from Digital Elevation Data. *Computer Vision, Graphics, and Image Processing*, 28:323–344.

Palacio, J., Aristizábal, E., Guthrie, R., and Echeverri, O. (2021a). DebrisFlow Predictor : Herramienta para la propagación de movimientos en masa tipo flujos . In *XVIII Congreso Colombiano de Geología*, Medellin, 18-20 August 2021. Sociedad Colombiana de Geología.

Palacio, J., Aristizábal, E., Mergili, M., and Echeverri, O. (2021b). Shallow landslide occurrence and propagation in tropical mountainous terrain with open source models . A case study in the Colombian Andes . In *EGU General Assembly 2021*, online, 19–30 Apr 2021.

Palacio, J., Gómez, F., Aristizábal, E., and Guthrie, R. (2022). Modelos empíricos para la evaluación de la amenaza por movimientos en masa tipo flujo. In *XXI Congreso Geológico Argentino*, page 3, Puerto Madryn, Chubut.

Palacio, J., Mergili, M., and Aristizábal, E. (2020). Probabilistic landslide susceptibility analysis in tropical mountainous terrain using the physically based r.slope.stability model. *Natural Hazards and Earth System Sciences*, 20:815–829.

Papa, M. N., Sarno, L., Vitiello, F. S., and Medina, V. (2018). Application of the 2D depth-averaged model, FLATModel, to pumiceous debris flows in the Amalfi Coast. *Water (Switzerland)*, 10(9).

Pastor, M., Blanc, T., Haddad, B., Petrone, S., Sanchez Morles, M., Drempetic, V., Issler, D., Crosta, G. B., Cascini, L., Sorbino, G., and Cuomo, S. (2014). Application of a SPH depth-integrated model to landslide run-out analysis. *Landslides*, 11(5):793–812.

Pastor, M., Haddad, B., Sorbino, G., Cuomo, S., and Drempetic, V. (2009). A depth-integrated, coupled SPH model for flow-like landslides and related phenomena. *Int. J. Numer. Anal. Meth. Geomech.*, 32:143–172.

Perla, R., Cheng, T. T., and McClung, D. (1980). A two–parameter model of snow–avalanche motion. *Journal of Glaciology*, 26(94):197–207.

Petley, D. (2008). The global occurrence of fatal landslides in 2007. In *Geophysical Research Abstracts, EGU General Assembly 2008*, page 3, Vienna, Austria.

Petley, D. (2012). Global patterns of loss of life from landslides. *Geology*, 40(10):927–930.

Pirulli, M. (2005). *Numerical Modelling of Landslides Runout*. Phd, Politecnico di Torino.

Poisel, R., Preh, A., and Hungr, O. (2008). Run Out of Landslides - Continuum Mechanics versus Discontinuum Mechanics Models. *Geomechanik und Tunnelbau*, 1(5):358–366.

Poveda, G. (2004). La hidroclimatología de Colombia : una síntesis desde la escala inter-decadal hasta la escala diurna. *Revista de la Academia Colombiana de Ciencias*, XXVIII(107):201–222.

Prada-Sarmiento, L. F., Cabrera, M. A., Camacho, R., Estrada, N., and Ramos-Cañón, A. M. (2019). The Mocoa Event on March 31 (2017): analysis of a series of mass movements in a tropical environment of the Andean-Amazonian Piedmont. *Landslides*, 16(12):2459–2468.

Pudasaini, S. P. (2012). A general two-phase debris flow model. *JGR Earth Surface*, 117(3):1–28.

Pudasaini, S. P. and Krautblatter, M. (2021). The mechanics of landslide mobility with erosion. *Nature Communications*, 12(1).

Pudasaini, S. P. and Mergili, M. (2019). A Multi-Phase Mass Flow Model. *Journal ofGeophysical Research: Earth Surface*, 124(12):2920–2942.

Qiu, C., Xie, M., and Esaki, T. (2007). Application of GIS Technique in Three-Dimensional Slope Stability Analysis. *COMPUTATIONAL MECHANICS*, 3(1):703–712.

Quan Luna, B., Remaître, A., van Asch, T. W., Malet, J. P., and van Westen, C. J. (2012). Analysis of debris flow behavior with a one dimensional run-out model incorporating entrainment. *Engineering Geology*, 128:63–75.

Quan Luna, B. R. (2012). *Dynamic numerical run out modeling for quantitative landslide risk assessment*. Phd, University of Twente, ITC.

Quinn, P., Beven, K., Chevallier, P., and Planchon, O. (1991). The prediction of hillslope flow paths for distributed hydrological modelling using digital terrain models. *Hydroloical Processes*, 5(October 1990):59–79.

Ramos Cañón, A. M., Merchán Reyes, A. A., Munévar Peña, M. A., Ruiz Peña, G. L., Machuca Castellanos, S. V., Rangel Flórez, M. S., Prada Sarmiento, L. F., Cabrera, M. Á., Rodríguez Pineda, C. E., Escobar Castañeda, N., Quintero Ortíz, C. A., Escobar Vargas, J. A., Juan Diego, G. O., Medina Orjuela, M. S., Durán Santana, L., Trujillo Osorio, D. E., Medina Ávila, D. F., Capachero Martínez, C. A., León Delgado, D., Ramírez Hernández, K. C., González Rojas, E. E., Rincón Chisino, S. L., Solarte Blandón, P. A., Castro Malaver, L. C., López Marín, C., Navarro Alarcón, S. d. R., and Pérez Moreno, M. A. (2021). *Guía metodológica para zonificación de amenaza por avenidas torrenciales*.

RCN Radio (2017). Aumenta el número de personas muertas por avalancha en Mocoa.

Rickenmann, D. (1999). Empirical relationships for Debris Flow. *Natural hazards*, 19(47):47–77.

Rickenmann, D. (2005). *Runout prediction methods*, pages 305–324. Springer Berlin Heidelberg, Berlin, Heidelberg.

Rickenmann, D. and Zimmermann, M. (1993). The 1987 debris flows in Switzerland: documentation and analysis. *Geomorphology*, 8(2-3):175–189.

Salm, B. (1993). Flow, flow transition and runout distances of flowing avalanches. *Annals of Glaciology*, 18:221–226.

Sassa, K. (1988). Geotechnical model for the motion of landslides. In *5th International Symposium on Landslides*, pages 37–55, Rotterdam.

Savage, S. B. and Hutter, K. (1989). The motion of a finite mass of granular material down a rough incline. *Journal of Fluid Mechanics*, 199(2697):177–215.

Savage, S. B. and Hutter, K. (1991). The dynamics of avalanches of granular materials from initiation to runout. Part I. Analysis. *Acta Mechanica*, 86:201–223.

Scheidegger, A. E. (1973). On the prediction of the reach and velocity of catastrophic landslides. *Rock Mechanics Felsmechanik Mécanique des Roches*, 5:231–236.

Scheidl, C. and Rickenmann, D. (2010). Empirical prediction of debris-flow mobility and deposition on fans. *Earth Surf. Process. Landforms*, 35(2):157–173.

Scheidl, C., Rickenmann, D., and McArdell, B. W. (2013). Runout prediction of debris flows and similar mass movements. *Landslide Science and Practice: Spatial Analysis and Modelling*, 3(September 2012):221–229.

Schilling, S. P. (1998). LAHARZ; GIS programs for automated mapping of lahar-inundation hazard zones. Technical report, USGS, Vancouver, Washington.

Schuster, R. and Highland, L. (2003). Impact of landslides and innovative landslide-mitigation measures on the natural environment. *Geologic Hazards Team, US Geological survey, Denver, Colorado, U.S.A.*

Schuster, R. L. (1996). Socioeconomic significance of landslides. In *Landslides investigation and mitigation*, chapter 2, pages 12–35. Washington, D.C.

Schuster, R. L. and Highland, L. (2001). Socioeconomic Impacts of Landslides in the Western Hemisphere. Technical report.

Sepúlveda, S. A. and Petley, D. N. (2015). Regional trends and controlling factors of fatal landslides in Latin America and the Caribbean. *Natural Hazards and Earth System Science*, 15(8):1821–1833.

SGC (2016). *Guía metodológica para estudios de amenaza, vulnerabilidad y riesgo por movimientos en masa*. Bogotá, D. C.

SGC (2017). Caracterización del movimiento en masa tipo flujo 31 de marzo 2017 en Mocoa-Putumayo. Technical report, Servicio Geológico Colombiano (SGC), Bogotá.

SGC (2017). *Guía metodológica para la zonificación de amenaza por movimientos en masa escala 1: 25.000*. Servicio Geológico Colombiano (SGC), Bogotá, D. C.

SGC (2017a). Sistema de Información de Movimientos en Masa - SIMMA.

SGC (2017b). Zonificación de susceptibilidad y amenaza por movimientos en masa de las subcuencas de las quebradas Taruca, Taruquita, San antonio, El carmen y los ríos Mulato y Sangoyaco del municipio de Mocoa – Putumayo. Escala 1:25.000. Technical report, Servicio Geológico Colombiano (SGC), Putumayo.

SGC (2018a). Amenaza por movimientos en masa tipo flujo de las cuencas de las quebradas Taruga, Taruquita, San Antonio y El Carmen y los ríos Mulato y Sangoyaco, municipio de Mocoa, escala 1:5000. Technical report, Servicio Geológico Colombiano (SGC), Bogotá.

SGC (2018b). Evaluación de la amenaza por movimientos en masa en el área urbana, periurbana y de expansión del municipio de Mocoa – Putumayo. Escala 1:5.000. Technical report, Servicio Geológico Colombiano (SGC), Mocoa.

Skempton, A. and Hutchinson, J. (1969). Stability of natural slopes and embankment foundations. pages 291–340.

Sovilla, B., Burlando, P., and Bartelt, P. (2006). Field experiments and numerical modeling of mass entrainment in snow avalanches. *Journal of Geophysical Research: Earth Surface*, 111(3):1–16.

Tarboton, D. G. (1997). A new method for the determination of flow directions and upslope areas in grid digital elevation models. *Water Resour. Res.*, 33(2):309–319.

Tayyebi, S. M., Pastor, M., Stickle, M. M., Yagüe, Á., Manzanal, D., Molinos, M., and Navas, P. (2022). SPH numerical modelling of landslide movements as coupled two-phase flows with a new solution for the interaction term. *European Journal of Mechanics, B/Fluids*, 96:1–14.

Te Chow, V. (1959). *Open-channel Hydraulics*. Civil engineering series. McGraw-Hill, New York.

UNGRD and Fundación Instituto Geofísico Universidad Javeriana (2016). Consultoría de estudios y diseño para la implementación del sistema de alerta temprana por avenidas torrenciales en la microcuenca de la quebrada la Liboriana, quebrada la Clara y río Barroso del municipio de Salgar (Antioquia). Technical report, Unidad Nacional para la Gestión del Riesgo de Desastres (UNGRD), Bogotá.

UNGRD and Universidad Pontificia Javeriana (2017). Consultoría de los estudios de diseño del sistema de alerta temprana para avenidas torrenciales y crecientes súbitas generadas por precipitaciones de la microcuenca de los ríos Mulato, Sangoyaco, quebradas Taruca y Taruquita del municipio de Mocoa. Technical report, Bogotá.

unico de informacion normativa, S. (2011). DECRETO 4131 DE 2011.

Varnes, D. J. (1978). Slope Movement Types and Processes. pages 11 – 33.

Varnes, D. J. (1984). *Landslide hazard zonation: a review of principles and practice*. Unesco, Paris, France.

Voellmy, A. (1955). Über die Zerstörungskraft von Lawinen. *Schweizerische Bauzeitung*, 73(15).

Von Neumann, J. (1966). *Theory of self-reproducing automata*.

von Ruette, J., Lehmann, P., and Or, D. (2016). Linking rainfall-induced landslides with predictions of debris flow runout distances. *Landslides*, 13(5):1097–1107.

Wang, F. and Sassa, K. (2000a). A modified geotechnical simulation model for the areal prediction of Landslide motion. *Annuals of Disas. Prev. Res. Inst.*, 43:6.

Wang, F. and Sassa, K. (2000b). A modified geotechnical simulation model for the areal prediction of Landslide motion. *Annuals of Disas. Prev. Res. Inst.*, 43:6.

Wang, Y., Hutter, K., and Pudasaini, S. P. (2004). The savage-hutter theory: A system of partial differential equations for avalanche flows of snow, debris, and mud. *ZAMM Zeitschrift fur Angewandte Mathematik und Mechanik*, 84(8):507–527.

Witt, A., Malamud, B. D., Rossi, M., Guzzetti, F., and Peruccacci, S. (2010). Temporal correlations and clustering of landslides. *Earth Surface Processes and Landforms*, 35(10):1138–1156.

Zimmermann, F., McArdell, B. W., Rickli, C., and Scheidl, C. (2020). 2D runout modelling of hillslope debris flows, based on well-documented events in Switzerland. *Geosciences*, 10(2):1–17.

Zimmermann, M. N., Mani, P., Gamma, P., Gsteiger, P., Heiniger, O., and Hunziker, G. (1997). Murganggefahr und klimaänderung - ein gis-basierter ansatz.